

(12)

# SYNTHESIS AND SURFACE MODIFICATION OF LWIR WINDOW MATERIALS

AD-A231 891

## FINAL REPORT

---

---

CONTRACT NO. N00014-85-C-0140

Prepared for

Office of Naval Research  
Code 1131  
800 N. Quincy Street  
Arlington, Virginia 22217-5000

Contract Monitor

Dr. Robert Schwartz  
Naval Weapons Center  
China Lake, CA

Prepared by

A.B. Harker  
Rockwell International  
Science Center  
1049 Camino Dos Rios  
Thousand Oaks, CA 91360

DISTRIBUTION STATEMENT A  
Approved for public release  
Declassify/Declassify



Rockwell International  
Science Center



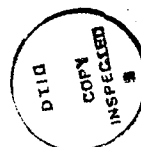
Rockwell International  
Science Center

SC5422.FR

## ABSTRACT

This report summarizes the results of a four-year Office of Naval Research (ONR) sponsored research program in three separate areas all directed toward the development of improved mechanical properties in materials suitable for use as long wavelength infrared (LWIR) window materials. The three areas under investigation were:

1. The use of directed chemical synthesis techniques to produce phase pure powders suitable for consolidation as polycrystalline LWIR window materials.
2. The use of surface layers and surface implantation approaches to improve the fracture toughness and tensile strength of LWIR window materials.
3. The investigation of the chemical and physical processes involved in the synthesis and post-fabrication polishing of polycrystalline diamond.



Statement "A" per telecon Dr. Robert Schwartz. Naval Weapons Center/Code 373. China Lake, CA 93555-6001

Accession For	
NTIS CR1&I	<input checked="" type="checkbox"/>
DTIC TAB	<input type="checkbox"/>
Unannounced	<input type="checkbox"/>
Justification	
By	
Distribution	
Availability Dates	
Dist	Avail. and/or Special
A-1	

**PROGRAM PARTICIPANTS:**

**Rockwell International Science Center Co-Investigators**

Dr. Alan B. Harker  
Dr. Peter E. D. Morgan  
Dr. Paul H. Kobrin  
Dr. Jeffery DeNatale  
Mr. John F. Flintoff

**Undergraduate Summer Students and Rockwell Youth Motivation Program High School Students**

**Mike Koutsoutis: YMP Student and Undergraduate UCLA, Summer Student (1986)**

**Eric Harmon: Undergraduate U.C. Davis, summer student (1987-88)**  
**Completed Electrical Engineering Degree (1988), Currently graduate student at Purdue in Electrical Engineering.**

**Jonathan Flintoff: Undergraduate U.C. Santa Barbara, Summer Student (1989), Completed Degree in Chemical Engineering (1989), currently employee Rockwell International Science Center.**

**Kristin Wilson: Undergraduate Duke, Summer Student (1988,1989,1990), Bachelor of Science in 1990, applying for graduate studies at U.C. Davis.**



## TABLE OF CONTENTS

	<u>Page</u>
1.0 INTRODUCTION .....	1
2.0 TECHNICAL RESULTS .....	2
2.1 Directed Chemical Synthesis of LWIR Window Materials .....	2
2.2 Surface Modification of LWIR Materials .....	4
2.3 Polycrystalline Diamond Materials Research .....	6



## 1.0 INTRODUCTION

The goals of this ONR sponsored research program include both the synthesis and modification of materials which are candidates for application as LWIR window materials with improved mechanical impact and thermal shock resistance. The research program, initiated in 1985, has extended over four years and has evolved based upon work in this and other laboratories to pursue the development of the most promising candidate materials and processes. The program has involved research in three separate areas. These include:

1. The use of directed chemical synthesis techniques to produce phase pure powders suitable for consolidation as polycrystalline LWIR window materials.
2. The use of surface layers and surface implantation approaches to improve the fracture toughness and tensile strength of LWIR window materials.
3. The investigation of the chemical and physical processes involved in the synthesis and post-fabrication polishing of polycrystalline diamond.

These significant results of these research efforts have been documented in the technical literature in the form of refereed journal and conference proceedings articles. These articles have been collected and are presented in sequence in this report with introductions to show the development of the research effort and to tie the work to the ultimate goals of the program.

## 2.0 TECHNICAL RESULTS

### 2.1 Directed Chemical Synthesis of LWIR Window Materials

#### Directed Fused Salt Synthesis of IR Window Materials

Investigator P.E.D. Morgan

Student M.S. Koutsoutis

Publication: Fused Salt Synthesis of Materials for IR Windows  
Mat. Res. Bull. vol. 22, pp.617-621 (1987)

At the initiation of this program it was recognized that a number of highly covalently bonded materials would have to be surveyed in an attempt to locate new IR window material candidates. To accomplish this synthesis techniques needed to be developed that not only could handle sulfide and phosphide compounds, but could also produce pure compounds as powders suitable for consolidation so that bulk optical and mechanical properties could be determined. It has been recognized that an effective means of producing high-density, fine grained ceramics is to start with uniform, highly compacted monosize particles. This achieves a high number of particle-particle contacts producing uniform densification during sintering, avoiding porosity which is deleterious to both mechanical and optical properties.

In this work, a fused salt synthesis technique was examined for the production of chalcogenides and pnictides, with an aim of attaining controlled monosized particles in the 0.1-1  $\mu\text{m}$  size range. Initial efforts addressed the synthesis of  $\text{CaLa}_2\text{S}_4$ , but were redirected to the study of  $\text{NaLaS}_2$  when this LWIR transparent material was produced with high purity.

Pellets of the sodium lanthanum sulfide were consolidated and made available to other participants in the ONR program for optical and mechanical characterization. The results of the characterization work was not published, but was presented at the annual program workshop. The decision to not pursue this particular material and the



Rockwell International  
Science Center

SC5422.FR

multication sulfides in general was based upon both their large thermal expansion coefficients and their absorption bands in the LWIR spectral region.

The following article summarizes the major findings of the synthesis efforts.

## FUSED SALT SYNTHESIS OF MATERIALS FOR IR WINDOWS

P.E.D. Morgan and M.S. Koutsoutis  
Rockwell International Science Center  
Thousand Oaks, CA 91360

(Received December 15, 1986; Refereed)

**ABSTRACT:** A fused salt technique for preparing nearly spherical, narrow size distribution particles of  $\text{NaLaS}_2$  is discussed. The method, a one-step synthesis and Ostwald ripening, appears to have great potential for complex, nonoxide materials.

**MATERIALS INDEX:** Sodium Lanthanum and Sulphides.

### INTRODUCTION

Fused salt synthesis of a chalcogenide powder for infrared (IR) window use in the 8-12  $\mu\text{m}$  regime of the "atmospheric window" has been investigated. Materials for this application require erosion resistance, high hardness and strength with good thermal shock resistance. Oxides, with the required mechanical properties, because of their strong M-O bonds, especially when M is a light element, however, absorb in this region and a more massive anion is required.

As narrow bandgap materials will not fill the bill, especially at higher temperatures, one is left apparently with only the more ionic chalcogenides or pnictides. One considers, therefore, bonds such as Zn-Se, Ca-S, La-S, Zn-P, and a few others. The choices are few, as chalcogenide or pnictide bonds are less strong, leading to weaker and softer structures with higher thermal expansivity. Thermal expansivity in an approximately close-packed structure is proportional to individual bond valence (1). Total strength can be related to total bond valence sum at the "cations and anions". The bonding requirements are therefore in conflict; strong bonds between light atoms are needed for mechanical properties, and weak bonds between heavier elements for IR transmittance. Compromise is the only solution.

Attempts at compromise have included  $\text{Zn}^{\text{IV}}\text{Si}^{\text{IV}}\text{P}^{\text{IV}}_2$  (Wurtzite type) (2) (Roman numerals denote atom coordination). The idea here is to use low coordination with stronger bonds (to keep thermal expansion down). Unfortunately, the absorption edge is too low (3). An alternative is to attempt to use many weaker bonds as in  $\text{Ca}^{\text{VIII}}\text{La}^{\text{VIII}}_2\text{S}^{\text{VI}}_4$

( $\text{Th}_3\text{P}_4$  structure type) (4,5), however, the thermal expansivity is high as each bond valence is low.

One possible compromise, as discussed here, may be to use a six coordinated solid such as  $\text{Na}^{\text{VI}}\text{La}^{\text{VI}}\text{S}_2^{\text{VI}}$

For the 3-5  $\mu\text{m}$  "atmospheric window", various oxides and nitrides,  $\text{Y}_2\text{O}_3$ ,  $\text{MgAl}_2\text{O}_4$ ,  $\text{AlN}$  and  $\text{AlON}$ , have been tried and sophisticated processing techniques (6) have been designed to fabricate them. This will be true for the 8-12  $\mu\text{m}$  candidates.

It has become recognized that one efficient way of producing high-density, fine-grain oxide ceramics is to start with uniformly highly compacted monosize particles (7). The aim is to achieve large numbers of particle-particle contacts, with uniform densification during sintering, so as to avoid the formation of large voids due to discontinuous effects (8), this danger has been recognized for many years, but only recently studied in detail. Voids, especially larger ones, are sources of fracture initiation and light scattering. In the case of an IR window, if unavoidable pores can be kept below the size corresponding to the wavelength of interest, then transparency will be little affected. This should be easy for the 8-12  $\mu\text{m}$  regime of interest.

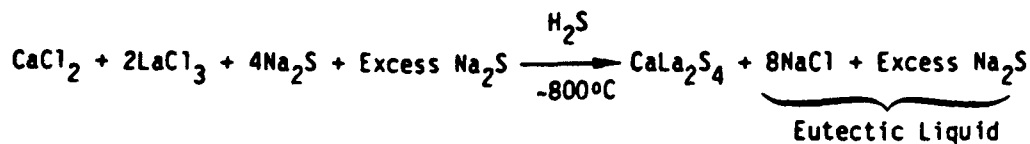
Less work has been done to produce chalcogenides of uniform particle size than for the case of oxides (9); for complex mixed chalcogenides, new challenges are expected. A further advantage of carefully controlled growth of uniform particles should be improvements in purity of the product. This is especially important with respect to oxygen, ubiquitously property degrading, but unfortunately almost ever-present. It is anticipated that uniform particles of complex chalcogenides or other appropriate IR transparent materials should be readily fabricable into IR windows.

Many chalcogenides, due to their more covalent nature, and therefore lower bulk and grain boundary diffusion values relative to coarsening mechanisms such as evaporation-condensation, do not readily sinter (10) (if at all) and must be hot-pressed or HIPed (hot iso-pressed). It is extremely desirable to keep temperatures of fabrication low to avoid simultaneous grain coarsening, and hence mechanical weakening, and thus minimize evaporation-condensation and stoichiometry variation.

For this work, we have chosen the fused salt synthesis technique (11-14) for producing chalcogenides or pnictides with the aim of attaining controlled monosized particles in the 0.1-1  $\mu\text{m}$  size range. The fused salt technique promises to be a better method of attaining good stoichiometry with high impurity and low oxygen content, which has been a persistent problem (15). This follows because the impurities and oxygen will tend to accumulate in the fused melt, while the particles are purified by solution-reprecipitation (Oswald ripening). The particles do not need to be milled (normally necessary to break up aggregates), thus eliminating a contaminating step. Initially, to establish the principles of the method, we attempted to use  $\text{CaLa}_2\text{S}_4$  as a prototype candidate. A surprise result led us instead to study  $\text{NaLaS}_2$ .

## EXPERIMENTAL AND RESULTS

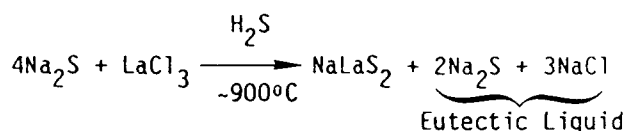
We wish to concentrate on cheap starting materials, potentially to be scaled up for later commercial use. We want the least number of steps to minimize labor, handling and contamination. Irreducibly simple, then, seemed to be the reaction in quartz inside a controlled atmosphere tube furnace:



With many tries, varying the ratios of the ingredients, surprisingly, no  $\text{CaLa}_2\text{S}_4$  was seen. Instead, recently discovered (16) rock salt structure  $\text{NaLaS}_2$ , and  $\text{CaS}$  were the predominant products. Even more surprising to us was that when the by-product  $\text{NaCl} + \text{Na}_2\text{S}$  was extracted by solution in cold water, the  $\text{NaLaS}_2$  was not noticeably attacked. Contaminant  $\text{La}_2\text{O}_2\text{S}$ , present in the preparation and not produced by reaction with the water, was seen, suggesting a method of further lowering the oxygen potential, beyond that achievable by  $\text{H}_2\text{S}$ , was needed. It was further observed that, indeed, the  $\text{NaCl}-\text{Na}_2\text{S}$  eutectic was in the region of  $800^\circ\text{C}$  (the  $\text{NaCl}-\text{Na}_2\text{S}$  phase diagram has not been done!).

$\text{NaLaS}_2$  has the rock salt structure, i.e.,  $\text{Na}^{\text{VI}}\text{La}^{\text{VI}}\text{S}_2^{\text{VI}}$ ; thus, its six-fold coordinated structure may give useably low thermal expansivity while still having weak enough bonds for the absorption edge to be at a sufficiently long wavelength. In any event, it represented a new candidate for further study of the method.

The incredibly simple reaction:



was used with the slightly higher temperature. Again,  $\text{La}_2\text{O}_2\text{S}$  appeared as a low-level impurity and varying ratios of ingredients did not remove it.

To reduce oxygen further, the test was redone in carbon disulfide vapor by bubbling argon gas through  $\text{CS}_2$  liquid. It was considered that this might produce some carbon deposits (it didn't), but even should they form with this method, the carbon would form floating on the fused salt, and thus be easily removed. It was found that by using a ratio of 2:1  $\text{Na}_2\text{S}:\text{LaCl}_3$ , almost pure  $\text{NaLaS}_2$  was achieved (< 5% of  $\text{La}_2\text{O}_2\text{S}$  remained). At this point, alternative extraction studies were commenced. It was found that ethanol effectively removed  $\text{NaCl}$  and  $\text{Na}_2\text{S}$  in a Soxhlet extraction under argon, but that the method was extremely slow with > 10 g amounts. If water was used for at least one day in a Soxhlet,  $\text{NaLaS}_2$  was decomposed (the water was  $\sim 60^\circ\text{C}$  in this case).

Using a ratio of 2:1,  $\text{Na}_2\text{S}$  to  $\text{LaCl}_3$ , produced purer  $\text{NaLaS}_2$  with only a trace of  $\text{La}_2\text{O}_2\text{S}$  after 7 h under  $\text{CS}_2$ . If the mix was held for one day at  $900^\circ\text{C}$  in  $\text{CS}_2$ , then  $\text{La}_2\text{S}_3$  was a minor impurity.

At this point, another minor impurity was encountered whose presence increased with more excess  $\text{Na}_2\text{S}$  (desirable to produce a lower melting flux - easier to dissolve in organic solvents). It was found that the impurity could be isolated from the mixed  $\text{NaLaS}_2$ /impurity product by treating with cold acetic acid which dissolves  $\text{NaLaS}_2$ . The impurity was examined by energy dispersive x-ray fluorescence (EDS) which indicated La, Na (trace), Si and S. Material purified in this way was x-rayed; the diffraction pattern was analyzed by computer unit cell finders and turned out to be a (new) apatite structure,  $\approx \text{Na}_{0.5}\text{La}_{4.5}(\text{SiO}_4)_3\text{S}$ , hexagonal  $P6_3/m$ ,  $a = 9.911\text{\AA}$ ,  $c = 7.025\text{\AA}$ ,  $c/a = 0.709$ .

After heating in air to  $1000^\circ\text{C}$ , the apatite became more poorly crystalline with cell parameters:  $a = 9.874\text{\AA}$ ,  $c = 7.016\text{\AA}$  and  $c/a = 0.711$ . For the known  $\text{NaLa}_4(\text{SiO}_4)_3\text{F}$  (17):  $a = 9.689\text{\AA}$ ,  $c = 7.1805\text{\AA}$  and  $c/a = 0.741$ . For a group of apatites (18), it is known that the  $c/a$  ratio falls when the trigonal site in apatite, i.e., the F site in  $\text{NaLa}_4(\text{SiO}_4)_3\text{F}$ , is occupied by a larger anion such as Cl. In our case, the  $c/a$  ratio indicates that the detected sulfur is probably in this site, as suggested above. We believe this is the first known apatite of this type. Naturally, the finding of Si in the impurity suggested that  $\text{Na}_2\text{S}$ , especially in excess, was attacking the quartz containers used to contain the flux

melt. We therefore switched to using carbon crucibles. At this point, no further impurity was seen, and the  $\text{Na}_2\text{S}$  content was conveniently increased to about 2:1  $\text{Na}_2\text{S}:\text{NaCl}$  in the flux.

Samples of  $\text{NaLaS}_2$ , which have been standing in ambient air for 14 months, still give XRD patterns that appear to be unchanged from the originals. However,  $\text{NaLaS}_2$  is attacked by hot water, so continuing studies have been carried out to remove the growth flux with organic solvents. We have found  $\text{C}_2\text{H}_5\text{OH}$  to be effective, but slow in a Soxhlet extraction. We now favor dimethyl formamide, DMF,  $\text{HCON}(\text{CH}_3)_2$ , in a well thermally insulated system where the Soxhlet thimble is at about 140°C. A resulting preparation of x-ray pure  $\text{NaLaS}_2$  is shown in the accompanying photograph, where well-rounded 10  $\mu\text{m}$  "apples" of  $\text{NaLaS}_2$  are shown (the reason for the curious shape is unknown). To obtain the desired  $\approx 1 \mu\text{m}$  size spheres, we will have to go to much shorter times of Oswald ripening. This is an immediate future task.

As an example of the relative uniformity in  $\text{NaLaS}_2$  product, Figure 1 shows SEM pictures of the product at indicated magnifications after extraction of the eutectic melt with cold water. The slight surface "contaminant" may be due to reaction with the water.

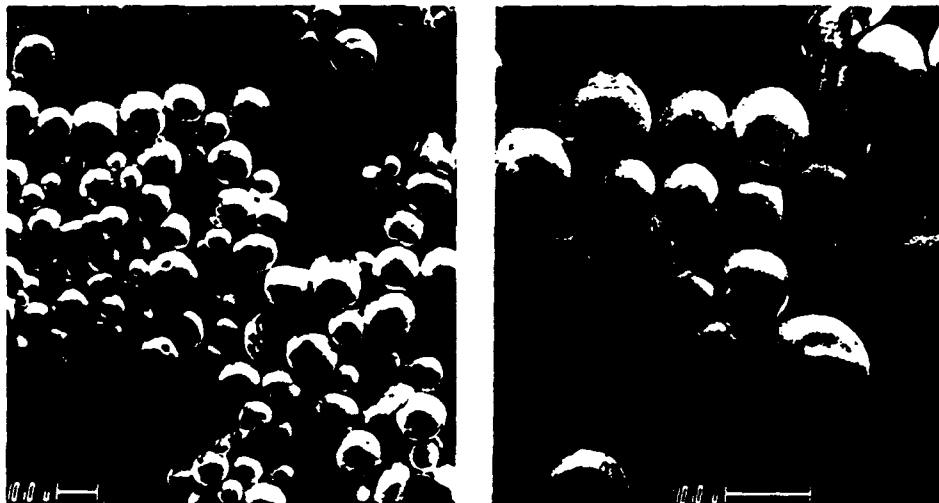


Figure 1 SEM of particles of  $\text{NaLaS}_2$ .

#### CONCLUSION

This type of very simple fused salt chemistry appears to be a viable approach to modern ceramic synthesis of monosize particles of complex sulfides or other chalcogenides.

#### ACKNOWLEDGEMENT

This research was supported by the Office of Naval Research and by the Rockwell International Science Center Youth Motivation Program.

## REFERENCES

1. R.M. Hazen and L.W. Finger, Comparative Crystal Chemistry, Wiley-Interscience (1982).
2. J. Covino, Proc. Int. Soc. for Opt. Eng. 505, Emerging Optical Materials, Aug. 21-24, 1984.
3. G.Q. Yao, H.S. Shen, R. Kershaw, K. Dwight and A. Wold, Technical Report No. 1, Office of Naval Research, Contract No. N00014-85-K-0177 (1986).
4. W.B. White, D. Chess, C.A. Chess and J.V. Biggers, SPIE 297, 38-43 (1981).
5. K.J. Saunders and R.L. Gentilman, Final Technical Report, Office of Naval Research, Contract No. N00014-82-C-0413 (1984).
6. W.H. Rhodes, J. Am. Ceram. Soc. 64, 13-19 (1981).
7. E.A. Barringer and H.K. Bowen, J. Am. Ceram. Soc. 65 (12), C199-C201 (1982).
8. K.D. Reeve, Am. Ceram. Soc. Bull. 42 (8), 452 (1963).
9. E. Matijevitch, Ultrastructure Processing of Ceramics, Glasses and Composites, eds., L.L. Hench and D.R. Ulrich, Wiley (1984), pp. 334-52.
10. P.E.D. Morgan, Sintering and Related Phenomena, Proc. Int. Conf., Notre Dame, IN (1965); 861-94, ed., G.C. Knuzyński, Gordon and Breach (1967).
11. D.G. Wickham, Ferrites, 105-7, Proc. Int. Conf., Kyoto, Japan (1970).
12. P.J. Walker and R.C.C. Ward, Mat. Res. Bull. 19, 717-725 (1984).
13. V.V. Leonov, Inorganic Materials 19, 1238-9 (1983).
14. H.J. Scheel, J. Crystal Growth 24/25, 669-73 (1974).
15. K.L. Lewis, J.A. Savage, K.J. Marsh and A.P.C. Jones, Proc. SPIE 400, 21-28 (1983).
16. M. Sato, G. Adachi and J. Shiokawa, Mat. Res. Bull. 19, 1215-1220 (1984).
17. PDF No. 21-1364, Center for Powder Diffraction Standards, Swarthmore, PA.
18. O.S. Bondareva and Yu. A. Malinovskii, Sov. Phys. Cryst. 31 (2), 136-138 (1986).

2.2 Surface Modification of LWIR Materials

Co-Investigators: Paul H. Kobrin and Alan B. Harker

The long-term goal of this program, to develop materials suitable for use as LWIR sensor windows in high temperature and high thermal-mechanical stress environments, places severe restrictions upon the available candidates. Most LWIR transmitting materials have a fairly low band-gap and become broad-band absorbers upon heating as electrons enter the conduction bands. Wider band-gap materials considered under the program include ZnS, ZnSe, ternary sulfides, new phosphides, and diamond. Other than diamond, all these candidate materials exhibit mechanical and thermal shock failure properties well below those of the fine grained polycrystalline and single crystal windows used in the short- and mid-wave infrared (sapphire, spinal, cubic yttria, fused silica, etc).

Relatively poor thermo-mechanical shock failure properties are intrinsic to most LWIR transmitting materials. This is the case since more strong chemical bonds generally improve mechanical properties and such strong bonds typically have phonon absorptions at wavelengths shorter than 10  $\mu\text{m}$  in the infrared. The exceptions to this generalization are materials with high coordination numbers in which the bonding is primarily covalent, ZnS, ZnSe, Ge, Si, diamond, and some narrow band gap semiconductors.

Given these intrinsic restrictions upon the properties of candidate LWIR materials, it was determined that investigating means of surface modification offered potential for improving the mechanical properties without severe LWIR transmission and emission penalties. The most promising method for improving fracture toughness and tensile strength involves the introduction of surface stress to inhibit crack propagation through the use of surface layers or the ion implantation of the surface.

It was found that the fracture toughness, as measured by Vickers indentation techniques, of single crystal and amorphous materials could be improved by compressive layers (up to 170% in single crystal sapphire). This measurement technique never showed the surface films to produce any direct improvement in the fracture toughness of polycrystalline ZnS, which was used as a base line material in the study. However,



tensile strength measurements using a ring on ring fracture approach did show a 40 to 60% improvement in coated and implanted ZnS samples.

Generally, the thin compressive surface layer coating modification approach was found to be more reproducible than ion implantation and could be qualitatively described by existing fracture models. The use of implantation was found to be highly dependent upon the implantation ion mass and energy as expected, but also dependent upon the temperature of implantation. Uncooled implantation runs produced sufficient heating in the samples to partially anneal out the surface damage caused by the process.

The results of the compressive layer study are described in the following article.

**The Effects of Thin Films on Indentation Fracture Toughness Measurements,  
Journal of Materials Science 24, 1363-1367 (1989).**

# The effects of thin compressive films on indentation fracture toughness measurements

P. H. KOBRIN, A. B. HARKER

Rockwell International Science Center, Thousand Oaks, California 91360, USA

Thin compressive films have been shown to decrease the lengths of radial cracks produced by a Vickers indentation in a variety of non-metallic materials. The intrinsic stress of sub-micrometre thick films deposited by reactive ion beam sputtering was measured by a cantilever technique. The change in the apparent indentation fracture toughness of the coated material was correlated with film thickness and stress, indentation load, and the nature of the substrate.

## 1. Introduction

The indentation fracture technique is a simple and rapid means of determining the fracture toughness,  $K_c$ , of brittle materials. In this method, a Vickers-shaped diamond indenter of a given load is used to produce radial cracks that can be viewed on the sample surface. The lengths of the cracks can then be directly related to the fracture toughness [1].

A thin stressed layer on the surface of a brittle material can significantly modify the lengths of the radial cracks and therefore also the computed value of the toughness. This phenomenon has been observed in ion-implanted materials by several groups [2-4]. Lawn and Fuller [5] have developed a model that relates thin-layer surface stresses to changes in indentation crack dimensions. Their model predicts a change in the computed fracture toughness,  $K$ , that is independent of indenter load. However, work with ion implantation surface layers [3, 4] shows that the change in  $K$  is smaller at larger loads than at smaller loads.

In this paper, a systematic study is described in which changes in the indentation fracture toughness of a variety of brittle materials are correlated with thin film stress and thickness, and with indenter load.

## 2. Experimental details

Reactive ion beam deposition was used to deposit thin ( $< 1 \mu\text{m}$ )  $\text{Si}_3\text{N}_4$ ,  $\text{SiO}_2$  and  $\text{Al}_2\text{O}_3$  films from elemental and ceramic targets. Depositions were made at room temperature. These sputtered films are intrinsically stressed as depicted in Fig. 1. This figure shows a model of the relaxed stress distribution of a film-substrate system [6]. The compressive stress in the film is balanced by a tensile stress in the bulk which will cause an unclamped substrate to bend. The resultant stress is highest near the film-substrate interface. This stress is intrinsic to the growth conditions and does not develop as a result of a mismatch in the thermal expansion coefficients of the film and substrate. Furthermore, for amorphous or polycrystalline films it is expected to be independent of the nature of the substrate.

The intrinsic stress of the films used in this study were measured by a sensitive bending plate technique with capacitive detection [7]. For this technique, a thin glass cover slip is coated on one side with 20 nm of aluminium metal to make it conductive. The cover slip is then clamped at one end so that it forms a parallel plate capacitor with a metal plate. When a stressed film is deposited on the uncoated side of the cover slip, the glass bends and the resulting change in capacitance is used to measure the film stress. Typically, 10 to 50 nm of film were deposited; the ion gun was turned off and the capacitive system was allowed to equilibrate thermally before the stress was determined. Additional depositions were made until 500 nm had been deposited.

Corroboration of the cantilever determined stress values was obtained by measuring the stress of a 400 nm thick  $\text{Si}_3\text{N}_4$  film on a thin, round  $\text{ZnS}$  substrate. Film stress caused the  $\text{ZnS}$  substrate to assume a spherical curvature that was measured by counting the Newton's rings under a sodium lamp. The seven rings that were measured from a  $0.4 \mu\text{m}$  thick  $\text{Si}_3\text{N}_4$  film corresponded to a film stress of 1.4 GPa. This is reasonably close to the 1.6 GPa value obtained by the cantilever system. The cover-slip cantilever system is coated while stationary, while all of the other substrates in this study were mounted on a rotating planetary substrate holder that produced uniform film coverage.

The Vickers indent technique was used to measure the fracture toughness. The fracture toughness,  $K_c$ , in an unstressed material is given by [1]

$$K_c = \chi P/c_0^{3/2} \quad (1)$$

where  $P$  is the load, and  $c_0$  is the radial crack length defined in Fig. 2. The coefficient  $\chi$  is defined by  $\chi = (0.016)(E/H)^{1/2}$ , where  $E$  and  $H$  are the Young's modulus and hardness, respectively. This technique provides a measure of the fracture toughness which is independent of the indenter load. Fig. 3a shows a glass sample that has been indented with a 1.0 kg load. The glass slide was broken along two of the cracks to expose the radial cracks lying beneath the surface. The full penny-like (or semicircular) shape of the radial

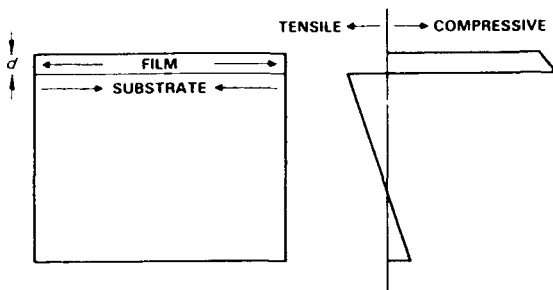


Figure 1 Stress distribution in a brittle material with a compressive surface film.

cracks did not develop because of a lateral crack 40  $\mu\text{m}$  below the surface. Note how the radial cracks intersect the surface at right angles.

A film-stressed system can alter the size and shape of the penny-like radial cracks as well as the indenter loading required to produce four symmetrical cracks. This crack alteration produces a different apparent fracture toughness. Fig. 3b shows the effect of adding a 0.4  $\mu\text{m}$  thick  $\text{Si}_3\text{N}_4$  film. The radial cracks are deflected near the surface which results in a shorter crack length on the surface. The shapes of the cracks are modified at a depth beneath the surface that is many times the film thickness. Deflected radial cracks were also observed for films on single crystal silicon substrates.

Films up to 1  $\mu\text{m}$  thick were initially grown on 1.2 mm thick soda lime glass (Erie Scientific, New Hampshire) and 0.3 mm thick (100) single crystal silicon substrates. Indents were made at several loadings and crack lengths were measured at least one day later. The delay between indentation and crack analysis was established since cracks in glass may continue to grow after the load is removed due to

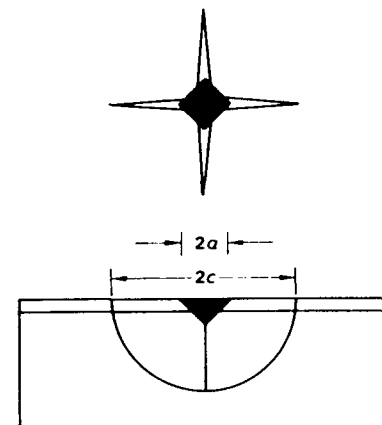


Figure 2 Schematic representation of a Vickers indent in a coated material.

moisture assistance. The rate of this postindentation growth decreases with time [1]. Silicon does not exhibit postindentation growth. Measurements made immediately after indentation provide a more accurate  $K_c$  for unstressed materials [1]. The indenter was aligned so that the cracks in silicon were always oriented along the  $\langle 100 \rangle$  directions.  $K$  was calculated for indents with four radial cracks and with  $c \geq 2b$ . This put a lower limit on the loads and the depths that were sampled. The hardness of the samples, which was also obtained from the Vickers indent, was not noticeably changed by the addition of these films.

### 3. Results and discussion

The cantilever stress system gives values of  $\sigma_s$  equal to 0.2, 1.0 and 1.6 GPa for films of  $\text{Al}_2\text{O}_3$ ,  $\text{SiO}_2$  and  $\text{Si}_3\text{N}_4$ , respectively. In all cases the accumulated stress was found to increase linearly with thickness.



Figure 3 Glass samples with a 1.0 kg load indent taken with an optical microscope (a) no film and (b) with a 0.4  $\mu\text{m}$  thick  $\text{Si}_3\text{N}_4$  film. The arrows point to the ends of the surface radial cracks.

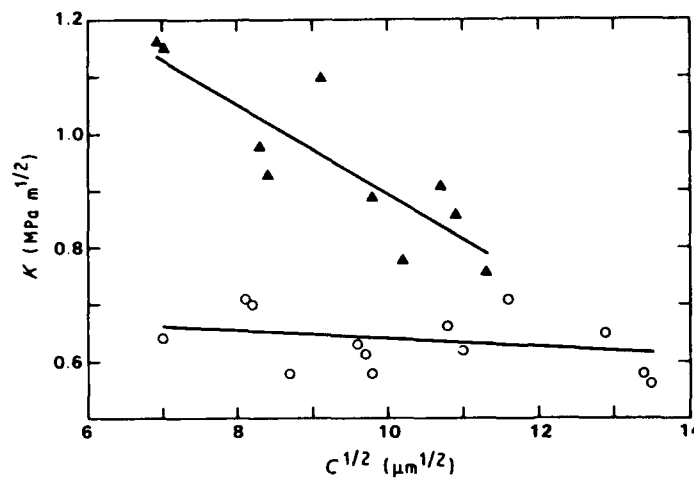


Figure 4 Measured fracture toughness of uncoated glass (○) and glass coated (▲) with a  $0.7\text{ }\mu\text{m}$  layer of  $\text{Si}_3\text{N}_4$  as a function of indent load.

While the stress of the  $\text{SiO}_2$  films is less than that of the  $\text{Si}_3\text{N}_4$ , it was observed that on glass the threshold load for crack production was higher with the  $\text{SiO}_2$  films. Glass with a  $1.0\text{ }\mu\text{m}$  thick  $\text{SiO}_2$  film required greater than a  $1.5\text{ kg}$  load for any radial cracks to form while uncoated glass gave four cracks with a  $0.2\text{ kg}$  load. Glass with a  $0.5\text{ }\mu\text{m}$  thick  $\text{Si}_3\text{N}_4$  film requires a  $0.4$  to  $0.7\text{ kg}$  load to crack. Thus, with an  $\text{SiO}_2$  film the crack initiation load increased by an order of magnitude. Greater adhesion or better protection against moisture-assisted crack growth in the  $\text{SiO}_2$ -glass system than in the  $\text{Si}_3\text{N}_4$ -glass system may be responsible for the larger threshold load.

As a first approximation to the change in fracture toughness, Lawn and Fuller [5] have derived a thin-film stress intensity factor for a penny-like crack system

$$K_f = 2\gamma\sigma_s d^{1/2} \quad (2)$$

where  $d$  is the film thickness,  $\gamma$  is a crack geometry term taken to be unity, and  $\sigma_s$  is the average surface stress of the film. Implicit in the derivation of Equation 2 is the assumption that the crack remains penny-like, which is not the case, as is shown in Fig. 3. Lawn and Fuller pointed out that this non penny-like shape will lead to some uncertainty in Equation 2.

The measured apparent fracture toughness,  $K$ , is given by the sum of the uncoated fracture toughness plus the thin film stress intensity factor

$$K = \chi P/c^{1/2} = K_c + K_f = K_c + 2\sigma_s d^{1/2} \quad (3)$$

Using the cantilever stress measurements, calculated  $K_f$  values for  $1.0\text{ }\mu\text{m}$  thick films are  $3.2$ ,  $2.0$  and  $0.4\text{ MPa m}^{1/2}$  for  $\text{Si}_3\text{N}_4$ ,  $\text{SiO}_2$  and  $\text{Al}_2\text{O}_3$ , respectively. Equation 3 predicts an increased fracture toughness which is independent of load and sampling depth. Equation 3 also predicts that the magnitude of the increased fracture toughness will be independent of the substrate since  $\sigma_s$  in the  $K_f$  term is independent of the substrate. The effect of tensile stress in the substrate may reduce the fracture toughness below that predicted by Equation 3 and this decrease may be dependent on load.

Fig. 4 shows the indent results for an uncoated glass and a  $\text{Si}_3\text{N}_4$ -coated glass sample. The measured fracture toughness of the coated glass is a strong function of load and therefore of sampled depth. In addition, the minimum load at which  $c = 2b$  is higher for the coated sample than for the uncoated sample. As was mentioned earlier, with coated glass and with some of the other substrates tested (except silicon), the

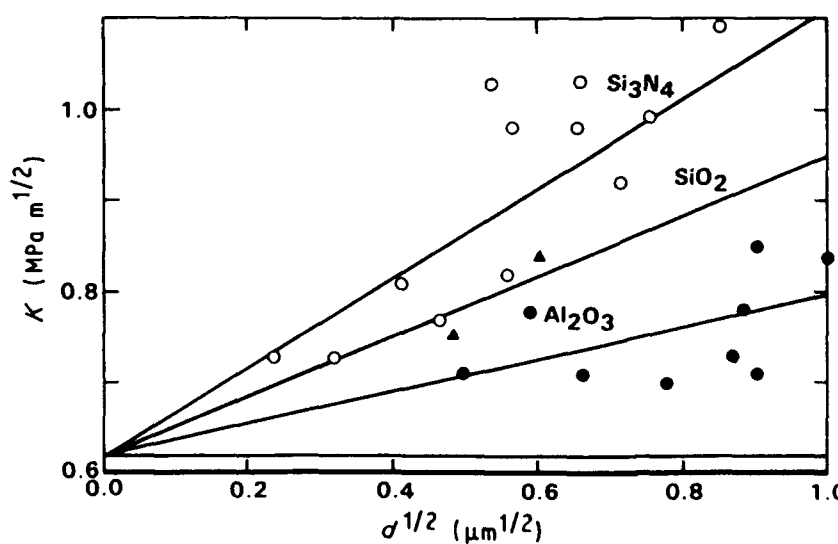


Figure 5 Surface fracture toughness of glass coated with (○)  $\text{Si}_3\text{N}_4$ , (▲)  $\text{SiO}_2$  and (●)  $\text{Al}_2\text{O}_3$  plotted as the square root of film thickness.

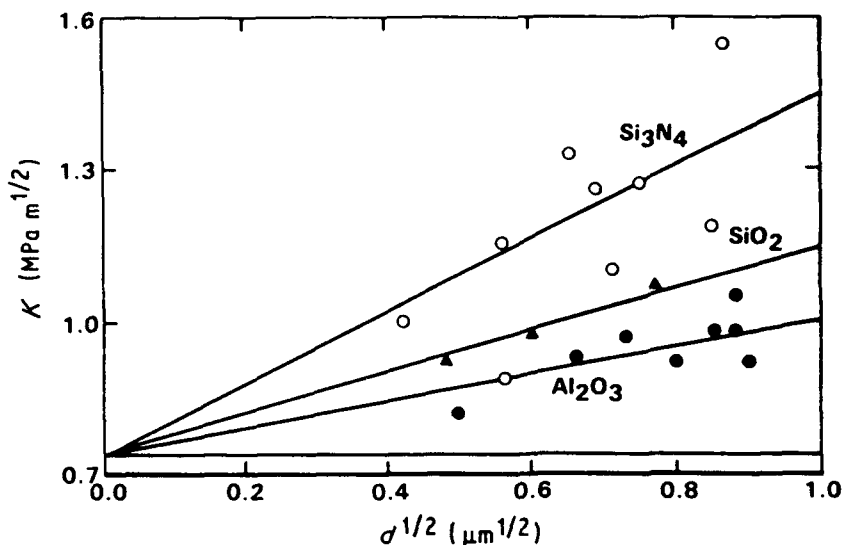


Figure 6 Fracture toughness of single crystal silicon coated with (○)  $\text{Si}_3\text{N}_4$ , (▲)  $\text{SiO}_2$  and (●)  $\text{Al}_2\text{O}_3$  plotted as the square root of the film thickness.

threshold load required to produce any radial cracks is increased considerably. This indicates that the coatings inhibit crack initiation.

The surface fracture toughness was taken as the value of  $K$  at a fixed crack length,  $c'$ , from a least squares fit of  $K$  against  $c'^2$ . Values of  $c'$  were chosen to be as small as possible for each substrate in order to maximize the measured change in fracture toughness. The values of  $c'$  for glass and silicon substrates were  $60 \mu\text{m}$  and  $16 \mu\text{m}$ , respectively. Figs 5 and 6 show these surface fracture toughness values as a function of the square-root of the film thickness.

Several other substrates were tested with  $\text{Si}_3\text{N}_4$  and/or  $\text{Al}_2\text{O}_3$  coatings. Only a few samples were coated in these cases so the data should be considered less reliable. Table I gives the uncoated fracture toughness, the crack length at which the surface toughness was determined, and the increased fracture toughness extrapolated to a  $1.0 \mu\text{m}$  thick film using Equation 2 (i.e., as  $d^{1/2}$ ). Also listed are the average grain sizes of the materials.

In most cases, the measured  $K_f$  is 2 to 6 times smaller than that predicted by Equation 3. This is most likely caused by the presence of the tensile stress

in the substrate or by the deviation from the penny-like shapes of the cracks. Those sampled substrates with the smaller cracks tended to give larger changes. When the silicon and glass data are plotted against  $c'^2$  and extrapolated to zero crack length, the changes in toughness are approximately twice as high as those listed in Table I.

Very high toughening was found for single crystal sapphire and no change was observed for fine grained  $\text{Si}_3\text{N}_4$  and  $\text{ZnS}$ . These anomalous results indicate that the toughening effect as measured by the Vickers indentation method may be dependent upon the mechanisms by which the surface stresses are accommodated in the substrate. The role of grain size and grain boundaries must be considered as must the levels of stresses in the bulk materials.

Complementary to this work, Burnett and Page [8] have made indent fracture measurements on ion-implanted sapphire. The implanted sapphire expands and produces a thin compressive layer near the surface. Using an implantation depth of  $0.2 \mu\text{m}$  for  $5.8 \times 10^{17} \text{ Y}^+ \text{ ions cm}^{-2}$  at  $300 \text{ keV}$  and a stress of  $5 \text{ GPa}$ , the calculated  $K_f$  is 10 times larger than that measured using a  $0.2 \text{ kg}$  load.

TABLE I Measured fracture toughness data from coated ceramic and single crystal substrates

Substrate	Grain size ( $\mu\text{m}$ )	$K_c$ ( $\text{MPa m}^{1/2}$ )	$c'$ ( $\mu\text{m}$ )	Increase in toughness $K_f$ ( $\text{MPa m}^{1/2}$ )		
				$\text{Si}_3\text{N}_4$	$\text{SiO}_2$	$\text{Al}_2\text{O}_3$
ZnS	4	0.8	100	< 0.1		< 0.1
$\text{Si}_3\text{N}_4$	0.5	4.1	100	< 0.1		
Glass	Amorphous	0.62	60	0.5	0.3	0.17
Glass	Amorphous	0.62	60	(ZnS Coated)*		0.2
$\text{As}_2\text{S}_3$	Amorphous	0.16	50			0.10
Silicon	Single crystal	0.74	16	0.7	0.4	0.3
Sapphire <sup>†</sup>	Single crystal	1.7	16	1.7		1.5
ALON	75	1.43	16			0.5
Germanium	> 100	0.5	15	0.6		0.6
Spinel	50	1.1	12			
Calculated <sup>‡</sup>				3.2	2.0	0.4

\* Zn<sup>2+</sup> film deposited by laser evaporation and independently determined to have an intrinsic stress of  $0.2 \text{ GPa}$ .

<sup>†</sup> (0001) surface

<sup>‡</sup> from Equation 3

#### 4. Conclusions

Thin compressive films deposited onto brittle substrates are found to increase the measured indentation fracture toughness of a variety of materials. For a given substrate, the change in fracture toughness with respect to film stress, film thickness, and indent load can be modelled semi-quantitatively. Anomalously large increases are found for single crystal sapphire while no change is measured with polycrystalline ZnS or Si<sub>3</sub>N<sub>4</sub>.

#### Acknowledgements

The authors acknowledge David Marshall for helpful discussions and Kristin Wilson for help with the fracture toughness measurements. This work was supported in part by the Office of Naval Research under Contract N00014-85-C-0140, and by the Rockwell International Science Center Youth Motivation Program.

#### References

1. G. R. ANSTIS, P. CHANTIKUL, B. R. LAWN and D. B. MARSHALL, *J. Amer. Ceram. Soc.* **64** (1981) 553.
2. C. J. MCHARGUE, M. B. LEWIS, B. R. APPLETON, H. NARAWMOTO, C. W. WHITE and J. M. WILLIAMS, Proceedings International Conference on Science of Hard Materials, Jackson, Wyoming, August 23-28, 1981 (Plenum, New York, 1983).
3. P. J. BURNETT and T. F. PAGE, *J. Mater. Sci.* **19** (1984) 3524.
4. T. HIOKI, A. ITOH, M. OHKUBO, S. NODA, H. DOI, J. KAWAMOTO and O. KAMAGAITO, *ibid.* **21** (1986) 1321.
5. B. R. LAWN and E. R. FULLER, *ibid.* **19** (1984) 4061.
6. P. CHAUDHARI, *IBM J. Res. Develop.* **13** (1969) 197.
7. M. LAUGIER, *J. Mater. Sci.* **15** (1980) 1147.
8. P. J. BURNETT and T. F. PAGE, *ibid.* **20** (1985) 4624.

*Received 29 February  
and accepted 4 May 1988*



## 2.3 Polycrystalline Diamond Materials Research

Co-Investigators: Alan B. Harker and Jeffrey F. DeNatale

From the inception of the ONR research program, it was evident that diamond was the most mechanically and thermally stable candidate window material. However, the growth of synthetic diamond by low-pressure processes was still in its first stage of development in 1985, and the controlling mechanisms were far from established. With the development of plasma processes for growing thin and thick polycrystalline diamond films, the emphasis of this program has shifted to address basic issues in rapidly moving technology.

### Microstructure

From the earliest synthetic diamond growth efforts, it was evident that the rough faceting in the polycrystalline microstructure was dominating both the mechanical and optical properties of the films. The super-micron columnar grained films exhibited intergranular fracture behavior and were highly scattering to wavelengths shorter than 20  $\mu\text{m}$ . Hence, efforts in this program were directed towards determining the mechanisms and parameters controlling the microstructure of the polycrystalline films and to the study of methodologies of reducing the optical scattering in the material by post growth reactive polishing.

The results of our work in describing the mechanisms involved in the growth and control of diamond film microstructure are published in a series of papers. These papers involve both the modification of the growth surface to control nucleation and the use of low growth temperatures to avoid large facet formation. The appended papers include:

**"Properties of Low Temperature Plasma CVD Diamond Films," A.B. Harker, Proceedings of Diamond Optics II, eds. A. Feldman and A. Holly, SPIE Proceedings Series Vol. 1146, 152-158 (1989).**



"Temperature and Reactive Etching Effects on the Microstructure of Micro-wave Plasma Deposited Diamond Films," A.B. Harker and J.F. DeNatale, Journal of Materials Research Vol. 5(4), 818-823 (1990).

"Microstructural Control of Diamond Thin Films By Micrographic Patterning," J.F. DeNatale, J.F. Flintoff, and A.B. Harker, Journal of Applied Physics 68(8), 4014-4019 (1990).

"Microstructure of Diamond Films as a Function of Deposition Conditions," A.B. Harker, J.F. DeNatale, and J.F. Flintoff, in press. Proceedings of Diamond Optics III, SPIE Meeting San Diego, CA, August, (1990).

"Adhesion Improvement in Diamond Films by Microlithographic Patterning," J.F. DeNatale, J.F. Flintoff, and A.B. Harker, submitted Journal of Material Science (Oct., 1990).

"Microstructure and Orientation Effects in Diamond Thin Films," J.F. DeNatale, A.B. Harker, and J.F. Flintoff, submitted Journal of Applied Physics (Nov., 1990).

#### Polishing

A consequence of the extreme hardness of diamond, is that the synthetic polycrystalline films are difficult to polish, particularly if the surface has curvature and cannot be placed flat on a standard high speed diamond powder in oil lapping wheel. In order to overcome this problem, high temperature surface reactions are being investigated to develop a methodology for improving the polycrystalline diamond surface finish. One method is the use of the heterogeneous reaction of diamond with iron at temperatures above 725°C. This chemical reaction carried out on a heated iron lapping wheel in a reduced pressure of hydrogen is capable of producing a high quality surface finish on diamond, but is again primarily limited to flat surfaces. Ion etching at high temperatures offers the best methodology for chemically polishing polycrystalline

diamond surfaces which have strong contours. Reactions with oxygen and argon are being investigated and future work is planned with other ionized gases.

The results of these efforts are described in:

"The Polishing of Polycrystalline Diamond Films," A.B. Harker, J.F. Flintoff, and J.F. DeNatale, to be published in Proceedings of Diamond Optics III, SPIE Symposium, San Diego, CA, (August, 1990).

# Properties of low temperature plasma CVD diamond films

Alan B. Harker

Rockwell International Science Center  
Thousand Oaks, CA 91360

## ABSTRACT

In the microwave plasma deposition (PECVD) of diamond from methane, the variables available for controlling the microstructure of the resulting films are the plasma composition and density, the substrate surface properties, and the temperature. It has been demonstrated that the competition between nucleation site formation and the rate of reactive plasma etching is the critical feature in the development of the film microstructure. Through reducing the deposition temperature and enhancing the etching rates of sp<sub>2</sub> carbon, fine grained optical quality diamond films have been produced.

## INTRODUCTION

A critical limitation in the exploitation of synthetic diamond films is the need to control their microstructure. Wide band-gap semiconductor applications require hetero-epitaxial films while highly smooth, fine grained polycrystalline films are needed for tribological and optical applications. In this work a parametric study has been carried out to determine the process variables controlling the microstructure and crystallinity of sp<sub>3</sub> bonded diamond films produced from a microwave-induced plasma composed of methane, hydrogen, and oxygen. The primary analytical tools used in the study were infrared spectroscopy, electron microscopy, and Raman scattering spectroscopy.

In the formation of diamond films the initial process involves the formation of chemical bonds between the substrate and carbon-carbon and carbon-hydrogen bonded molecules. These nucleation centers then act as sites for the bonding of additional adatoms and clusters. This typical film growth process is limited, however, by the reactive etching of the growing film by the excited hydrogen, oxygen, and radical species such as OH present in the plasma environment. The ability to produce pure crystalline diamond relies on the process conditions being established in which the sp<sub>2</sub> bonded, graphitic carbon, and carbon-hydrogen bonds are etched away at a rate sufficiently fast that only the more strongly bonded metastable sp<sub>3</sub> diamond carbon remains in the growing film. Hence, the process of attempting to control the microstructure in the diamond films must be considered as one of balancing the rates of the nucleation, growth, and etching processes occurring in the system.

## EXPERIMENTAL

The deposition experiments were carried out in a turbomolecular pumped stainless steel vacuum chamber equipped with an Applied Science and Technology 1000 W magnetron plasma source. The chamber had a baked base pressure of 10<sup>-8</sup> torr. Experimental conditions ranged from pressures of 12 to 50 torr with substrate temperatures of 450 to 1150°C as measured by infrared pyrometry. In all cases the pyrometric measurements were made on Si wafers with an assumed emission of 0.96. Gas mixtures were typically hydrogen containing 1 volume percent methane and 0.25 volume percent oxygen. Substrates used in the experiments were (100) oriented silicon wafers, fused quartz, random oriented sapphire, (100) germanium, and (100) natural diamond.

Microstructural characterization of the films was carried out by electron microscopy using a Phillips 400 and CM-30 for transmission electron microscopy (TEM) and selected area electron diffraction (SAD) analysis. Scanning electron microscopy (SEM) and selected area electron channeling were also used. Spectroscopic analysis included infrared transmission and reflection measurements with a scanning dual beam spectrophotometer, integrating sphere light scattering measurements at 3.39  $\mu\text{m}$ , and micro-Raman scattering. The micro-Raman scattering measurements were made with a nominal 5  $\mu\text{m}$  spot size, which could be defocused to obtain broader area analysis.

### RESULTS AND DISCUSSION

As previously reported by other investigators,<sup>1, 2, 3</sup> a plasma discharge of 1%  $\text{CH}_4$  in  $\text{H}_2$  at low pressures and temperatures between 800 and 1200°C produces the nucleation and growth of diamond and diamond-graphite films. These films are typically polycrystalline, highly faceted, and have individual grains with linear dimensions ranging from 3 to 10  $\mu\text{m}$  as shown in the scanning electron micrograph in Figure 1. The film microstructure in Figure 1 is from a region of film growing directly below the visible discharge in the chamber at 1040°C. The grains are strongly faceted and show the dominance of individual grain growth over nucleation. The major limitation in the out-of-plane growth of the individual crystallites is the high density of twinning and stress induced defects. These defects cause continual reorientation of the crystalline faces during deposition, inhibiting grain growth and reducing any orientation of the film to the substrate. The size of the individual grains is determined in part by the density of the initial nucleation centers and in part by the development of new growth directions in the individual crystallites.



Fig. 1. Scanning electron micrograph of a highly faceted diamond film deposited at 1040°C.

The density of nucleation sites is relatively low due to the high mobility of the plasma generated species arriving at the substrate, and the high temperature of the substrate itself. Lattice matching and several surface pretreatments, such as scratching with diamond grit, can enhance the density of nucleation centers, but such high temperature films typically have super-micron grain size and rough faceted surfaces which cause light scattering.

### Oriented Grain Growth

For optical and electronic applications epitaxial film growth or at least grain-oriented polycrystalline films with smooth surfaces are desired. In order to achieve such growth, both the lattice match between the diamond film and substrate and the etching versus deposition rate must be maximized. High lattice match optimizes the potential nucleation site formation with direct relationship to the substrate lattice, while increasing the etching process favors the removal of less stable defect based growth sites. Further enhancement in orientation comes from reducing the deposition temperature to limit stacking faults, twinning, and other stress related defects.

By maintaining all conditions the same as described above, but dropping the deposition temperature to nominally 450°C, a significant reduction in the degree of stress related defects can be achieved as shown by TEM analysis. The result of the lower density of defects in the nucleating grains is that existing grains have the opportunity to grow while maintaining their original orientation to the substrate.

The effect of reducing the stress in the growing film, while enhancing the formation of nucleation centers at lower temperatures is the formation of finer grained, oriented films on (100) Si substrates and the formation of stress free homo-epitaxial films on (100) natural diamond substrates. Figure 2 shows SEM micrographs of two films formed on (100) silicon substrates at a nominal substrate temperature of 450°C at different distances from the plasma ball. The finer grained film, formed 1.5 cm from the plasma is randomly oriented. The slightly coarser film, formed directly beneath the plasma ball, is oriented with 220 plane parallel to the 100 plane of the substrate. The orientation of the textured film can be seen by the significant enhancement of the 220 Bragg reflection in Figure 3.

When a natural (100) oriented diamond substrate was coated under the same conditions as used for the oriented film on silicon (30 torr, 1% CH<sub>4</sub> in H<sub>2</sub>, 0.25% O<sub>2</sub>, 450°C) a homo-epitaxial film was formed. The epitaxial nature of the film was confirmed by X-ray diffraction and electron channeling in the SEM. The channeling pattern in Figure 4 which shows the diamond cubic symmetry propagated throughout the film, would be totally absent if any significant stress or lack of orientation was present in upper 100 nm of the film. Raman and IR analysis of the films shows them to be true diamond with little sp<sub>2</sub> bonding contribution (Figure 5). Figure 6 shows the calculated (assuming a refractive index of 2.4) and observed transmission from a 1.9  $\mu$ m thick diamond film on silicon formed at 450°C. The good agreement shows the lack of scattering and adsorption in the 6 to 50  $\mu$ m spectral region of the IR.

### CONCLUSIONS

The microstructure and orientation in diamond films formed on silicon substrates from a microwave-induced plasma of CH<sub>4</sub> in H<sub>2</sub> can be highly modified by the addition of reactive etchants such as oxygen, altering the deposition temperature, and altering the distance of the substrate from the plasma center. Higher temperatures favor low nucleation rates, enhanced grain growth and high defect levels. Lower temperatures favor nucleation, lower stress, and sustained orientation to the substrate. The presence of oxygen in the plasma serves to enhance faceted growth through the preferential etching of non sp<sub>3</sub> bonded species forming on the film

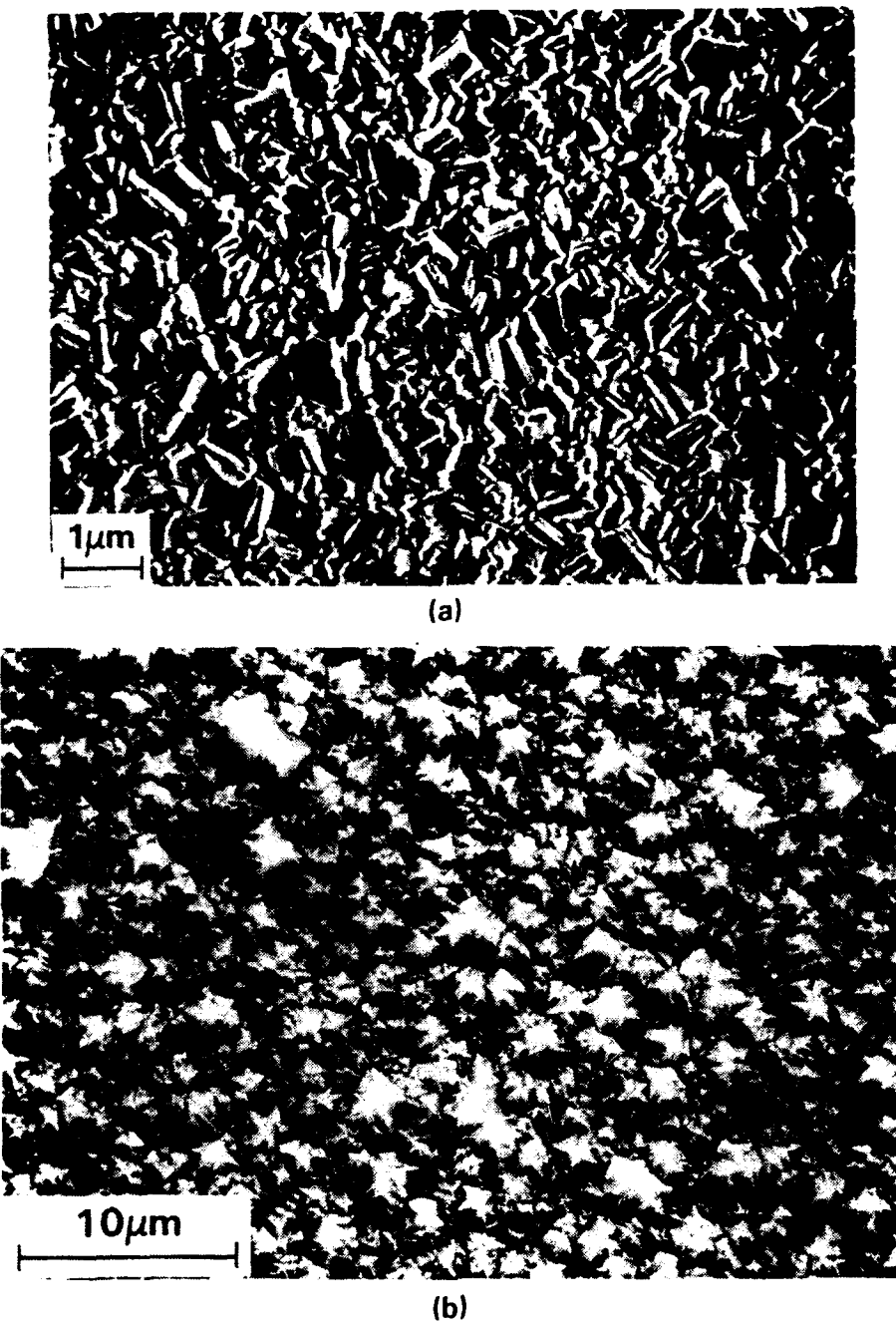


Fig. 2. Scanning electron micrographs of (a) a fine grain randomly oriented diamond film on (100) silicon and (b) an oriented diamond film on (100) silicon, both deposited at a nominal surface temperature of 450°C.

surface. At substrate temperatures below 500°C fine grained oriented diamond films have been produced upon (100) silicon and full epitaxy has been achieved on natural (100) diamond.

#### ACKNOWLEDGEMENT

Portions of this work were sponsored by the United States Office of Naval Research.

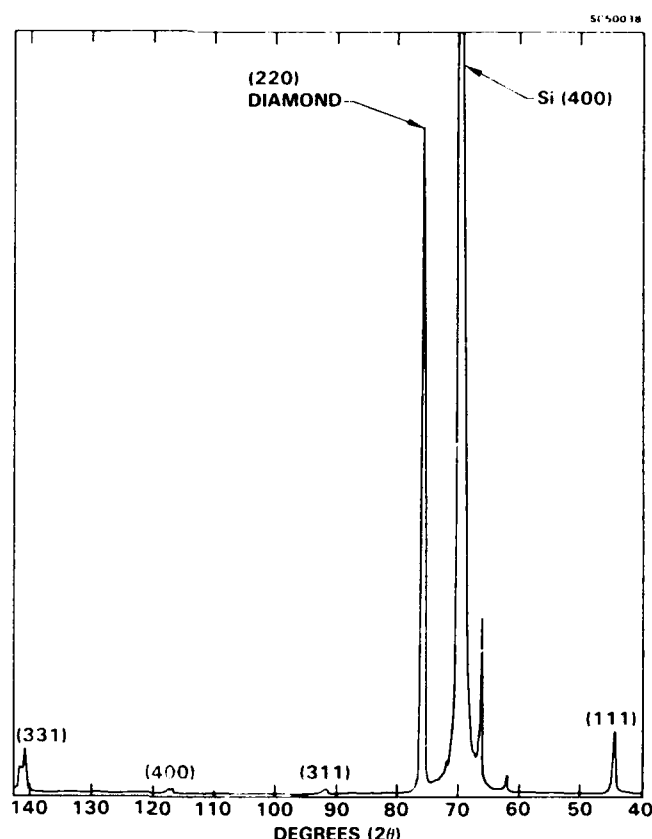


Fig. 3. Scanning x-ray diffraction pattern of a (220) oriented diamond film formed on (100) silicon.

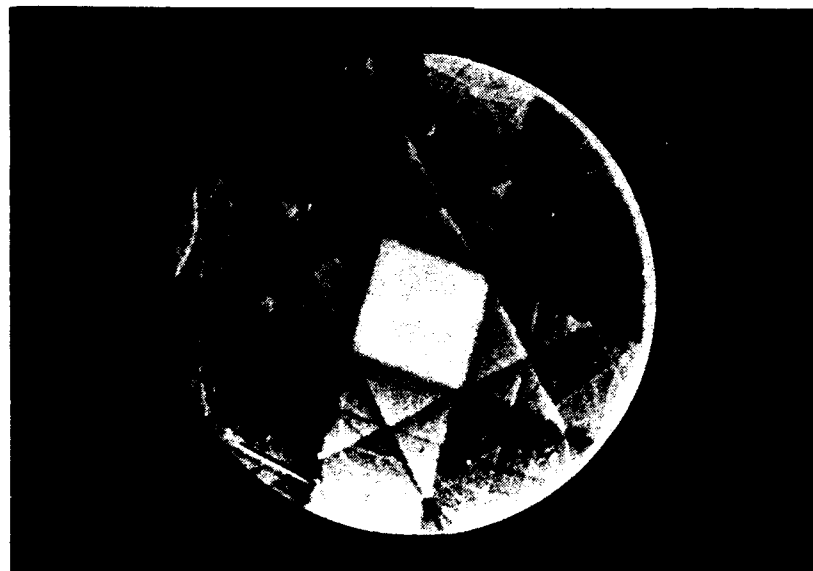


Fig. 4. An electron channeling pattern produced from a  $2\ \mu\text{m}$  thick homo-epitaxial diamond film formed on a type 2A (100) natural diamond.

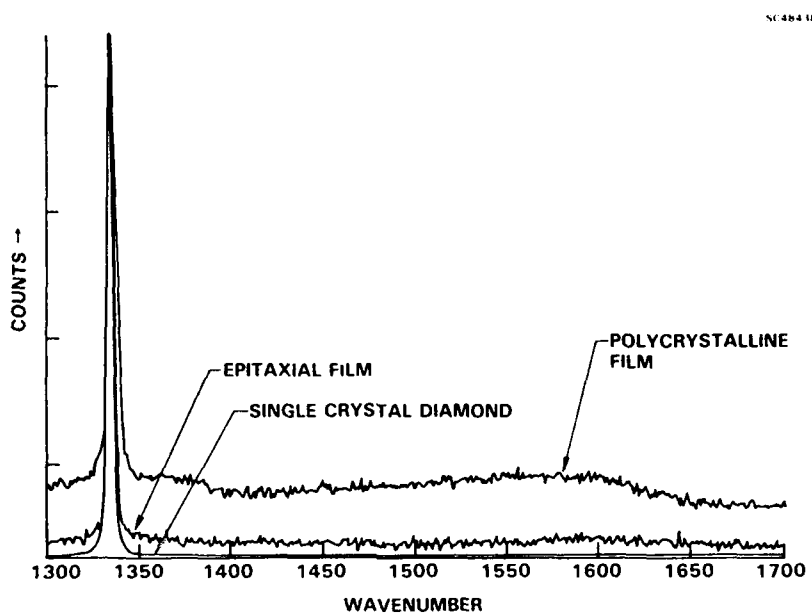


Fig. 5. Micro-Raman spectra taken from a homo-epitaxial diamond film and a polycrystalline random diamond film formed at 450°C.

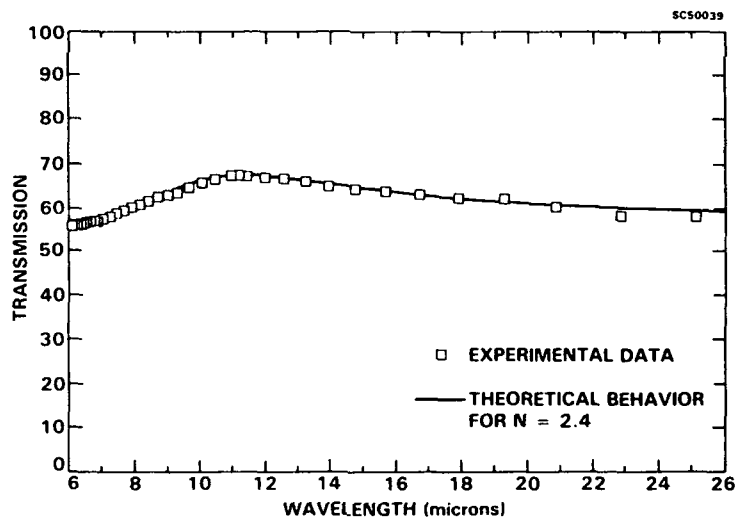


Fig. 6. The calculated and observed (squares) transmission of a diamond film on silicon. The film is 1.9  $\mu\text{m}$  thick with an assumed optical index of refraction of 2.4.

## REFERENCES

1. M. Kamo, Y. Saito, S. Matsumoto, and N. Setaka, "Diamond Synthesis for Gas Phase in Microwave Plasma," *J. Crystal Growth*, vol. 62, pp. 642-644 (1983).
2. A.R. Badzian, T. Badzian, R. Roy, R. Messier, and K.E. Spear, "Crystallization of Diamond Crystals and Films By Microwave Assisted CVD (Part II)," *Mat. Res. Bull.* 23(4), pp. 531-548 (1988).
3. Y. Saito, K. Sato, K. Gomi, and H. Miyadera, "Synthesis and Application of Diamond or Diamond-Like Films from CO-H<sub>2</sub> Plasma," *Proc. Symp. Plasma Chem.*, Vol. 1, pp. 303-308 (1988).

## Temperature and reactive etching effects on the microstructure of microwave plasma deposited diamond films

Alan B. Harker and Jeffery F. DeNatale

*Rockwell International Science Center, Thousand Oaks, California 91362*

(Received 22 September 1989; accepted 21 December 1989)

In the microwave induced plasma deposition of diamond from methane-hydrogen-oxygen mixtures, the variables available for controlling the microstructure of the resulting films are the plasma composition and density, the substrate surface properties, and the temperature. It has been demonstrated that the competition between nucleation site formation and the rate of reactive plasma etching is the critical feature in the development of the film microstructure on silicon substrates. On diamond substrates, the favorable lattice match dominates and homo-epitaxial films are formed over a wide temperature range. Raman scattering studies also demonstrate that the reactive etching of the diamond surface by oxygen-containing species is critical to the removal of non-diamond carbon species over the temperature range 450–1050 °C.

### I. INTRODUCTION

A critical limitation in the exploitation of synthetic diamond films is the need to control their microstructure. Wide band-gap semiconductor applications require single crystal films while highly smooth, polycrystalline films are needed for tribological and optical applications. In this work a parametric study has been carried out to determine the process variables controlling the microstructure and crystallinity of sp<sup>3</sup> bonded diamond films produced from a microwave induced discharge of mixtures of methane, hydrogen, and oxygen. The primary analytical tools used in the study were infrared spectroscopy, electron microscopy, and Raman scattering spectroscopy.

In the formation of diamond films the initial process involves the formation of chemical bonds between the substrate and crystallized clusters of carbon-carbon and carbon-hydrogen bonded molecules. These nucleation centers then act as sites for the bonding of additional adatoms and clusters. This typical film growth process is limited, however, by the reactive etching of the growing film by the excited species present in the plasma environment. The ability to produce pure crystalline diamond relies on the process conditions being established in which the sp<sup>2</sup> bonded, graphitic carbon, and carbon-hydrogen bonds are etched away at a rate sufficiently fast that only sp<sup>3</sup> diamond bonded carbon remains in the growing film. Hence, the process of attempting to control the microstructure in the diamond films must be considered as one of balancing the rates of the nucleation, growth, and etching processes occurring in the system.

### II. EXPERIMENTAL

The deposition experiments were carried out in a turbomolecular pumped stainless steel vacuum chamber

equipped with an Applied Science and Technology 1500 W magnetron plasma source. The chamber had a baked base pressure of 10<sup>-8</sup> Torr. Experimental conditions ranged from pressures of 3 to 50 Torr with substrate temperatures of 450 to 1150 °C as measured by infrared pyrometry. In all cases the pyrometric measurements were made on Si wafers with an assumed emission of 0.96. Gas mixtures were typically hydrogen containing 0.3 to 1 vol. % methane and up to 1 vol. % oxygen. Substrates used in the experiments were (100) oriented silicon wafers and (100) type 2A natural diamond.

Microstructural characterization of the films was carried out by electron microscopy using a Phillips CM-30 for transmission electron microscopy (TEM) and selected area electron diffraction (SAD) analysis. Scanning electron microscopy (SEM) and selected area electron channeling were also used. Spectroscopic analysis included infrared transmission and reflection measurements with a scanning dual beam spectrophotometer, and micro-Raman scattering. The micro-Raman scattering measurements were made with a nominal 5 micron spot size, which could be defocused to obtain broader area analysis.

### III. RESULTS AND DISCUSSION

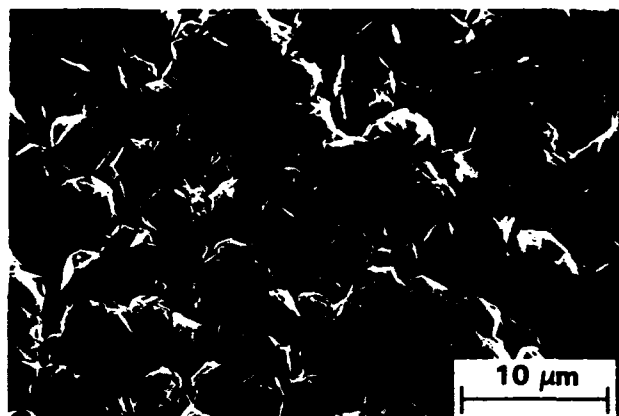
As previously reported by other investigators,<sup>1–4</sup> a microwave induced plasma of CH<sub>4</sub> and O<sub>2</sub> in H<sub>2</sub> at low pressures and temperatures between 800 and 1200 °C produces the nucleation and growth of diamond and diamond-graphite films on a range of substrate materials. These films are typically polycrystalline, highly faceted, and have individual grains with linear dimensions ranging from 3 to 50 micrometers. The large grain size is indicative of a low density of nucleation sites in the films formed at high temperatures. This can be caused by poor lattice match to the substrate and by the

high mobility of the plasma generated species arriving at the substrate. Lattice matching and several surface pretreatments, such as scratching with diamond grit, can enhance the density of nucleation centers. In the microwave induced plasma films produced in this work at temperatures of 850 to 1050 °C with low nucleation densities, nearly isotropic growth in the developing grains and polycrystalline particles was observed. As shown in the SEM micrographs in Fig. 1, the developing diamond particles on silicon produce regular, near spherical overall shapes induced by high levels of crystallographic twinning and defects. The individual crystalline particles show uniform growth rates and ultimately form a continuous film as proximity leads to particle overlap.

When surface pretreatments such as diamond grit scratching are applied to the substrate surface, the density of nucleation sites is typically increased. In these cases a continuous film forms when the growing particles impinge upon one another. The degree of faceting in the individual diamond particles in the continuous films has been found to be a function of the growth versus reactive etching rates in the system. In Fig. 2, the SEM micrographs give a comparison between the morphology of continuous films produced at 1 vol. % CH<sub>4</sub>, with and without the presence of 0.25 vol. % O<sub>2</sub>. In the absence of oxygen the individual diamond particles have very high defect densities and are nearly spherical. With oxygen present the reactive etching leads to strongly faceted individual grains. In these films

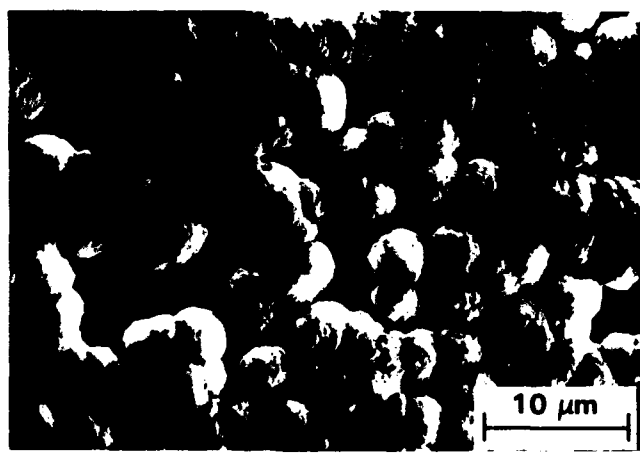


(a)

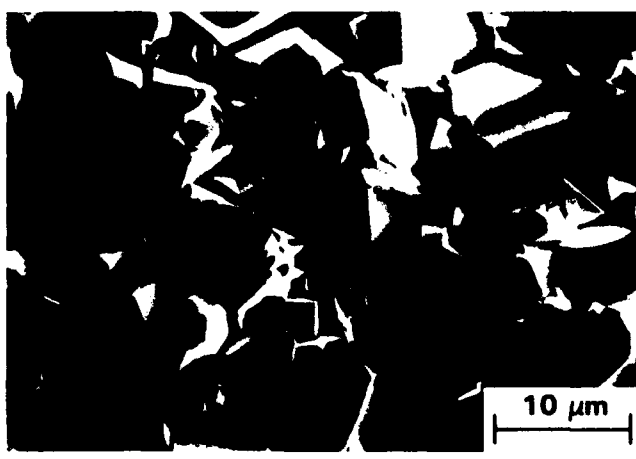


(b)

FIG. 1. (a) Scanning electron micrograph of discrete, faceted diamond particles forming on (100) Si at 1040 °C which show near isotropic growth. (b) Scanning electron micrograph of a continuous diamond film forming from the overlap of discrete particles.



(a)



(b)

FIG. 2. (a) SEM micrograph of the microstructure of diamond film formed at 1040 °C on Si with no O<sub>2</sub>. (b) SEM micrograph of a highly faceted diamond film formed at 1040 °C with 0.25% O<sub>2</sub>.

[Fig. 2(b)] the individual crystallite growth is limited by proximity effects and the formation of new growth directions at twin and defect sites on the crystalline facets.

The high density of defects plays a dominant role in determining the morphology of the diamond films at the higher temperatures. These defects appear very early in the film deposition process and may be stress related. The major crystallographic defect observed in the films is a multiple twinning on the {111} planes in <211> directions. This can lead to extremely high defect densities in the grains, as illustrated by the TEM micrograph, Fig. 3. Successive generation of this twin structure around the <011> axes can generate the five-fold defect structure, shown in Fig. 4, which is commonly reported to be present in the high-temperature diamond films.<sup>5</sup> This defect forms early in the individual grain development, as can be seen in the extremely fine-scale crystallites in the TEM micrograph. This defect was found to be present in a large fraction of the grains in the high-temperature formed films. Once formed, the fivefold defect structure is able to propagate and determine the shape of some of the crystalline grains even as they develop to super-micron size, as previously shown in Fig. 1.

Interestingly, while the polycrystalline films show a high level of defects, single crystal homo-epitaxial films can be formed under the same conditions. Figure 5

shows an electron channeling pattern of a 2-micron thick epitaxial diamond film produced on a (100) type 2A diamond surface. The pattern shows the cubic symmetry of the substrate to be fully propagated through the single crystal film. The film thickness was determined by masking an edge of the substrate with a second diamond. The channeling pattern would not be produced from the diamond film surface if there were any appreciable stress or loss of long-range order in the top 100 nm. Infrared transmission measurements showed no increase in absorption in the 250-micron thick diamond from the presence of the film.

While the homo-epitaxial films formed at 800–1100 °C are suitable for electronic studies, the high defect densities and very rough surfaces of the polycrystalline films formed in this temperature range do not have properties suitable for electronic, optical, or tribological applications. In order to obtain smoother film surfaces, finer grained polycrystalline films are required. To achieve this, both the lattice match between the diamond film and substrate and the etching versus deposition rate must be maximized. High lattice match optimizes the potential nucleation site formation, while increasing the rate of the etching processes favors the removal of less stable defect based growth sites. Further enhancement comes from reducing the deposition temperature to limit stacking faults, twinning, and other stress related defects.

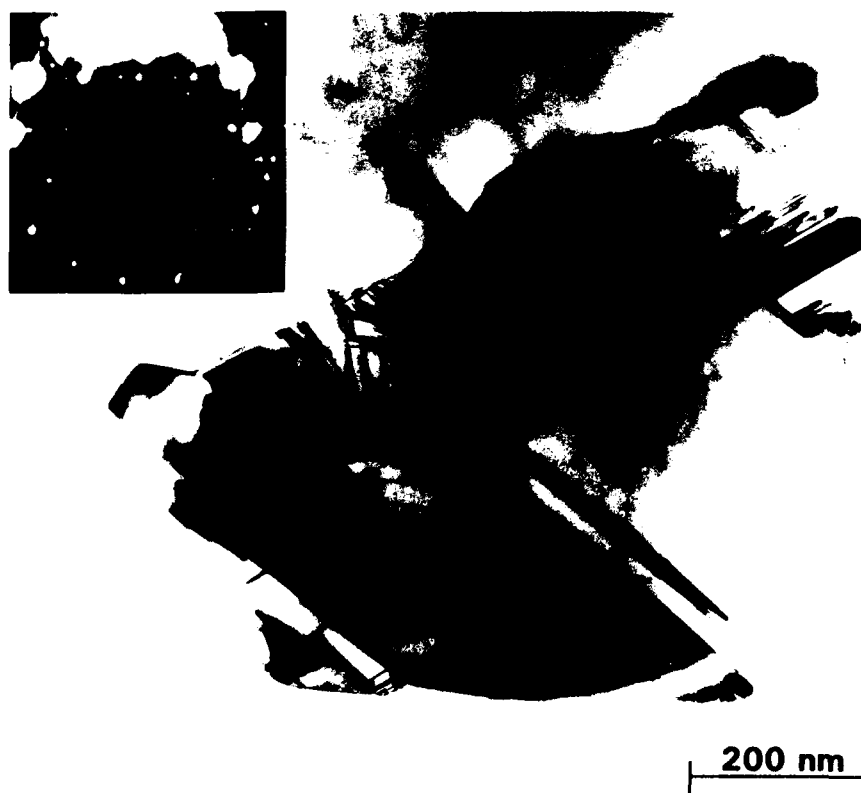


FIG. 3. Transmission electron micrograph and selected area electron diffraction pattern illustrating the high defect densities from multiple twinning in high temperature formed diamond films.

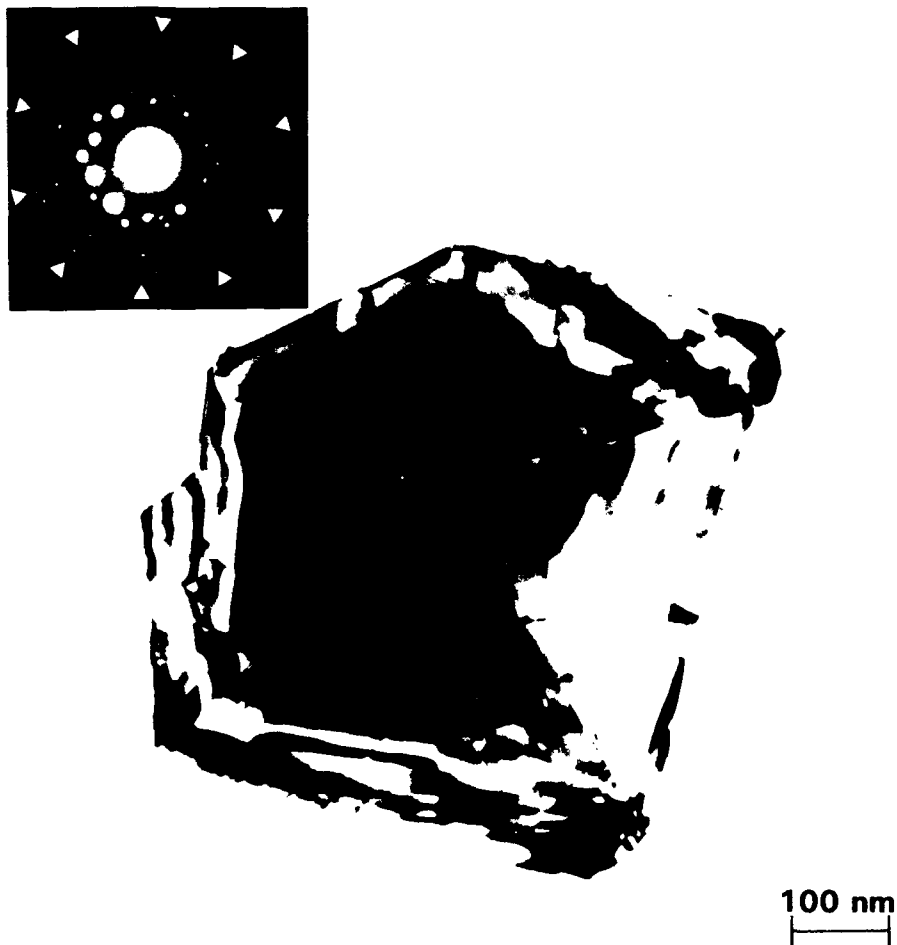


FIG. 4. Transmission electron micrograph and electron diffraction pattern of the fivefold twin defect structure commonly occurring in high temperature formed diamond films.

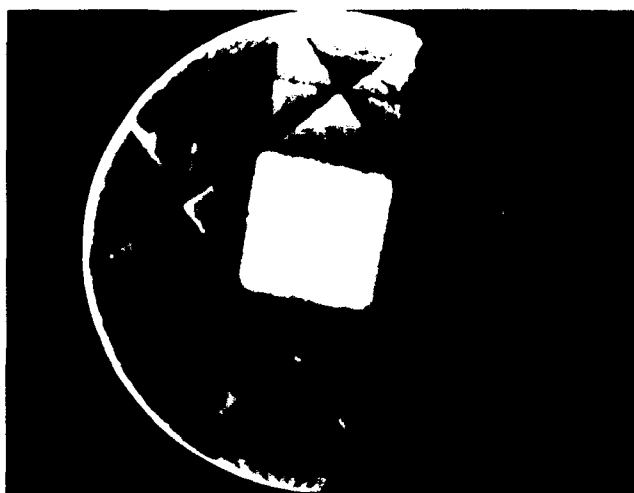
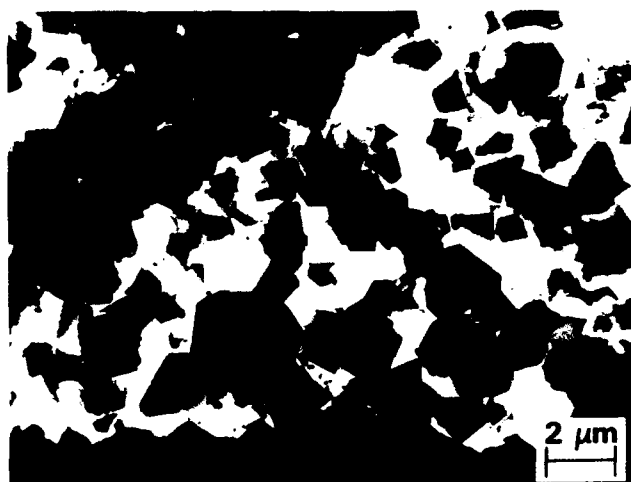


FIG. 5. A scanning electron channeling pattern formed from a homo-epitaxial diamond film grown on (100) type 2A diamond at 1040 °C.

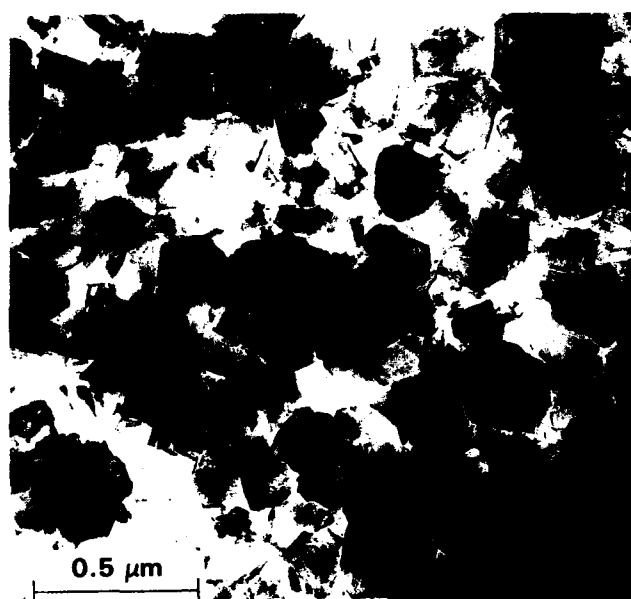
The role of temperature in determining the nucleation, defect structure, and growth morphology of the diamond films can be seen by TEM. Figure 6(a) shows

a TEM micrograph of a diamond film deposited at 1040 °C on Si. The bulk of the grains contains defects of the type described earlier, with the film microstructure defined by the impingement of large grains originating from highly separated nucleation centers. The morphology of these films is also characterized by the extensive out-of-plane growth shown in Figs. 1–3. By maintaining all conditions the same, but dropping the deposition temperature to 450 °C, a significant improvement in the film morphology can be achieved [Fig. 6(b)]. The lower temperature deposited films exhibit planar twinning similar to the higher temperature films, but little of the fivefold twin structure is present. The finer grain size and more uniform nucleation in these lower temperature films leads to higher film densities and reduced surface irregularities from out-of-plane growth.

The major effect of lowering the diamond deposition temperature is the formation of finer grained polycrystalline films and oriented films on (100) Si substrates. Figure 7 shows SEM micrographs of two films formed on (100) Si at a nominal substrate temperature of 450 °C at different distances from the



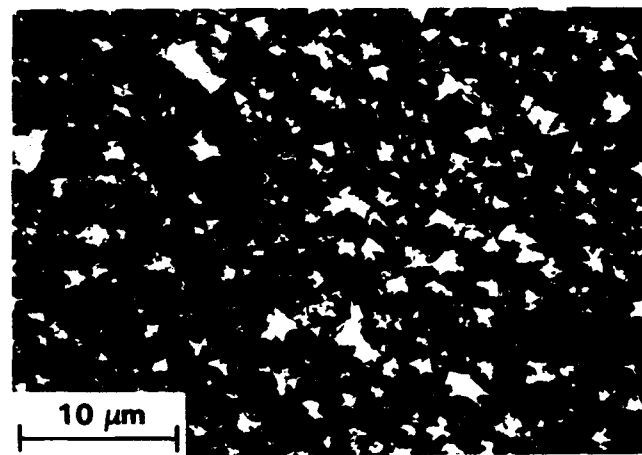
(a)



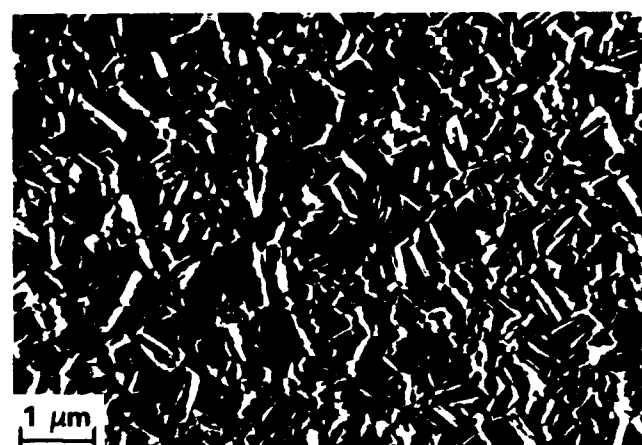
(b)

FIG. 6. (a) Transmission electron micrograph showing the coarse microstructure and high defect densities of a diamond film grown at 1040 °C on Si. (b) Transmission electron micrograph of a fine-grained diamond film grown at 450 °C on Si.

plasma ball. The finer grained film, formed 1.5 cm from the plasma, is randomly oriented. The slightly coarser film, formed directly beneath the plasma ball, is oriented with (220) plane parallel to the (100) plane of the substrate. The orientation of the textured film can be seen by the significant enhancement of the (220) Bragg reflection in Fig. 8. When a natural (100) oriented diamond substrate was coated under the same conditions as used for the oriented film on silicon (30 Torr, 1%  $\text{CH}_4$  and 0.25%  $\text{O}_2$  in  $\text{H}_2$ , 450 °C), a homo-epitaxial film was formed.



(a)



(b)

FIG. 7. (a) Scanning electron micrograph of a (220) oriented diamond film grown at 450 °C on (100) Si. (b) A random oriented fine-grain diamond film grown on (100) Si at 450 °C.

The role of oxygen at these lower temperatures seems primarily to be the etching away of  $\text{sp}^2$  bonded carbon. Raman spectra of films grown at the lower temperatures without oxygen showed the broad scattering line at  $1550 \text{ cm}^{-1}$  characteristic of  $\text{sp}^2$  bonded carbon.<sup>6</sup> Conversely, with oxygen present, the spectra were dominated by the diamond Raman line observed at  $1334.5 \text{ cm}^{-1}$ . The Raman scattering spectra in Fig. 9 are from the (100) face of a natural diamond, a homo-epitaxial film, and a fine grained (220) oriented diamond film on (100) Si formed at 450 °C. The polycrystalline film has a slightly broader  $\text{sp}^3$  scattering peak than the natural diamond and epitaxial film; however, it shows only a minor contribution of  $\text{sp}^2$  bonded carbon.

#### IV. CONCLUSIONS

The microstructure and orientation in diamond films formed on Si substrates by microwave induced

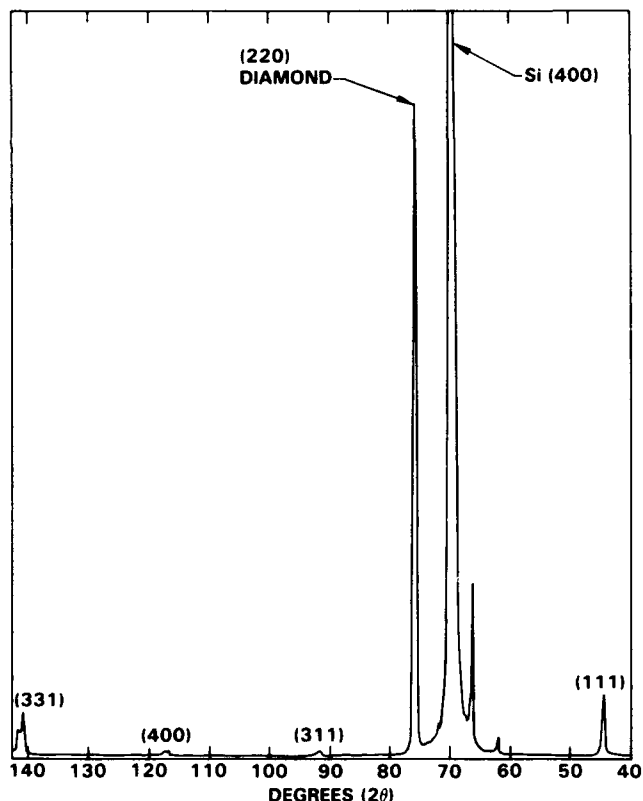


FIG. 8. X-ray diffraction pattern of the oriented diamond film on (100) Si shown in the SEM micrograph in Fig. 7(a).

plasma discharge of  $\text{CH}_4$  in  $\text{H}_2$  can be highly modified by the use of reactive etchants such as  $\text{O}_2$ , altering the deposition temperature, and altering the distance of the substrate from the plasma center. Higher temperatures favor low nucleation rates, enhanced grain growth, and high defect levels. Lower temperatures favor nucleation and sustained orientation to the substrate. The presence of  $\text{O}_2$  in the plasma serves to enhance faceted growth through the preferential etching of non  $\text{sp}^3$  bonded species forming on the film surface. At substrate temperatures below 500 °C fine-grained oriented diamond films have been produced upon (100) silicon and full epitaxy has been achieved on natural (100) diamond.

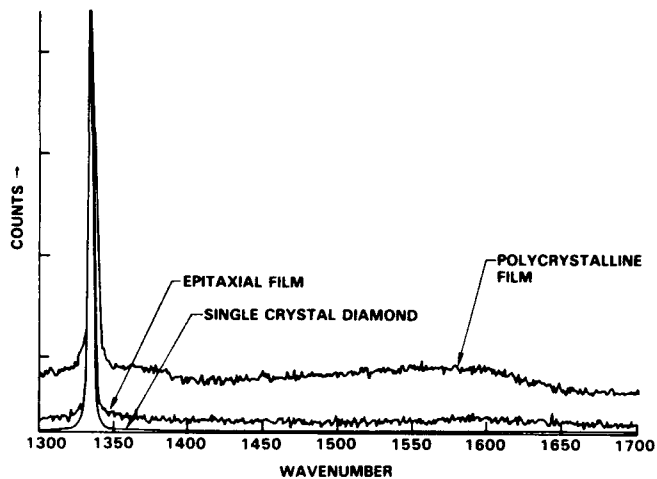


FIG. 9. Raman scattering spectra of a homo-epitaxial diamond film and a polycrystalline diamond film grown at 450 °C compared to that of 2A diamond.

#### ACKNOWLEDGMENTS

This research was sponsored in part by the Office of Naval Research. The authors also acknowledge the contribution of Mr. John F. Flintoff who performed the scanning electron microscopy for this work.

#### REFERENCES

- 1M. Kamo, Y. Saito, S. Matsumoto, and N. Setaka, *J. Cryst. Growth* **62**, 642–644 (1983).
- 2A. R. Badzian, T. Badzian, R. Roy, R. Messier, and K. E. Spear, *Mater. Res. Bull.* **23** (4), 531–548 (1988).
- 3Y. Saito, K. Sato, K. Gomi, and H. Miyadera, *Proc. Symp. Plasma Chem.* **1**, 303–308 (1988).
- 4A. B. Harker, "Proceedings of Diamond Optics II," SPIE 33rd Annual Int. Symp. on Optical and Optoelectronic Applied Science & Engineering, San Diego, CA (Aug. 6–11, 1989).
- 5J. Narayan, A. R. Srivatsa, M. Peters, S. Yokota, and K. V. Ravi, *Appl. Phys. Lett.* **53** (19), 1823 (1988).
- 6D. S. Knight and W. B. White, *Raman Scattering, Luminescence, and Spectroscopic Instrumentation in Technology*, SPIE **1055**, 144–151 (1989).

# Microstructural control of diamond thin films by microlithographic patterning

J. F. DeNatale, J. F. Flintoff, and A. B. Harker  
Rockwell International Science Center, Thousand Oaks, California 91360

(Received 7 May 1990; accepted for publication 22 June 1990)

Microlithographic patterning has been used to elucidate the mechanisms controlling diamond film nucleation and grain growth. The approach is capable of establishing a degree of control over diamond nucleation on the substrate, which can be used to improve film uniformity and enhance fine grained microstructure. The observed microstructures in the patterned films are consistent with an intrinsic growth mechanism based upon defect-initiated renucleation.

## I. INTRODUCTION

The application of current synthetic diamond films as optical and friction-reduction coatings is greatly limited by the surface roughness of the as-deposited polycrystalline material. The high degree of defects in the faceted crystalline films as well as the supermicron grain size characteristic of most plasma and filament chemical vapor deposition (CVD) diamond films produces a surface roughness on the order of 500–5000 nm.<sup>1–3</sup> Such roughness causes a high degree of optical scattering extending from the visible through the long wavelength infrared,<sup>4</sup> and produces a surface which is too abrasive for direct application as a bearing surface for wear reduction.

Methods currently exist and are being further developed for the post-deposition polishing of the polycrystalline diamond surfaces,<sup>5,6</sup> but these processes are made more difficult to implement by the surface roughness in the films due to the large, irregular grain sizes. Hence, it is highly desirable for specific applications to not only limit grain growth in the diamond films, but also to produce a dense, uniform microstructure amenable to post-deposition surface polishing.

Deposition of the polycrystalline diamond thin films is inherently different from that of conventional optical thin film materials. For the diamond films, the film morphology is controlled by the nucleation and growth of the individual crystalline diamond grains on the substrate surface. To achieve microstructures consistent with optical applications, one must generate uniform, fine-grained nucleation geometries and restrict out-of-plane growth of large diamond particulates. Microlithographic patterning is being investigated in this laboratory as a means of establishing such a uniform distribution of nucleation centers on the film and a degree of control over the film microstructure. Both Kirkpatrick *et al.*<sup>7</sup> and Ma *et al.*<sup>8,9</sup> have demonstrated that selective nucleation can be achieved using micropatterning of the substrate before deposition. Both groups achieved point nucleation of large ( $> 10 \mu\text{m}$ ) diamond particulates, whose growth was primarily limited by physical impingement. This paper demonstrates microlithographic processing techniques that provide both the fine grain size and spatial uniformity desired for the optical and

wear-reduction applications of diamond films. A general mechanism for the controlled grain growth is also discussed.

## II. EXPERIMENT

Single-crystal silicon wafers were patterned by standard photolithography techniques prior to growth using a proprietary high-temperature resist. The pattern used for the initial experiments was a square grid of 1- $\mu\text{m}$ -wide lines exposing the bare silicon substrate, separated by 10  $\mu\text{m}$  of resist. Investigations of the linewidth-dependence used a pattern of parallel lines ranging between 0.5 and 1.5  $\mu\text{m}$  wide. The films were grown using microwave-plasma-assisted CVD (PACVD) with a source gas composition of 1%  $\text{CH}_4$ , 0.5%  $\text{O}_2$ , and the balance  $\text{H}_2$ . Substrate growth temperatures of 650 °C were used as determined by optical pyrometry. The substrates were prepared both with and without the use of a diamond polish pretreatment to establish the relative roles of topology and “seeding” on nucleation behavior. Growths were first conducted for a short time to establish diamond formation in the grid lines. The substrates were then removed, the resist was stripped, and the substrates were returned to the chamber for additional film growth.

## III. RESULTS

Preliminary experiments were conducted to determine the appropriate length of time for the initial growth on the patterned substrate. The development of the microstructure with increasing time is illustrated in the sequence of scanning electron micrographs in Fig. 1. The diamond was found to nucleate preferentially on the exposed silicon substrate as opposed to the resist. This allowed a significant particle density to be achieved in the lithographed pattern prior to removal of the resist, with a crystallite size of approximately 200 nm. After the three-hour initial deposition, the diamond crystallites in the grid had already impinged upon each other, and growth was extending beyond the pattern. This overgrowth of the diamond film made removal of the resist difficult; and so for the later experiments, a two-hour initial growth was used prior to resist removal. Experiments using thicker resist layers, however, demonstrated that substantial pattern thicknesses can be

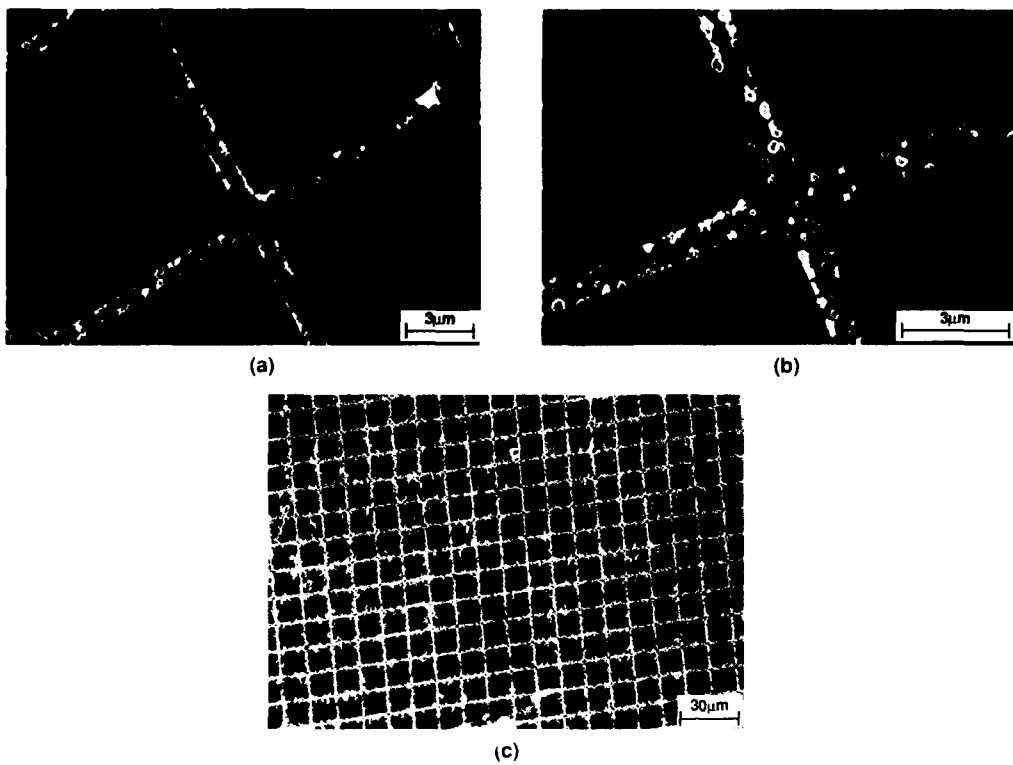


FIG. 1. Diamond crystallite growth on microlithographed Si substrates with increasing growth time. (a) 1 h; (b) 2 h; (c) 3 h.

generated by this technique (Fig. 2), while maintaining an extremely fine grain structure.

Experimental control substrates patterned but prepared without the diamond polish pretreatment exhibited no appreciable diamond nucleation on either the resist or the silicon over a period of approximately 20 h.

After grid nucleation, resist removal, and additional growth, the open areas between the grid lines filled in completely to form a continuous film. The diamond film maintained the fine grain structure of the initial nucleated particles, and the pattern was still evident on the surface (Fig. 3). With continued growth, however, this surface pattern became less distinct (Fig. 4).

The effect of the microlithographic pretreatment on the microstructure of the film was clearly demonstrated by comparison of the patterned and unpatterned regions of the substrate. The unpatterned regions provide a reference for the microstructural development that occurs on the bare substrate under the identical growth conditions. The boundary of the patterned region is clearly evident in the

scanning electron micrograph in Fig. 5, taken after 24 h of diamond growth. In the unpatterned areas of the silicon substrate, the diamond morphology is characteristic of large, faceted crystal growth and low net particle number densities. These diamond particle microstructures are characteristic of low nucleation density films formed on silicon under the PACVD growth conditions used in this study.<sup>3</sup> In contrast, the patterned areas are characterized by finer grains and higher particle densities, more consistent with the requirements of optical applications. With further growth, the larger particles on the unpatterned regions eventually impinge, as shown in Fig. 6. However, the film growth in the unpatterned region continues with the larger grain size. The transition from the fine-grained structure to the coarse-grained structure at the pattern boundary is extremely abrupt, with the microstructural differences arising within 1–2  $\mu\text{m}$  as seen in the micrograph in Fig. 7.

Extended microscopic examination of the patterned region of the diamond films showed a very uniform micro-

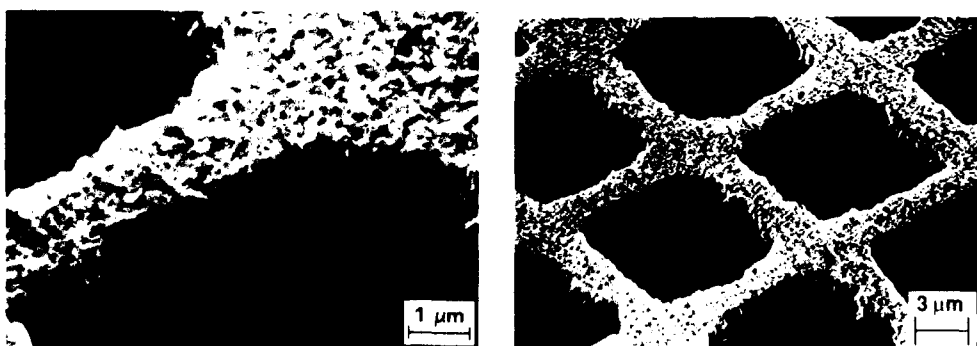


FIG. 2. Microlithographed diamond grid structure grown using thick resist layer.

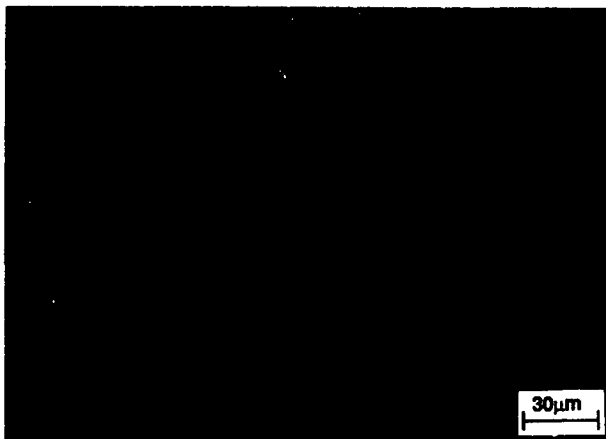


FIG. 3. Development of continuous diamond film on microlithographed Si after resist removal and subsequent growth.

structure over the entire  $2.5 \times 2.5$  cm pattern size. Often, spatial nonuniformities in sample temperature or plasma distribution lead to significant variations in film microstructure over this scale. Cross-sectional analysis in the scanning electron microscope (SEM) showed this diamond film to have no observable porosity in its microstructure in the patterned region, including both the microlithographed grid area and the initially masked areas (Fig. 8). The individual grains are distinctly columnar in nature over the entire thickness of the film.

The effect of the initial line width on the nucleation morphology was studied using a microlithographed pattern containing lines ranging from 0.5 to 1.5  $\mu\text{m}$  wide. The initial stages of growth, prior to resist removal, are shown in Fig. 9. As was seen in Fig. 1, nucleation preferentially occurred at the edges of the lines in all cases. For the 0.5  $\mu\text{m}$  line, a single row of crystallites was generated. For the line widths greater than 0.5  $\mu\text{m}$ , the crystal size remained constant, with an additional row forming at the opposite

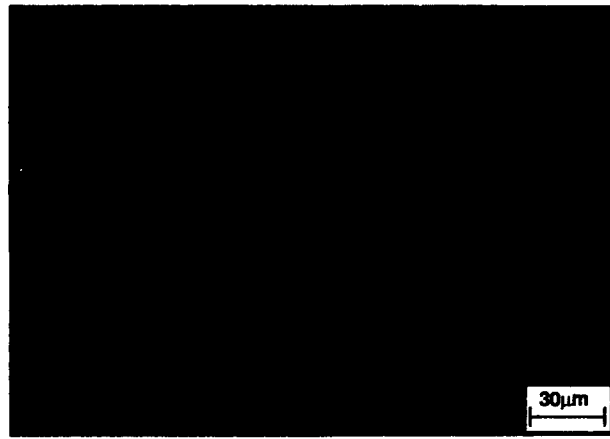
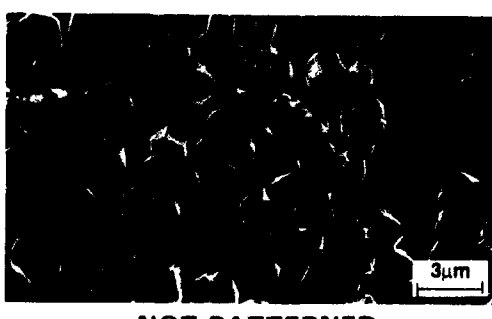


FIG. 4. Surface morphology of initially patterned Si after continued diamond film growth.

line edge. As the pattern linewidth was increased beyond this point, the crystallite particle size remained constant, with the spacing between the deposited rows of diamond particles progressively increasing with the lithographed linewidth.

#### IV. DISCUSSION

The importance of surface pretreatment to nucleation behavior in diamond thin films is well established. This work is consistent with the bulk of the literature which demonstrates a large increase in diamond nucleation density associated with a diamond abrasive preparation of the substrate surface. The action of surface polishing of a substrate with diamond paste both adds surface topology (by scratching) for diamond nucleation and "seeds" the surface with imbedded diamond particles. In the current experiments, the microlithographic patterns provide numerous sites for nucleation independent of the diamond

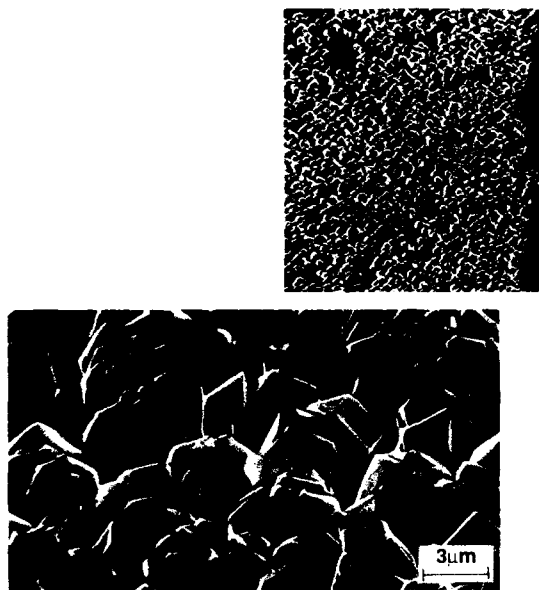


NOT PATTERNED

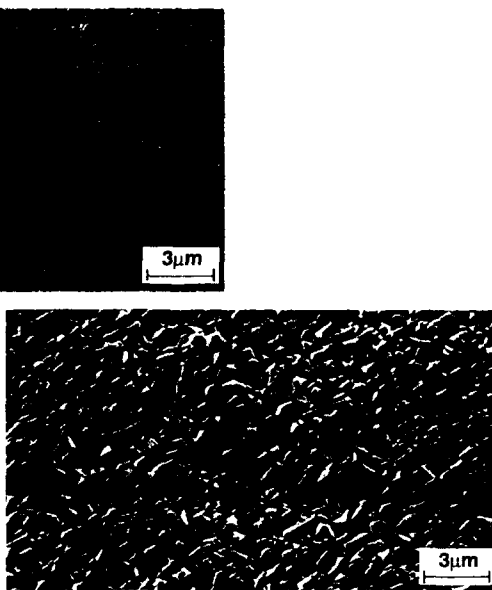


PATTERNED

FIG. 5. Comparison of microstructural development on patterned and nonpatterned regions of Si substrate after 24 h of growth.



NOT PATTERNED



PATTERNED

polishing, and yet the diamond pretreatment was still required to induce significant film nucleation. This is in contrast to the results of Kirkpatrick *et al.*,<sup>7</sup> who observed preferential nucleation of carbonaceous material at the sites of ion milled craters in silicon without seeding, although the nature of the deposited material is not reported. Bachmann *et al.*<sup>10</sup> used polished Si substrates oriented slightly off the  $\langle 100 \rangle$  axis, and noted that the crystallographic ledges so produced had no impact on diamond nucleation. This is consistent with the observations reported here using much larger scale topographic features. The current work supports the conclusion that the presence of the diamond particles from the surface pretreatment, i.e., the "seeding," is the critical step in enhancing the film nucleation. The work of Bachmann *et al.*,<sup>10</sup> performed at higher growth temperatures, supports this conclusion and further indicates that nondiamond particles can also lead to significant increases in film nucleation.

The nucleation morphologies of Figs. 1 and 9 indicate that the diamond particles "seeded" by the surface treat-

ment are located at the edges within the microlithographed channels, and that growth of subsequent film grains initially propagate in a similar manner along the same edges until impingement occurs. This is reasonable, since these sites provide two surfaces for film attachment. This is the same morphology observed by Ma *et al.*,<sup>8,9</sup> although their  $\text{Ar}^+$  irradiation step limited the nucleation to the edge region shadowed from the ion beam. The observed morphologies in this work are consistent with the residual diamond particles from the initial surface preparation being attached to the inside edges of these channels. Whether this attachment is electrostatic or not has not been determined. The work of Geis<sup>11</sup> reports comparable diamond seed texture development on Si, fused quartz, and chrome-coated substrates, which would tend to discount electrostatic attachment. The selective removal of the seed crystals by Ma *et al.*<sup>8,9</sup> by  $\text{Ar}^+$  ion irradiation, however, could be due to either physical sputtering or electronic processes. The absence of significant nucleation in the resist-covered areas in this work (i.e., prior to resist removal) indicates that significant numbers of particles are not being physically em-



FIG. 7. Detail of boundary between patterned and nonpatterned regions of Si substrate.



FIG. 8. Cross-sectional SEM micrograph illustrating dense, columnar structure.

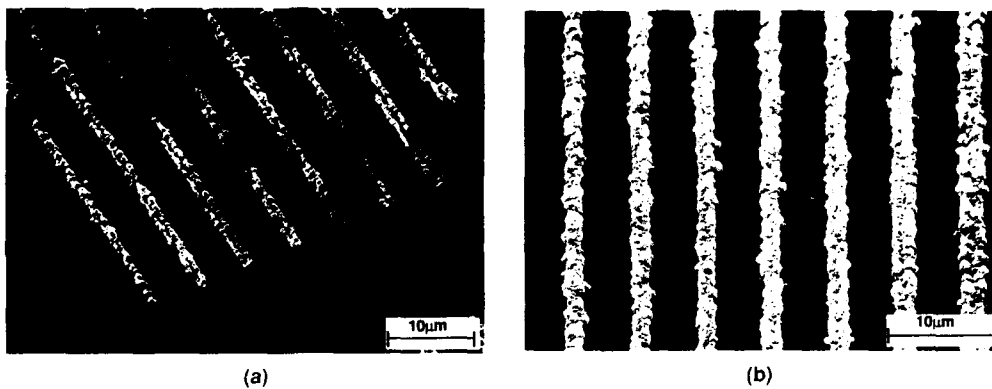


FIG. 9. Effect of pattern linewidth on diamond crystallite nucleation geometry. (a) early stage development; (b) later stage development.

bedded in the surface, as these would give rise to uniform diamond nucleation. In contrast, the diamond nucleation was found to be highly selective, forming almost exclusively within the microlithographed grid lines. Such attachment would undoubtably depend on particle size, and it is likely that the grids are retaining the finer particles in the overall distribution. Indeed, previous work has reported differences in film nucleation and growth associated with the use of different size diamond grit for the surface pretreatment.<sup>10,12</sup> Thus, both the geometry and scale of the pattern, as well as the size and distribution of the seeding material, will affect the final film microstructure, thus providing a degree of control over the film development.

In addition to illustrating the nature of nucleation in the diamond films, this work also elucidates critical factors inherent to diamond film growth. Most striking is the apparent propagation of grain size with continued film growth. Under identical growth conditions, the (patterned) fine grained regions of the sample remained fine and the (unpatterned) coarse-grained regions remained coarse. When a grain renucleates a new crystal adjacent to it, that new crystal appears to achieve the same size as the original one. For a film with a uniform microstructure, such constant grain size could be attributed to control by the growth conditions. However, in this instance different microstructures coexist under the same growth conditions and appear to be self-propagating. This self-propagation of grain size was observed both in the initial growth stages, where growth is occurring in plane, and also in the later stages when full coverage has occurred and out-of-plane growth is occurring. Examination of the early stage growth morphologies, both for the coarse-grained and fine-grained regions, indicates that this effect is not produced by proximity effects due to simple impingement of similar sized crystals. In the initial stages of growth, before significant impingement occurs, the crystal renucleation process appears distinctly linear in nature; i.e., the crystals tend to form in continuous chains, with each uniformly sized crystallite nucleating another in succession.

A mechanism to describe the reproducibility of the diamond crystal particle size during growth must be based on crystallographic factors. Here, nucleation of a new crystal from an existing one must be favored on a particular site on the existing crystal. Under the growth conditions of

this work, the nucleation of the new crystal must on average consume an equal number of these sites as it produces. Such behavior would produce growth in a chainlike fashion. Otherwise, if each new crystal provided multiple nucleation sites, the total number of available sites would rapidly grow and produce isotropic growth geometries. This would suggest that the renucleation step preferentially occurs at a defect site. Furthermore, the establishment of a steady state number of these sites would tend to indicate that the defect is linear, rather than planar, in nature. Such a growth mechanism in which there is an energetically favored site would likely be significant only at the lower growth temperatures used in this work. It is expected that at the higher temperatures of 850–1050 °C normally reported for diamond film growth, the nucleation process would be dominated by thermal energetics. Indeed, the increase in film nucleation and growth rates with increasing temperature is well established.<sup>10</sup>

The observed reproducibility in the diamond crystallite particle size, even in unconstrained growth conditions, would indicate that the initial defect density of the particle acts to establish an upper limit on its size. Work in this laboratory as well as by others has shown that under proper experimental conditions, diamond crystals can be grown to considerable sizes. An example given in Fig. 10 is

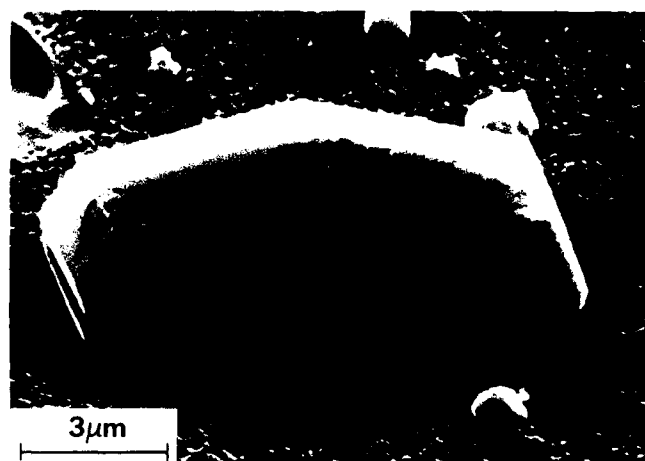


FIG. 10. Large, planar diamond crystal formed on  $\text{SiO}_2$  by plasma-enhanced CVD.

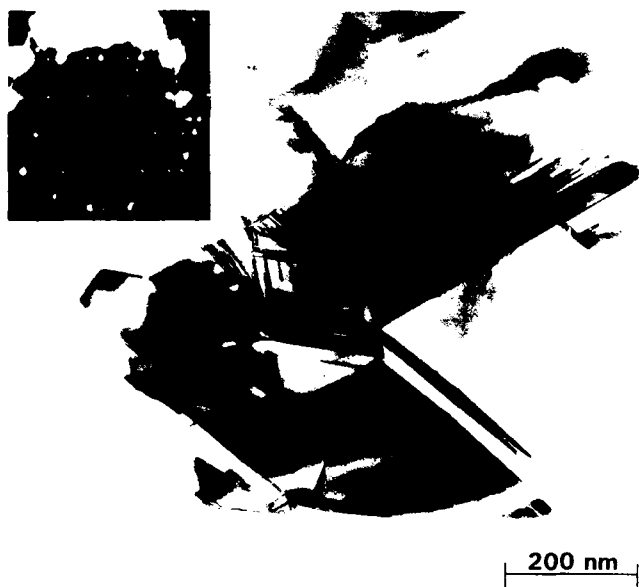


FIG. 11. Multiple twinning occurring in diamond film on Si.

of a regular, faceted platelet grown on  $\text{SiO}_2$  by plasma-enhanced CVD. It is likely that the achievement of this large size is controlled to a significant degree by the crystalline perfection of the lattice. Films that were grown under alternate conditions and that developed much smaller crystal dimensions were found to be highly defective,<sup>13</sup> containing significant amounts of crystallographic twinning. An example of this multiple twinning is shown in Fig. 11, which can give rise to the apparent five-fold faceting commonly reported. Thus, while growth conditions are of unquestionable importance in developing appropriate microstructures in diamond thin films, the nucleation and early stages of growth also appear critical in defining the defect concentration, and hence the microstructure, of the final film.

## V. CONCLUSIONS

Microlithographic patterning of substrate surfaces can enhance film uniformity over a large spatial area and can assist the formation of fine-grained microstructures. This is especially useful for optical applications, where fine-

grained films are preferred for reduced scatter losses. If post-deposition polishing is required, then the patterned growth serves as a useful precursor by improving spatial uniformity and reducing the initial surface roughness.

Examination of the nature of the nucleation and growth of the microlithographed films indicates that the intrinsic film growth mechanism is controlled by renucleation on crystallographic defects. This gives rise to a constant number of growth sites and results in generation of a steady state grain size that is controlled by the early stage film structure. The microlithographic patterning is believed to retain the smallest diamond particles in the initial surface pretreatment, predisposing the later stage film growth to a fine-grained morphology.

## ACKNOWLEDGMENTS

The authors are grateful to Dr. D. G. Howitt at the University of California, Davis, for valuable discussions on crystal growth mechanisms. This work was supported in part through the Office of Naval Research.

- <sup>1</sup>M. Kamo, Y. Saito, S. Matsumoto, and N. Setaka, *J. Cryst. Growth* **62**, 642 (1983).
- <sup>2</sup>A. R. Badzian, T. Badzian, R. Roy, R. Messier, and K. E. Spear, *Mater. Res. Bull.* **23**, 531 (1988).
- <sup>3</sup>A. B. Harker and J. F. DeNatale, *J. Mater. Res.*, April 1990.
- <sup>4</sup>Tom Feng, in *Diamond Optics II*, SPIE Proceedings Vol. 1146, 159 (1989).
- <sup>5</sup>H. Diao, T. Kobata, S. Morimoto, J. Satoh, and M. Yoshikawa, "Diamond Low Resistance Polishing Method," Preprint from Showa Electrical Engineering and Tokyo Engineering University, Tokodai, Japan (1989).
- <sup>6</sup>A. B. Harker, J. F. Flintoff, and J. F. DeNatale, in the Proceedings of *Diamond Optics III*, SPIE Meeting, San Diego, CA, July, 1990 (to be published).
- <sup>7</sup>A. R. Kirkpatrick, B. W. Ward, and N. P. Economou, *J. Vac. Sci. Technol. B* **7**, 1947 (1989).
- <sup>8</sup>Jing Sheng Ma, Hiroshi Kawarada, Takao Yonehara, Jun-Ichi Suzuki, Jin Wei, Yoshihiro Yokota, and Akio Hiraki, *Appl. Phys. Lett.* **55**, 1071 (1989).
- <sup>9</sup>Jing Sheng Ma, Hiroshi Kawarada, Takao Yonehara, Jun-Ichi Suzuki, Yoshihiro Yokota, and Akio Hiraki, *J. Cryst. Growth* **99**, 1206 (1990).
- <sup>10</sup>P. K. Bachmann, W. Drawl, D. Knight, R. Weimer, and R. F. Messier, in *Diamond and Diamond-Like Materials Synthesis*, EA-15, edited by A. Badzian, M. Geis, and G. Johnson (Materials Research Society, Pittsburgh, PA, 1988), pp. 99-102.
- <sup>11</sup>M. W. Geis, *Appl. Phys. Lett.* **55**, 550 (1989).
- <sup>12</sup>S.-C. Yu, H.-S. Chun, and F.-S. Guo, *J. Cryst. Growth* **99**, 1196 (1990).
- <sup>13</sup>A. B. Harker, *R&D Magazine* **32**, 84 (1990).

# PROCEEDINGS REPRINT



SPIE—The International Society for Optical Engineering

*Reprinted from*

## Diamond Optics III

**9-11 July 1990**  
**San Diego, California**



**Volume 1325**

# Microstructure of diamond films as a function of deposition conditions

A.B. Harker, J.F. DeNatale, and J.F. Flintoff

Rockwell International Science Center  
P.O. Box 1085  
1049 Camino Dos Rios  
Thousand Oaks, CA 91360

## ABSTRACT

The microstructure of polycrystalline diamond films grown by microwave plasma assisted chemical vapor deposition (PACVD) have been observed as a function of growth temperature, substrate identity and surface condition. Our highest microwave PACVD growth rates have been achieved in (110) axis normal oriented polycrystalline diamond films. Results indicate that at growth temperatures below 650°C kinetically dominated processes induce the formation of a preferential (110) axis normal orientation in diamond films with micron scale microstructure. This orientation can be sustained on silicon, boron nitride, and silicon nitride substrates to film thicknesses in excess of 60 microns through the occurrence of (111) twin defects. Such films have the high density and generally uniform microstructure required for optical applications.

## 1. INTRODUCTION

The rate of growth of PACVD diamond films is intimately tied to the availability of low energy growth sites. Such low energy sites will be associated with the most rapidly growing crystalline faces. In general, those crystalline faces having the highest growth rates rapidly fill their available bonding sites and cease growth. Hence, the exposed facets on a randomly oriented crystalline film would be expected to be those exhibiting the slowest growth. In the case of diamond films, the dominance of (100) and (111) faceting on the exposed surfaces indicates that these are the slow growth faces (Fig. 1) and explains the need to have continued renucleation to sustain reasonable growth rates. In order to achieve a situation in which the film development is controlled by a growth rather than a renucleation mechanism it would be necessary to provide a continuous source of the most favored growth sites. In this work it has been shown that such a situation can be achieved through the continued propagation of a highly twinned (110) axis normal oriented diamond film.

8C62308

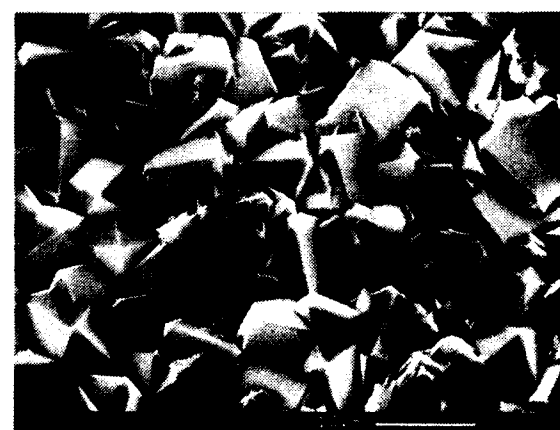


Fig. 1 Scanning electron micrograph of a random polycrystalline diamond film surface grown at 1000°C by microwave PACVD.

In this research we have investigated the degree to which the microstructure of PACVD polycrystalline diamond films can be modified and controlled through the use of various substrates, substrate surface preparations, and deposition conditions. The primary deposition variable investigated was temperature, with films being deposited over the range 450 to 1000°C. Substrates investigations included (100), (110), and (111) Type 2A diamond single crystals, pyrolytic polycrystalline boron nitride (PBN), polycrystalline silicon nitride, (100) silicon, and fused silica.

## 2. EXPERIMENTAL

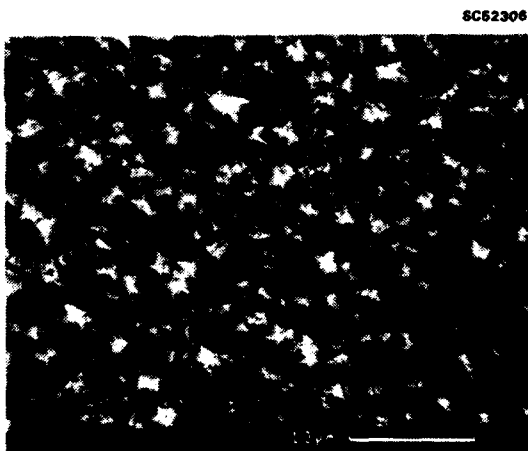
All films were grown in a standard stainless steel ASTEX 1.5 KW microwave reactor with an inductively heated graphite sample holder. The chamber is equipped with windows to permit sample surface temperature monitoring by optical pyrometry. The gas composition used for growth was 99% hydrogen, 0.7% methane, and 0.3% oxygen. Films were analyzed by scanning electron microscopy, micro-Raman scattering, and x-ray diffraction. Growth rates were determined by infrared reflectance measurements.

## 3. RESULTS

The initial growth temperature variation experiments were conducted with (100) silicon substrates polished with submicron diamond paste. These experiments, previously reported,<sup>1</sup> revealed that (110) axis normal oriented diamond films could be produced at growth temperatures of 450 to 650°C when the samples were located in the plasma region of highest growth rate. Outside of the direct plasma impingement zone, only randomly oriented films have been observed.

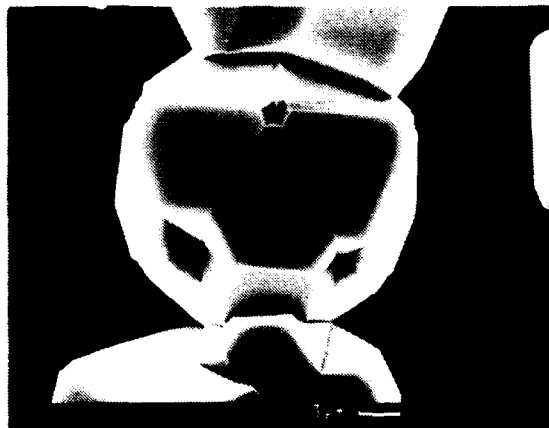
Our study has shown that such (110) oriented films can be produced upon polycrystalline silicon nitride and boron nitride substrates as well as on (100) silicon with growth rates of 0.5 to 1.0  $\mu\text{m}$  per hour at 650°C. Figure 2 shows an electron micrograph of a 25  $\mu\text{m}$  thick (110) oriented diamond film on polycrystalline silicon nitride. The microstructure of the one-dimensionally oriented film is generally more regular than that of a random film. The surface appearance is dominated by the exposed edges of crystallites multiply twinned along the (111) planes. The observation that such oriented films can be grown on polycrystalline substrates as well as single crystal (100) silicon indicates that under these growth conditions the crystal structures of the non-lattice matched substrates do not significantly affect the nucleation energetics. This observation is consistent with the high surface energy of diamond.

Fig. 2 Scanning electron micrograph of a (110) axis normal polycrystalline diamond film grown on diamond polished polycrystalline silicon nitride at 650°C.

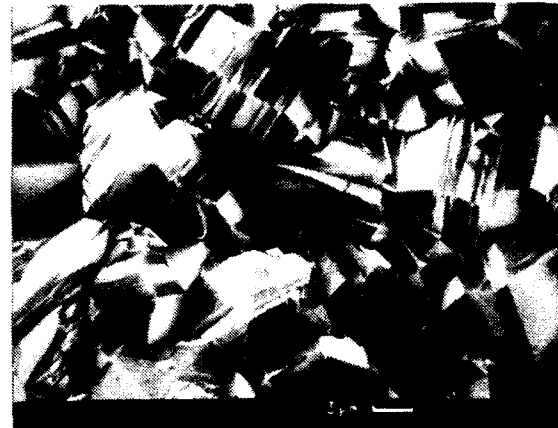


To observe the effects of substrate identity in the growth process, diamond films were produced by PACVD under identical conditions at 650°C on a range of single crystal, polycrystalline, and amorphous substrates. The resulting film properties are tabulated below.

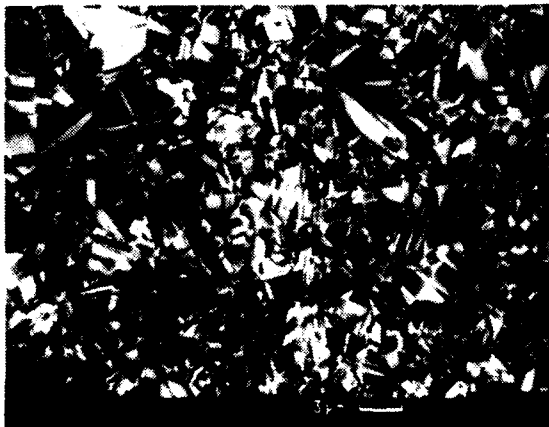
The microstructures of some of the films are shown in the electron micrographs in Fig. 3. The similarities of the microstructures in the (110) oriented films on Si, PBN, and Si<sub>3</sub>N<sub>4</sub> are apparent, as are the dramatic differences between the films grown on the Si samples polished with boron nitride and diamond. To provide a consistent description of the various microstructures one must consider surface energies, the types of expected crystalline defects, and the metastable nature of the low pressure diamond synthesis environment in which etching is occurring concurrently with film growth.



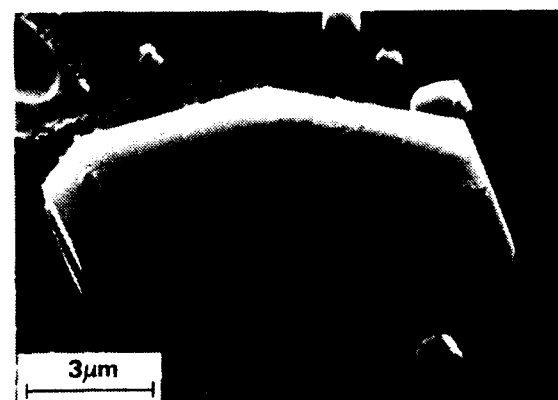
POLYCRYSTALLINE DIAMOND  
ON (100) SILICON, CUBIC BORON  
NITRIDE POLISH (45 MESH)



(110) ORIENTED DIAMOND  
ON (100) SILICON, SUBMICRON  
DIAMOND PASTE POLISH



(110) ORIENTED DIAMOND ON  
PYROLYtic BORON NITRIDE,  
SUBMICRON DIAMOND PASTE POLISH



POLYCRYSTALLINE DIAMOND ON  
FUSED SILICA, SUBMICRON  
DIAMOND PASTE POLISH

Fig. 3 Scanning electron micrographs showing the morphology of poly-  
polycrystalline diamond films grown on a range of substrates.

Table 1

Microstructure of Diamond Films as a Function of Substrate Identity and Surface Preparation. Boron Nitride Polishes Were Done with a Cubic 45 Mesh Powder

SUBSTRATE	FILM PROPERTIES
(100) Type 2A Diamond	Epitaxial Film, very low defects
(111) Type 2A Diamond	Epitaxial Film, surface defects
(110) Type 2A Diamond	Grain Oriented Polycrystalline (Highest Growth Rate)
(100) Silicon (BN polish)	Well Formed Low Defect Crystallites
(100) Silicon (Dia. Polish)	(110) Oriented Polycrystalline Film
Fused Silica (Dia. Polish)	Well Formed Low Defect Crystallites
Silicon Nitride* (Dia. Polish)	(110) Oriented Polycrystalline
Boron Nitride* (Dia. Polish)	(110) Oriented Polycrystalline

\* - Polycrystalline Material

Since the three single crystal diamond substrates all produced fully orientated films, it is clear that substrate crystallography can be significant to homoepitaxy under the deposition conditions of this work. The high surface energy of the (100) crystal and the absence of any periodic bonding chains<sup>2</sup> correlates well with its epitaxial nature and low defect density surface.<sup>3,4</sup> Similarly, the appearance of triangular defects on the generally epitaxial (111) growth surface is consistent with the lower surface energy of that plane and the presence of three periodic bonding chains<sup>3</sup> that can produce triangular growth hillocks on that face. However, the more rapid growth rate and grain oriented polycrystalline nature of the film on the (110) diamond crystal require that the nature of the defects generated in the film be considered to explain the results.

The (110) plane of diamond is intersected by the (111) planes that generate the single periodic bonding chain on the (110) face. The (111) planes are subject to both stacking and slip plane faults that are known to produce striations in natural diamond crystals.<sup>5</sup> Similarly, fairly regular twinning defects along the (111) plane produce the striated or layered morphology seen in the grains of the (110) oriented polycrystalline films (Fig. 4). Hence, we conclude that the formation of defects along the (111) planes on the (110) diamond growth surface provides both a low energy state for preferential bonding of the radical species producing growth and a very high surface area of unsatisfied chemical bonds to enhance the growth rate. Additionally, Zheng et al.<sup>5</sup> have reported that the (110) face of diamond shows a lower oxidation rate than either the (100) or (111) face, which would favor (110) film growth.

The generation of oriented films on the non-diamond substrates is consistent with the observed homo-epitaxial film growth behavior. The global (110) orientation on is believed due to the interplay between anisotropic growth modes and anisotropic etching, favoring the (110) oriented growth. For small diamond seed crystals, the plasma etching occurring during the initial stages of growth will tend to alter the crystallographic distribution of seed crystals towards (110) orientation. Coupled with this is the enhanced growth rates observed on the (110) single crystal diamond surface. The combination of these two factors imposes a strong preference for (110) oriented polycrystalline film development under the low temperature conditions used in this work. For higher growth temperatures, it is likely that the energetic differences associated with crystallographically favored growth modes will be much less significant, and the nucleation time associated with "seed" etching will be reduced, favoring random film development. This transition to random growth morphologies at higher temperatures has indeed been experimentally demonstrated.



Fig. 4 Higher resolution electron micrographs of the twin defects generated at the intersection of the octahedral and dodecahedral planes of diamond in a (110) oriented diamond film on (100) silicon.

The samples not exhibiting this type of growth at  $T < 650^{\circ}\text{C}$  were the films grown on fused silica and (100) silicon polished with a coarse 45 mesh cubic boron nitride powder. On these samples growth of individual faceted particles dominated. In the boron nitride polished samples, growth was occurring upon the faceted super-micron boron nitride crystal surfaces. In this growth dominated regime little nucleation was occurring and very smooth faceted particles were produced. Similarly, in the case of fused silica, the reaction of the surface with the plasma (producing pitting in the micrograph in Fig. 3) releases significant oxygen near the surface. This not only etches the smaller diamond particles left by the abrasion process, but also inhibits the general nucleation of polycrystalline diamond. In this case, growth is again limited to the larger diamond particulate seeds on the surface and well defined particle growth morphologies result.

#### 4. CONCLUSIONS

The preferential growth of (110) oriented polycrystalline diamond films, at temperatures below  $650^{\circ}\text{C}$  by microwave PACVD can be ascribed to a combination of defect enhanced anisotropic growth and anisotropic etching. The oriented film microstructure is fairly regular and is dominated by the presence of layered planar micron scale crystallites and striations induced by multiple twinning defects on the (111) plane. These defects lead to continuous propagation of the a (110) oriented growth surface and permit the orientation to persist with increasing film thickness. The generation of large grained, low defect diamond crystals by PACVD under the growth conditions of this work is limited to those cases in which larger seed crystals grow while general polycrystalline diamond nucleation is inhibited by the absence of sufficient small diamond "seeds" or through the reactive etching of the nucleation sites.

#### 5. ACKNOWLEDGEMENTS

Portions of this research were sponsored by the Office of Naval Research.

## 6. REFERENCES

1. A.B. Harker and J.F. DeNatale, "Temperature and Reactive Etching Effects on the Microstructure of Microwave Plasma Deposited Diamond Films," *J. Mater. Res.* 5, pp. 818-823 (1990).
2. P. Hartmon and W.G. Perdok, "On the Relations Between Structure and Morphology of Crystals, III," *Acta Cryst.* 8, p. 49, 521, 525 (1955).
3. I. Sunagawa, "Growth and Morphology of Diamond Crystals Under Stable and Metastable Conditions," *J. Crystal Growth* 99, pp. 1156-1161 (1990).
4. M. Moore, "Optical Studies of Diamonds and Their Surfaces," in Properties of Diamond, ed. J.E. Field (Academic Press, London, 1979) 261.
5. Z. Zheng, H. Kanda, T. Ohsawa, S. Yamaoka, "Inhomogeneous Oxidation Rate Measured on the (110) Cross-Section of Synthetic Diamonds," *J. Mat. Sci. Lett.* 9, pp. 331-333, 1990.

ADHESION IMPROVEMENT IN DIAMOND FILMS BY MICROLITHOGRAPHIC PATTERNING

J.F. DeNatale, J.F. Flintoff, and A.B. Harker, Rockwell International Science Center, Thousand Oaks, CA 91360

ABSTRACT

The use of microlithographic surface patterning has been investigated as a means of modifying the nucleation and adhesion of diamond films on noncompatible substrates. Significant improvements in film adhesion were achieved using this technique, to the point that interfacial integrity was maintained even at stress levels which induced sub-surface fracture in the supporting substrate.

## INTRODUCTION

The recent advances in the low-pressure synthesis of diamond thin films have the potential to impact numerous technologies due to diamond's unique combination of optical, mechanical, and electrical properties. Formation of these films from hydrogen-hydrocarbon gas mixtures has been demonstrated by a variety of techniques including hot filaments, microwave plasmas, and high velocity torches [1]. The vast majority of the work described in the literature documents growth and characterization of diamond films on Si and carbide forming metallic substrates due to the relative ease of growth and adherence to these materials. On many substrate materials, however, the diamond films tend to exhibit poor adherence, and typically disbond at thicknesses on the order of a few microns due to the development of intrinsic growth and thermal mismatch stresses. To fully exploit the potential of the diamond films, fabrication on less-compatible substrates must be addressed. One approach investigated in this work has been the use of microlithographic patterning of the substrate surface prior to film deposition in order to improve film adhesion. The surface patterning provides increased surface area for bonding, enhances film uniformity [2] and, if the pattern is undercut, offers a means of physically "locking" the film onto the substrate. This approach has been found to significantly improve film adhesion.

## EXPERIMENTAL

Fused silica windows were patterned by standard photolithography and dry etching techniques prior to film growth. This produced grid patterns of 1 micron wide etched lines separated by 10 micron square spaces of unetched silica and 3 micron lines separated by 15 microns. The depths of the etched lines were approximately 1 micron in all cases. Processing conditions that gave both sharp sided and rounded etch profiles, respectively, (figure 1) were used to determine the effects of profile geometry on film adhesion. Diamond films were deposited using microwave plasma CVD with a source gas composition of 0.5%  $\text{CH}_4$ , 0.2%  $\text{O}_2$ , and the balance  $\text{H}_2$ . Substrate growth temperatures of 750 C were used as determined by optical pyrometry. Unpatterned substrates were also included in the depositions for experimental comparison. All substrates were prepared using identical diamond polish pre-treatments to enhance film nucleation.

## RESULTS

In the initial experiment, after approximately 16 hours of growth local film delamination was observed on the unpatterned substrate, so no further film growth was

conducted on this substrate. The patterned substrate with the rounded etch profile exhibited local film adhesion, although much of the film had already disbonded. The films on the substrates patterned with sharp etch profiles, however, maintained their integrity, demonstrating an improvement in adhesion associated with the patterning. The diamond film surfaces were characterized by highly faceted grains approximately 1-2 microns in size.

Diamond growth was continued on these substrates, and even after a film thickness of 9 microns, the topology of the initial pattern was still clearly evident in the film (figure 2). Subsequent tests showed evidence of the pattern to persist to film thicknesses of over 24 microns. By this thickness, cracks had become apparent in the film (figure 2). Cross sectional SEM revealed, however, that these were not the result of film delamination. Rather, the stresses generated by the growing film and the high temperature processing induced sub-surface fracture in the silica substrate itself (figure 3). The integrity of the film-substrate interface was still maintained even after the substrate fracture. These micrographs further indicated a strongly columnar grain structure, with the etched lines characterized by slightly inward sloping sides.

A filamentary structure was observed in the regions of the cracks (figure 4). This is attributed to H<sub>2</sub> etching of the SiO<sub>2</sub> substrate and the subsequent redeposition of reduced material. A similar structure was observed to occur

on Si substrates with sharp surface discontinuities where the plasma intensity profile is highly nonuniform.

## DISCUSSION

Microlithographic patterning has been applied to diamond film growth for controlled seeding [2-4] and microstructural control [2]. The current work demonstrates that, in addition to these uses, the technique offers potential improvements in film adhesion.

Even though the profiles of the initial etched lines did not have the desired undercut to physically constrain or "dovetail" the film into the substrate, the process still produced substantial improvement in film adhesion. This is believed partially due to increased surface area for film-substrate bonding and enhancement of fine grain nucleation and dense film microstructure. The diamond crystallites are able to grow around the sharp steps of the etched lines, following the contours of the substrate surface pattern (figure 5). This provides a means of resisting both planar and normal stresses which could induce film delamination. The minimal improvement in film adhesion provided by the rounded etched lines confirms that the sharp steps are critical to the effect; we anticipate that with refinement of the etching profiles, even further enhancements in film adhesion will be possible.

The cross sectional microstructure of the diamond film immediately above the patterned regions differed

significantly from the nonpatterned regions, with the individual columns of the former growing at acute angles to each other and strongly impinging (figure 6). The cross-sectional structure far from the unetched regions was similar to that of the unetched control sample, with parallel columnar grains over the entire film thickness. The expanding, columnar structure associated with the etched lines may be instrumental in the stress characteristics of the film. An unpatterned diamond film on Si may develop significant stresses of either compressive or tensile nature during growth as evidenced by the degree of substrate curvature. The expanding columnar grain geometries in the patterned films would tend to impose compressive stresses into the films as the columns grow and impinge. These stresses may actually help to balance the net stress in otherwise tensile films. Indeed, if this is the case then by tailoring the periodic spacing of these features, one may be able to independently exercise control over the stress state of a diamond thin film. In films that would otherwise be compressive in nature, the patterning would accentuate the degree of stress. This is most likely the case in the present experiments, with the combined stresses ultimately exceeding the fracture strength of the silica substrate.

The ultimate fracture of the  $\text{SiO}_2$  surface is likely due to a combination of intrinsic growth stresses and thermal expansion mismatch at the high processing temperatures. Additional reduction of the surface mechanical strength

could have resulted from the hydrogen plasma environment, and further studies are required to establish this. The subsurface fracture of a substrate by a tensile thin film has been modeled by Drory and Evans [5] and Drory et al [6]. The observed crack geometries in this work are identical to those described above, with both shallow and deep substrate cracks running parallel to the film interface.

Quantitative comparisons of the observed behavior can be made to the crack depths predicted by the theoretical models and experimental validations of refs 5 and 6. A substrate to film thickness ratio of 100 and an elastic modulus ratio of approximately 10 are appropriate for the current experiments. The observed ratio of crack depths to film thickness are 10 and 3.5 for the deep and shallow cracks, respectively. This compares to values of approximately 8 and 2, respectively for the predictions of ref 6.

## CONCLUSIONS

Microlithographic patterning of a substrate surface prior to diamond growth provides a means of improving film adhesion beyond that of nonpatterned substrates. This technique has significant application to the growth of diamond films on noncompatible substrates. The alteration of the growth geometries in the regions of the patterning may be responsible for modification of the film stress,

providing a means of control over the mechanical state of the resultant diamond film. Implementation of this technique to thicker film growth for which intrinsic compressive stresses may be large, however, will require the substrate fracture stresses to be considered.

## REFERENCES

1. K. Spear, J. Amer. Ceram. Soc. 72, 171 (1989).
2. J.F. DeNatale, J.F. Flintoff, and A.B. Harker, J. Appl. Phys. To be published Oct. 1990.
3. Jing Sheng Ma, Hiroshi Kawarada, Takao Yonehara, Jun-Ichi Suzuki, Jin Wei, Yoshihiro Yokota, and Akio Hiraki, Appl. Phys. Lett. 55 (11), 1071-1073 (1989).
4. A.R. Kirkpatrick, B.W. Ward, and N.P. Economou, J. Vac. Sci. Technol. B 7 (6), 1947-1949 (1989).
5. M.D. Drory and A.G. Evans, J. Amer. Ceram. Soc. 73 (3) 634-38 (1990).
6. M.D. Drory, M.D. Thouless, and A.G. Evans, Acta Metall. 36 (8), 2019-2028 (1988).

## FIGURE CAPTIONS

1. Comparison between  $\text{SiO}_2$  substrates with sharp and rounded etch profiles, respectively, prior to diamond growth.
2. Surface morphology of diamond growth on patterned  $\text{SiO}_2$ . Film thickness approximately 9 microns. Note development of surface cracks.
3. Cross sectional SEM micrograph illustrating subsurface fracture in  $\text{SiO}_2$  substrate after extended diamond growth.
4. Filamentary microstructure observed in subsurface cracks attributed to redeposition of reduced substrate material.
5. SEM micrograph of diamond crystallite growing around etched feature on Si substrate.
6. Cross sectional SEM micrograph illustrating expanding columnar geometry in regions of sharply etched features in  $\text{SiO}_2$ .



Figure 1

Figure 2

100  $\mu$ m

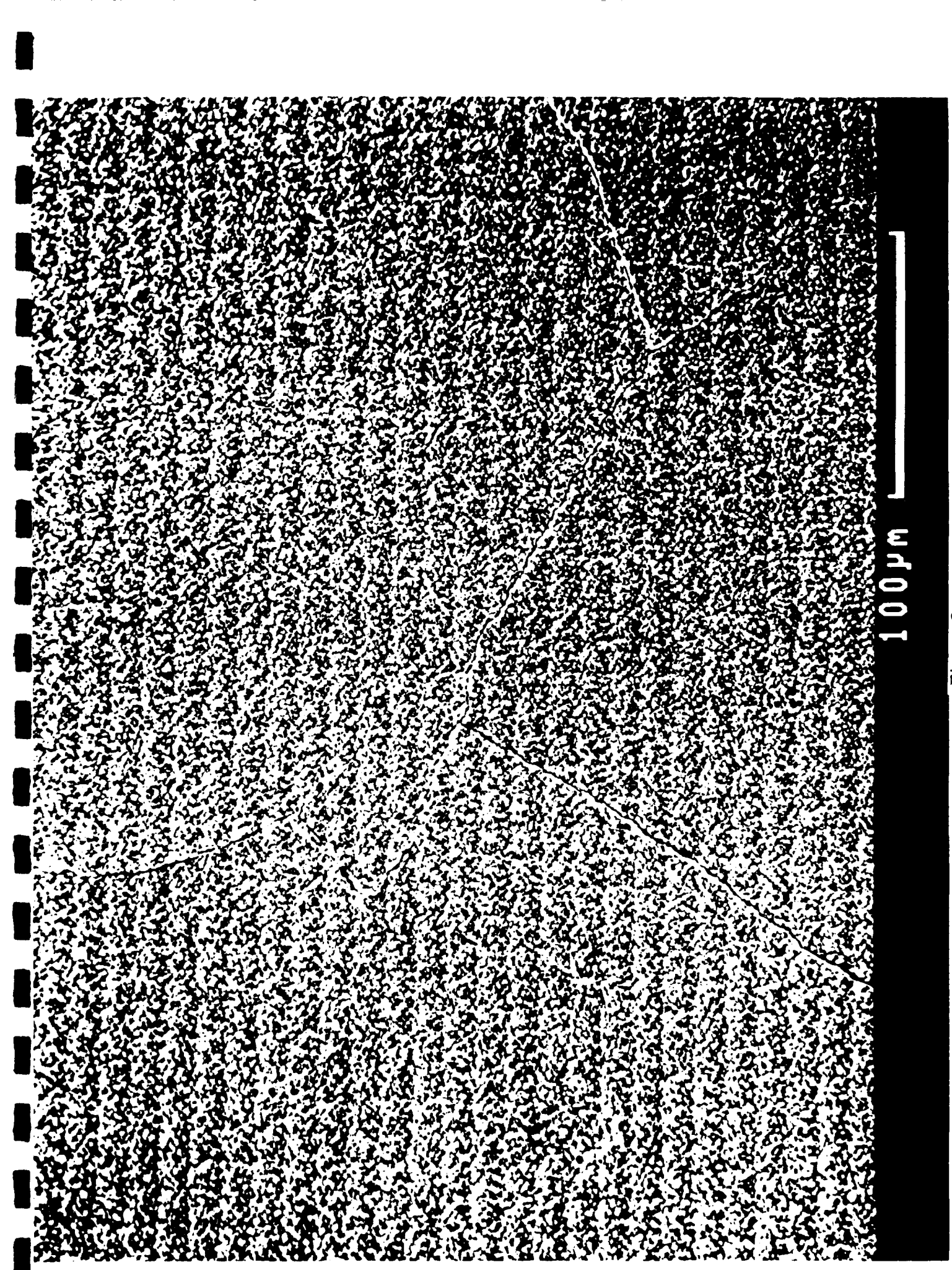
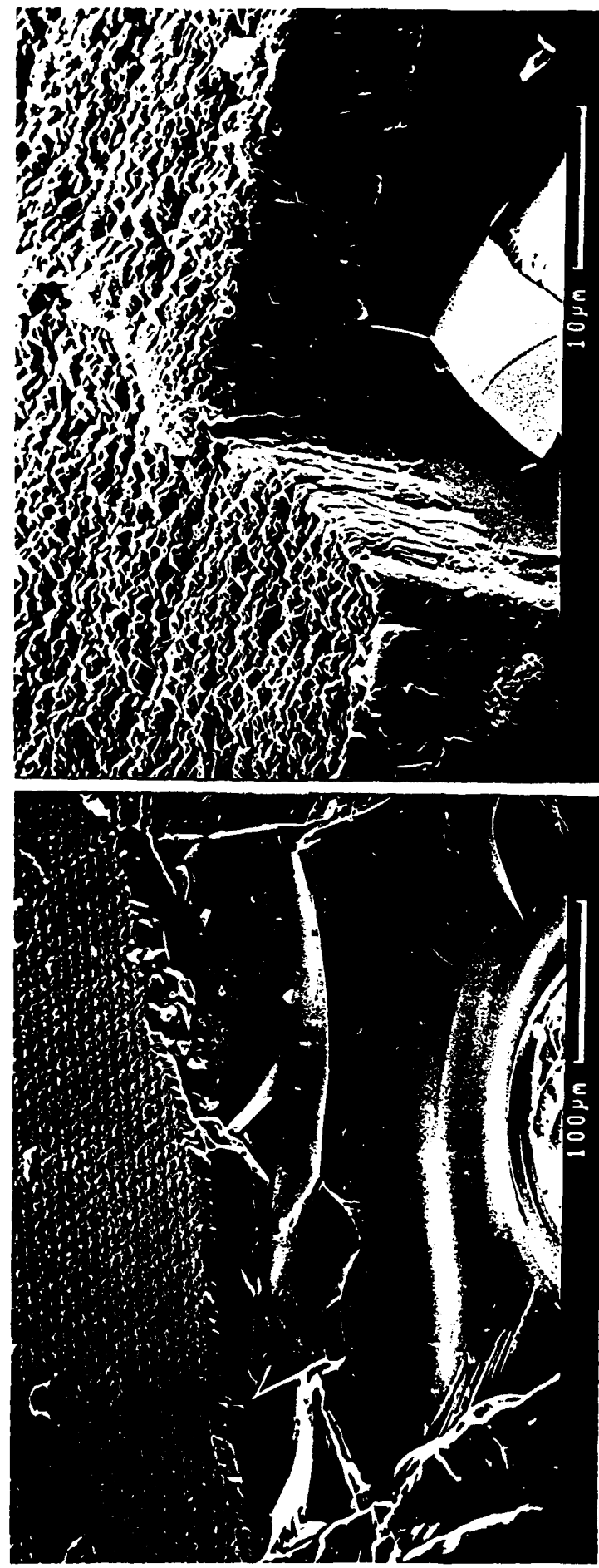


Figure 3



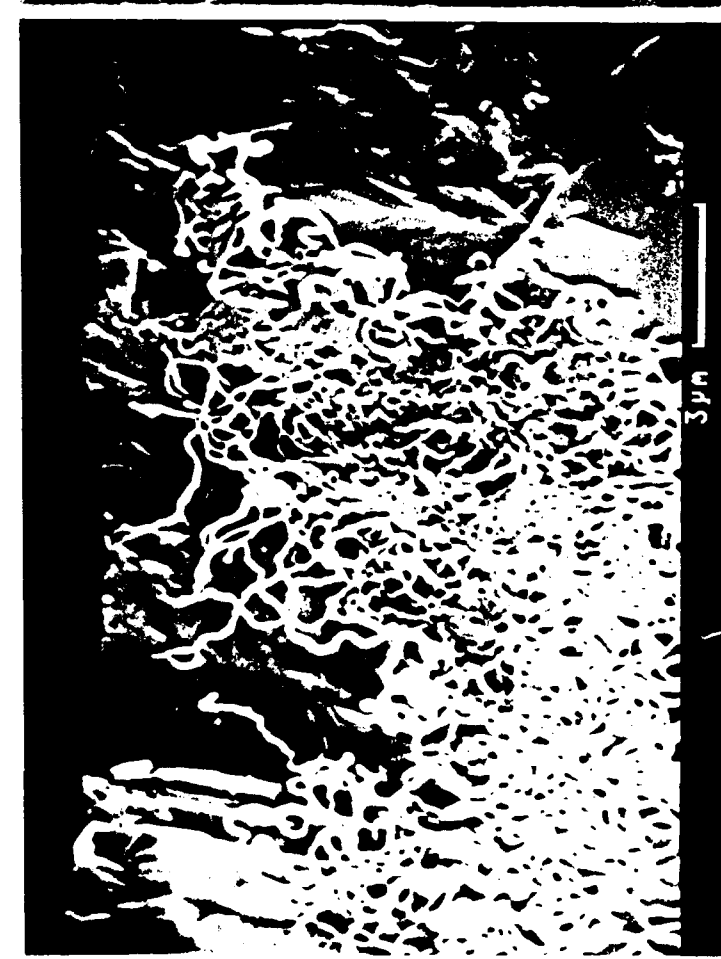


Figure 4

Figure 5

1  $\mu$ m

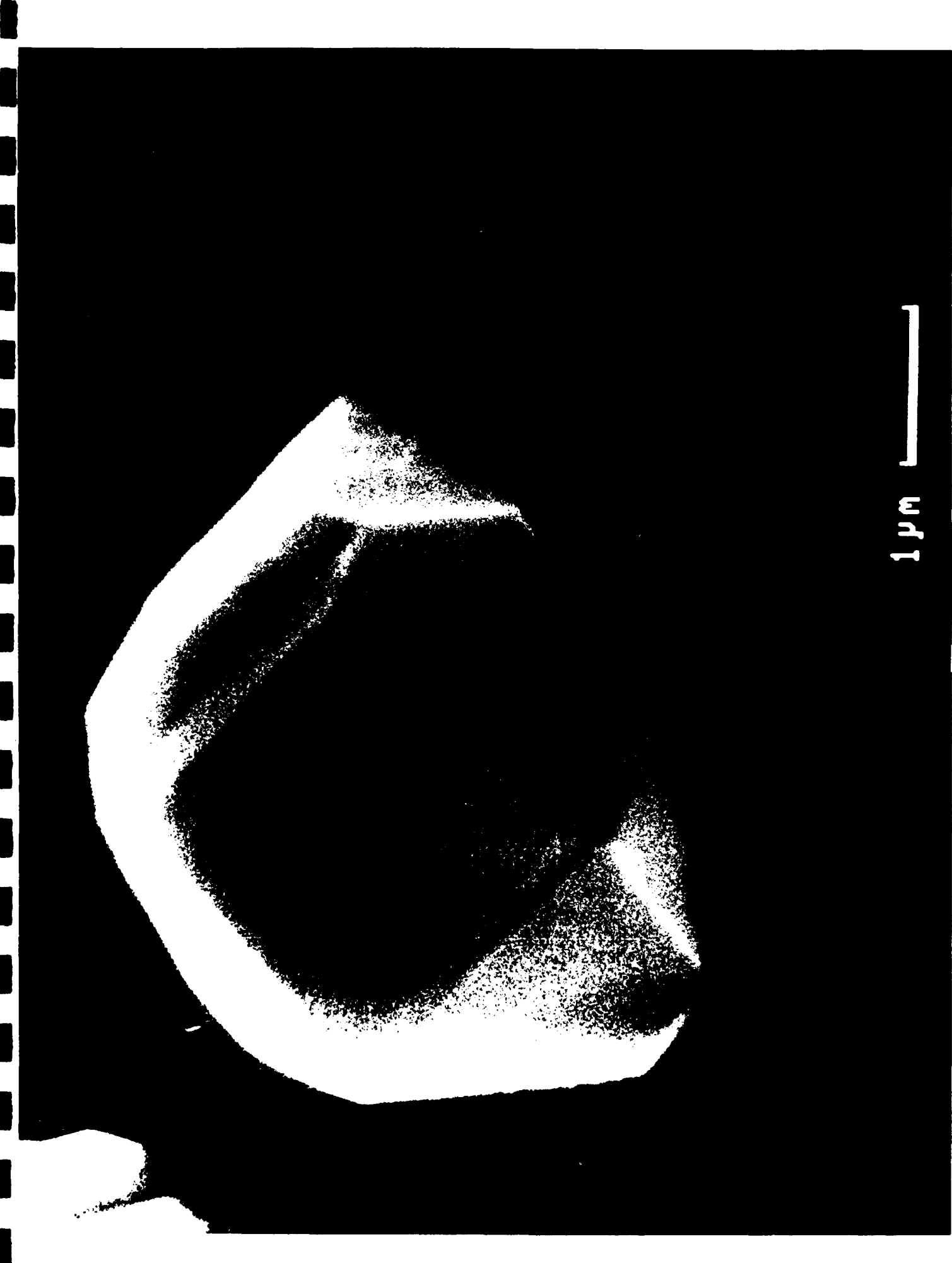


Figure 6



# MICROSTRUCTURE AND ORIENTATION EFFECTS IN DIAMOND THIN FILMS

J.F. DeNatale, A.B. Harker, and J.F. Flintoff

Rockwell International Science Center

Thousand Oaks, CA 91358

## ABSTRACT

The microstructure and orientation of diamond thin films grown by plasma assisted chemical vapor deposition (PACVD) have been studied as functions of growth temperature, substrate identity and substrate pre-treatment. Results indicate that for growth temperatures below 650 °C, competition between film growth and etching can lead to preferential (110) oriented films on a variety of substrate materials. This orientation can be globally sustained during growth by the occurrence of (111) planar defects.

## INTRODUCTION

The growth of diamond thin films by low-pressure techniques occurs through a complex kinetic balance between the nucleation, growth, and etching of both diamond and non-diamond species. The importance of these competing processes to the final film properties has been documented extensively in the literature, detailing the strong effect film deposition conditions have on the microstructures and Raman signatures of the resulting films.

In this work, we have investigated the degree to which the microstructure and orientation of PACVD diamond films can be modified by the use of various substrates, substrate surface preparations, and deposition conditions. This has illuminated the role of crystalline defects in the growth and morphology of polycrystalline and homoepitaxial diamond thin films.

## EXPERIMENTAL

Films were grown by plasma assisted CVD (PACVD) using an ASTEX 1.5 kW microwave reactor and an inductively heated graphite sample holder. The source gas composition used for this work was 99% hydrogen, 0.7% methane, and 0.3% oxygen. Film temperature was determined by optical pyrometry. Films

were grown on both diamond and non-diamond substrates. The diamonds were natural type 2A single crystals, oriented with (100), (110), and (111) surfaces, respectively. The non-diamond substrates included (100) single crystal silicon, fused silica, polycrystalline silicon nitride, and (hexagonal) polycrystalline pyrolytic boron nitride (PBN). Surface pretreatment with submicron diamond paste was performed on the non-diamond substrates to enhance film nucleation. In addition, a (100) silicon substrate which had been polished with a 45 mesh cubic boron nitride powder was included in the deposition.

Films were analyzed by scanning electron microscopy (SEM), micro-Raman scattering, and x-ray diffraction. Growth rates were established by infrared reflectance spectroscopy.

## RESULTS

A growth temperature of 650 °C was used for the depositions on the single crystal diamond substrates. The resulting films on all three substrate orientations produced fully oriented films, as evidenced by x-ray diffraction and SEM electron channeling contrast (Fig. 1). Imaging of both the (100) and (111) films indicated them to be epitaxial, although they differed in their surface morphologies (Fig. 2). The (100) film had a low level of observable structural

defects, although it did show some fine scale texture development. The (111) film exhibited well-defined triangular defects on an otherwise exceedingly smooth surface. The Raman spectra of these films showed a sharp peak at  $1332.5\text{ cm}^{-1}$  (Fig. 3), characteristic of natural single crystal diamond.

In contrast to the morphologies of the previous two substrates, the film on the (110) diamond substrate exhibited a high degree of fairly coarse surface texture (Fig. 2). In addition, the (110) film was characterized by a growth rate approximately twice that of the other two orientations.

The initial experiments investigating the effects of growth temperature on the non-diamond substrates were conducted using (100) Si substrates polished with submicron diamond paste. These experiments, previously reported [1], revealed that (110)-oriented polycrystalline diamond films could be produced at growth temperatures of 450 to  $650\text{ }^{\circ}\text{C}$  when the samples were located in the plasma region of highest growth rate. At higher growth temperatures or outside of the direct plasma impingement zone, only randomly oriented films have been observed. Based on these results, a growth temperature of  $650\text{ }^{\circ}\text{C}$  was used for the experiments reported here.

The current experiments revealed that similar (110)-oriented films can be produced on polycrystalline boron nitride and silicon nitride substrates as well as on (100)

Si with growth rates of 0.5 to 1.0  $\mu\text{m}$  per hour. X-ray diffraction analysis indicated that the ratio of the peak intensity of the diamond 220 reflection to that of the 111 reflection was approximately a factor of 25 higher than in a random film.

The microstructures of the one-dimensionally oriented films on the various substrate materials all exhibited certain similarities. These films were generally more regular than the random films, with their surface appearance dominated by the presence of large numbers of planar growth twins (Figs. 4,5). In contrast, the films on fused silica and BN-polished (100) Si showed no tendency for preferred orientation.

The observations of film morphology and properties for the various substrates and surface preparations are summarized in Table 1.

#### DISCUSSION

The homoepitaxial growth of the diamond films on the various diamond substrates indicates that substrate crystallography can significantly affect the microstructure and growth kinetics of the films. The observed surface morphologies and growth rates in these experiments are consistent with the directional bonding of the diamond structure. As noted by Hartman and Perdok [2] and Sunagawa

[3], the (110) face contains one periodic bond chain (PBC) in plane. In addition, by symmetry, one PBC vector also exists normal to the surface. This provides continuously available bonding sites for both in-plane propagation of the surface by atomic attachment as well as strong bonding sites for the attachment of subsequent layers. The observed growth rate and rough surface morphology of the homoepitaxial film on (110) diamond is attributed to the presence of (equivalently) favorable growth modes for both in-plane and out-of-plane growth.

The (111) face of diamond, on the other hand, contains three PBC's [3]. This predicts smooth growth faces with relatively low displacement velocities, as observed experimentally in the homoepitaxial films. The relatively smooth (100) face, in contrast, would not be expected to occur in a perfect diamond structure based solely on PBC analysis [3]. Surface reconstruction, however, can allow this face to develop into a habit-controlling face, and these cube faces are commonly observed in synthetic diamonds fabricated by a variety of techniques [3]. The lower number of PBC's on this face, and the possibility of local distortions in the surface reconstruction may contribute to the greater surface texture observed on the (100) homoepitaxial film as compared with the (111) film.

The observations of substantially higher growth rates for the (110) oriented polycrystalline films on the non-diamond substrates are consistent with their observed growth

morphologies as well as with the observed behavior of the homoepitaxial films. The rate of growth of a thin film is intimately associated with the availability of low-energy bonding sites. Such sites will in turn be associated with the most rapidly growing faces. In general, the crystalline faces having the highest growth rates rapidly fill their available bonding sites and cease growth. At this point, growth can continue only on the slower growing faces or by renucleation of a new crystallite, and this becomes the rate-limiting step in the growth kinetics. Hence, the exposed facets on a randomly oriented crystalline film would be expected to be those exhibiting the slowest growth. In the case of a random diamond film, the dominance of (100) and (111) faceting on the exposed surfaces suggests these are the slow growth faces (Fig. 6). Indeed, Zheng et al. [4] have reported that the (110) face of natural diamond shows a lower oxidation rate than either the (100) or (111) faces, suggesting that the atoms on this face have a higher bonding energy. The dominance of (100) and (111) faceting in natural diamond crystals further establishes this, and is consistent with the PBC analysis of Hartmon and Perdok [2] and Sunagawa [3].

The (110) plane of diamond is intersected by the (111) planes, generating the periodic bonding chains on the (110) faces. The (111) planes are subject to both stacking and slip plane faults that are known to produce striations in natural diamond crystals [3]. Similarly, these regular

planar growth twin defects on (111) planes produce striated morphologies in the grains of the oriented polycrystalline diamond films.

We propose that the formation of (111) twin defects on the (110) diamond growth surface provides low-energy sites for preferential bonding of the radical species, leading to an enhancement of the growth rate. Similarly, the presence of these defects leads to a continued propagation of the low-energy bonding sites. This is illustrated in Fig. 7. For a faceted perfect crystal oriented with a (110) surface plane, rapid growth along the (110) faces consumes all the available sites, leading to a crystal bounded by the slower growing faces. At this stage, crystal growth is stopped and renucleation of a new crystallite must occur for bulk film growth to continue. This step is known to be comparatively slow at low temperatures for PACVD diamond films. In the presence of the planar (111) twin defects, however, the growth along the (110) faces does not lead to a consumption of the preferred bonding sites due to the lack of crystallographic equivalence across the defect boundary. This leads to a propagation of the defective structure, with the net growth rate controlled now by the rate of radical attachment instead of by crystal renucleation.

The generation of oriented films on the non-diamond substrates is consistent with the observed homoepitaxial film growth behavior. The global (110) orientation on the non-diamond substrates is believed due to the interplay

between anisotropic growth modes and anisotropic etching, with both factors favoring the (110) growth. For small diamond seed crystals, the plasma etching occurring during the initial stages of film formation will tend to alter the crystallographic distribution of the seeds towards a (110) orientation. Coupled with this are the enhanced growth rates observed on the (110) single crystal diamond surface. The combination of these two factors imposes a strong preference for global (110) oriented polycrystalline film development under the low deposition temperatures used in this work. For higher growth temperatures, it is likely that the energetic differences associated with the crystallographically favored growth modes will be much less significant, and the nucleation time during which seed etching occurs will be reduced, favoring random film development. This transition to random growth morphologies at higher growth temperatures has indeed been experimentally demonstrated. Furthermore, the observation that such oriented films can be grown on a variety of polycrystalline substrates as well as on single crystal (100) silicon indicates that under these growth conditions the crystal structure of the non-lattice matched substrates do not significantly affect the nucleation energetics. This observation is consistent with the high surface energy of diamond [5]. For high surface energy substrates, such as diamond itself, substrate crystallography has been shown to play a role.

The samples not exhibiting the oriented growth at these low temperatures (<650 °C) were the (100) Si polished with coarse cubic boron nitride powder and the fused silica substrate. On the silicon sample, growth was initiated on the individual boron nitride crystal surfaces (Fig. 8). While smaller particles did initiate some growth on the Si surface, the morphology was dominated by large, isolated diamond crystals with smooth faceted geometries (Fig. 9). The lack of global orientation and the reduced growth rate in this sample were consistent with the proposed mechanisms for oriented growth in the diamond seeded films.

For the fused silica substrate, the different growth behavior is attributed to oxygen release during surface reduction. The interaction of the plasma with the substrate surface is clear, as evidenced by the pitting observed in the micrograph of Fig. 10. Oxygen released during this reaction will not only etch the smaller diamond particles embedded by the polishing process, but will also inhibit the general nucleation of the polycrystalline diamond film by surface disruption. In this case, growth is again limited to the larger diamond particulate seeds on the surface, and well-defined particle growth morphologies result. It has been noted in this laboratory that diamond films grown on fused silica are extremely white, containing little of the graphitic components which tend to darken the films. This is consistent with a higher local oxygen content at the

reaction surface, which preferentially removes the  $sp^2$  bonded carbons [6].

### CONCLUSIONS

The preferential growth of globally oriented (110) polycrystalline diamond films below 650 °C can be ascribed to a combination of anisotropic etching of diamond nuclei and anisotropic growth enhanced by the presence of crystallographic planar defects. These films tend to be described by regular microstructures dominated by multiple (111) growth twins. These defects provide a source of preferred attachment sites for the growing film and lead to a propagation of a (110) oriented growth surface. This tends to maintain the film in a growth-limited mode as opposed to a renucleation-limited mode, resulting in a significant increase in the net film growth rate.

### ACKNOWLEDGEMENTS

Portions of this research were sponsored by the Office of Naval Research.

REFERENCES

1. A. B. Harker and J.F. DeNatale, "Temperature and Reactive Etching Effects on the Microstructure of Microwave Plasma Deposited Diamond Films," *J. Mater. Res.* 5, pp. 818-823 (1990).
2. P. Hartmon and W.G. Perdok, "On the Relations Between Structure and Morphology of Crystals. I," *Acta. Cryst.* 8, pp. 49-52 (1955).
3. I. Sunagawa, "Growth and Morphology of Diamond Crystals Under Stable and Metastable Conditions," *J. Crystal Growth* 99, pp. 1156-1161 (1990).
4. A. Zheng, H. Kanda, T. Ohsawa, S. Yamaoka, "Inhomogeneous Oxidation Rate Measured on the (110) Cross-Section of Synthetic Diamonds," *J. Mat. Sci. Lett.* 9, pp. 331-333 (1990).
5. R.Kern, G. Le Lay, and J.J. Metois, "Basic Mechanisms in the Early Stages of Epitaxy, " in *Current Topics in Materials Science*, Vol. 3, Ed. E. Kaldis (North Holland, 1979).

6. S.J. Harris and A.M. Weiner, "Effects of Oxygen on Diamond Growth," *Appl. Phys. Lett.* 55(21), pp.2179-2181(1989).

FIGURE CAPTIONS

Fig 1. Electron channeling patterns of PACVD epitaxial diamond films on single crystal type 2A diamond.

Fig. 2. Surface morphology of homoepitaxial films on type 2A diamond.

Fig. 3. Raman spectra comparing homoepitaxial diamond film and type 2A diamond substrate. Also shown is spectra of polycrystalline film on Si.

Fig. 4. Surface microstructures of (110) oriented polycrystalline diamond films. (a) Silicon Nitride substrate; (b) Boron Nitride substrate; (c) (100) Si substrate.

Fig. 5. Detail of multiply twinned grain in (110) oriented diamond film on (100) Si.

Fig. 6 SEM micrograph of grain development in a random diamond film grown by PACVD.

Fig. 7. Schematic of (110) growth surface propagation in a multiply twinned diamond crystal.

Fig. 8. Preferential growth of diamond crystals on coarse cubic boron nitride particles.

Fig. 9. Faceted diamond crystal morphology observed on BN-seeded (100) Si.

Fig. 10. Diamond particle morphology for random film grown on fused silica.

TABLE 1: Microstructure of Diamond Films as a function of Substrate Identity and Surface Preparation.

SUBSTRATE	FILM PROPERTIES
(100) Type 2A Diamond	Epitaxial, low Defect, textured
(111) Type 2A Diamond	Epitaxial, smooth, isolated defects
(110) Type 2A Diamond	Epitaxial, rough surface, highest growth rate
(100) Si (Dia. Polish)	(110) Oriented Polycrystalline
(110) Si (c-BN Polish)	Random Polycrystalline
Fused Silica (Dia Polish)	Random Polycrystalline
Silicon Nitride (Dia. Polish)	(110) Oriented Polycrystalline
Boron Nitride (Dia. Polish)	(110) Oriented Polycrystalline

SC02697



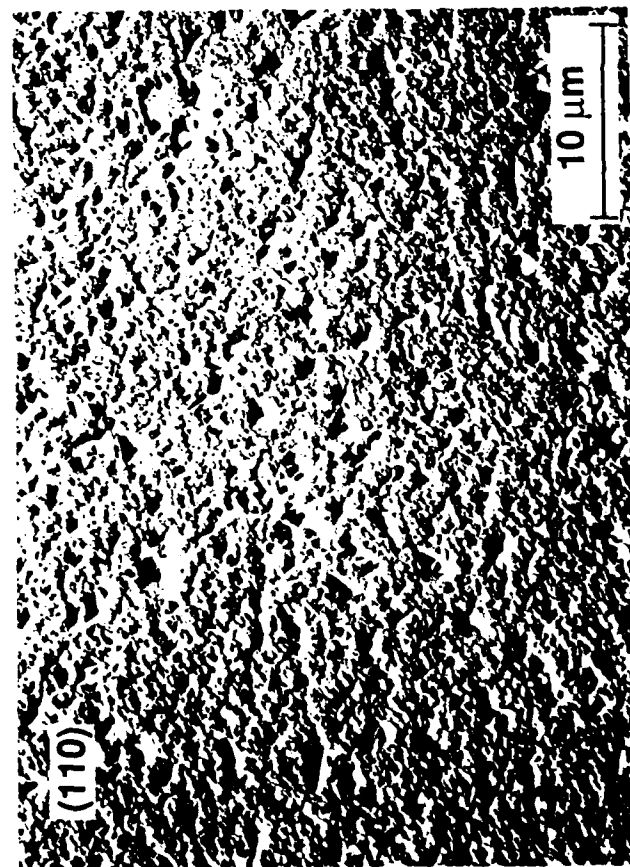
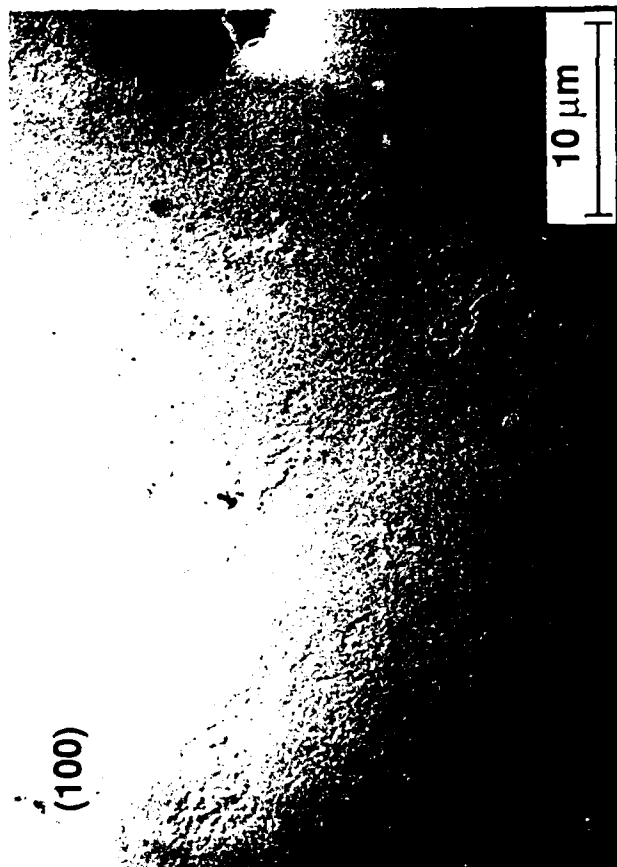
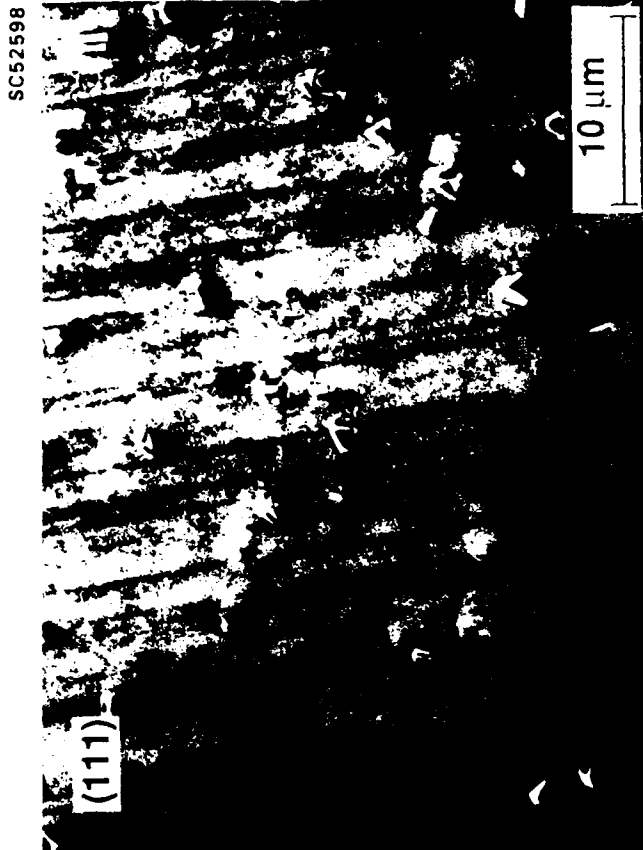
(100)



(110)

# Electron channelling patterns of microwave plasma CVD epitaxial films on the faces of type 2A diamond

Figure 1



Surface morphology of  
homo-epitaxial films on the faces  
of type 2A diamond

Figure 2

SC48438

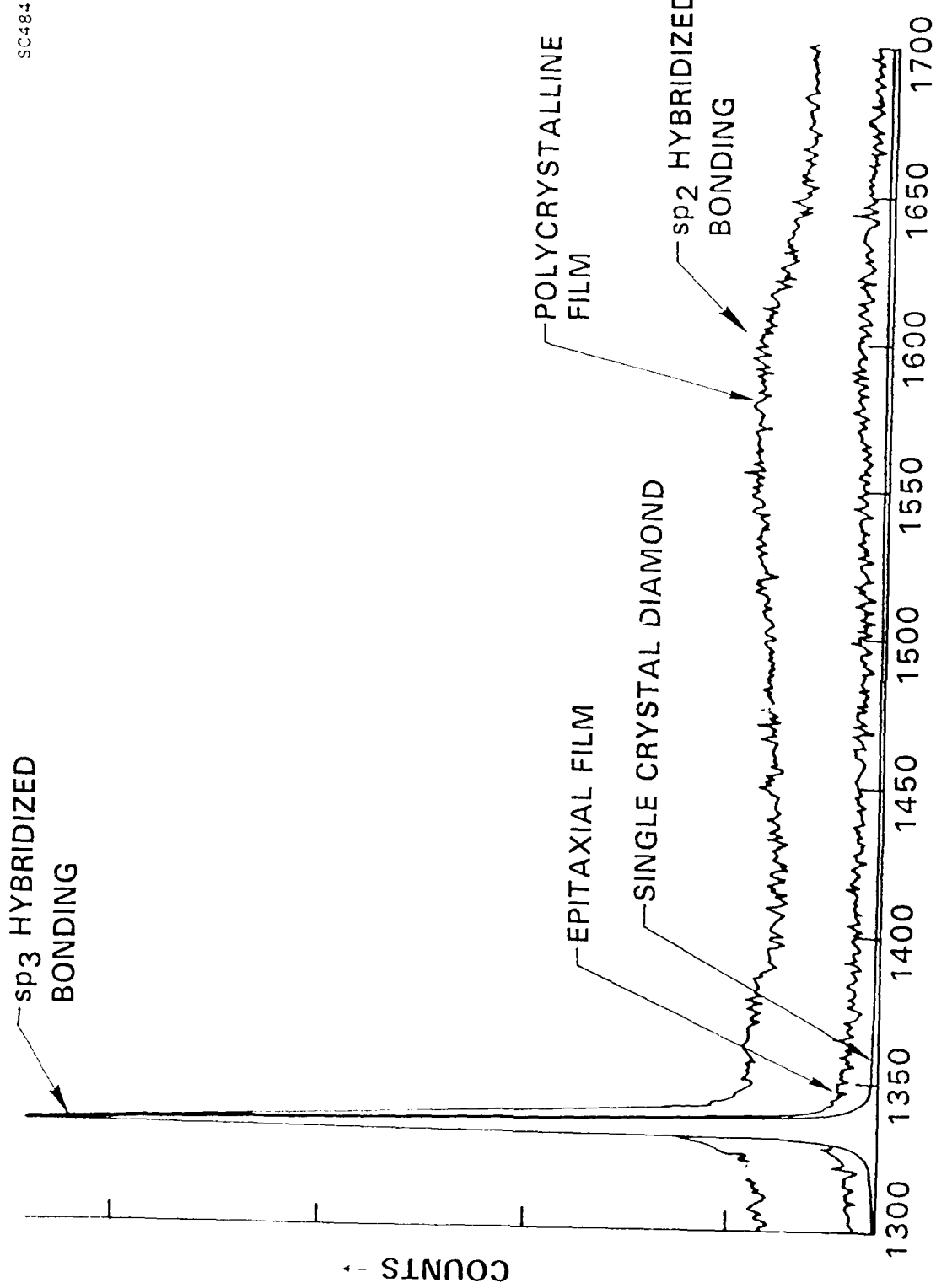


Figure 3



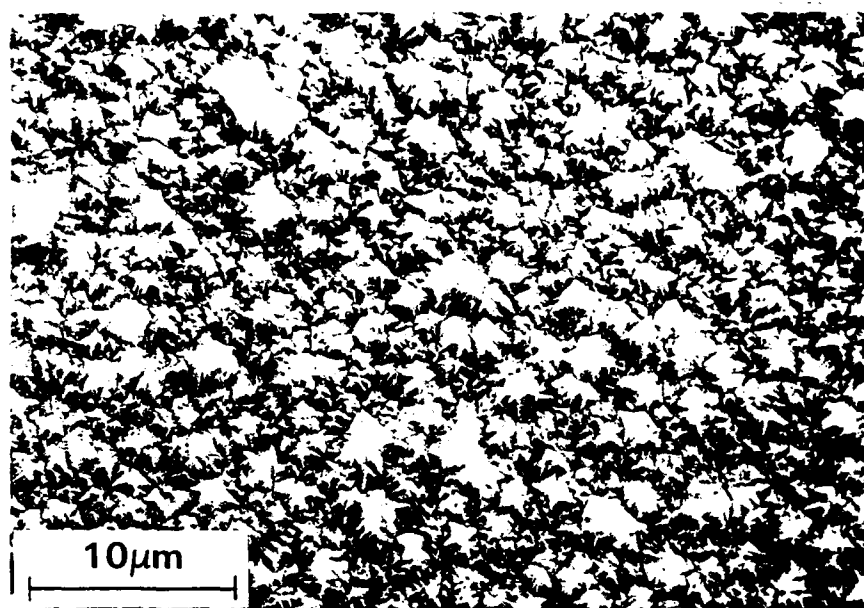
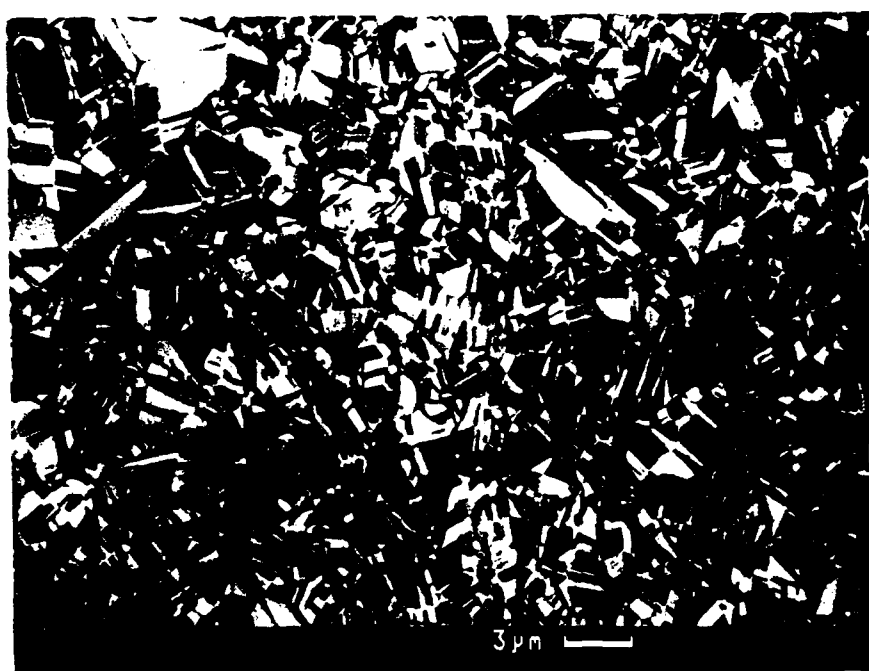
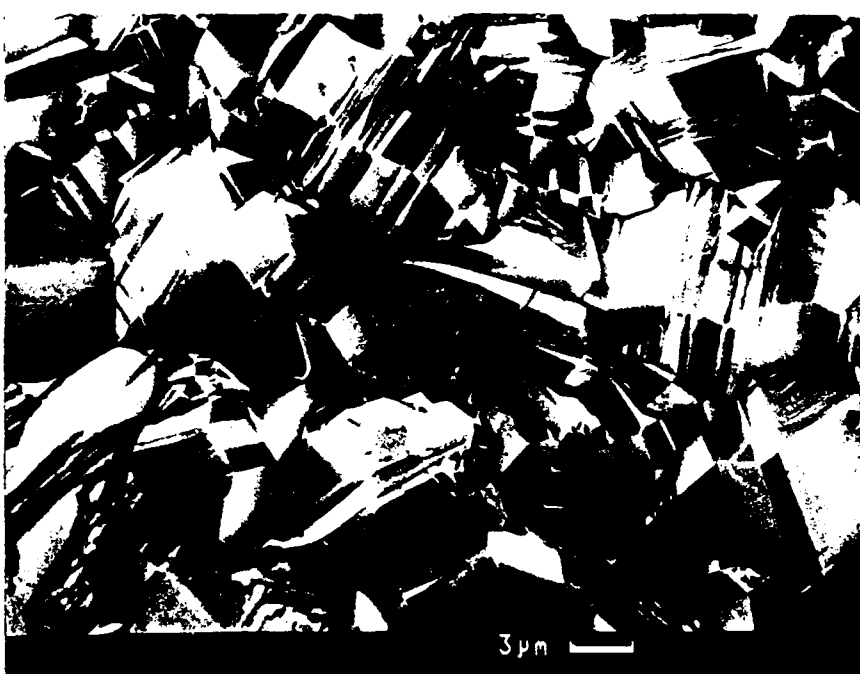


Figure 4a



**(110) ORIENTED DIAMOND ON  
PYROLYtic BORON NITRIDE,  
SUBMICRON DIAMOND PASTE POLISH**

Figure 4b



**(110) ORIENTED DIAMOND  
ON (100) SILICON, SUBMICRON  
DIAMOND PASTE POLISH**

Figure 4c

SC62307



Figure 5

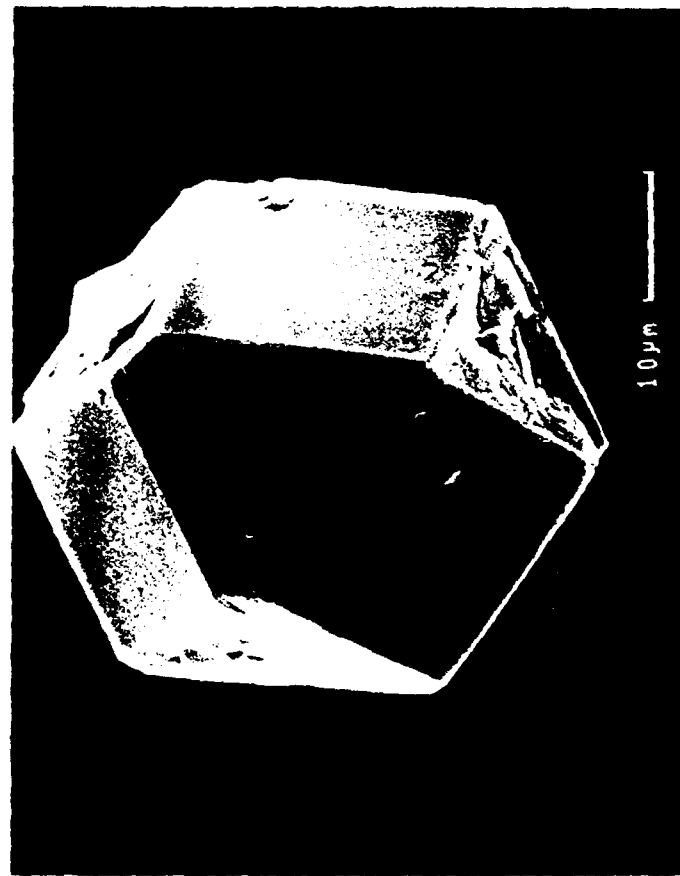
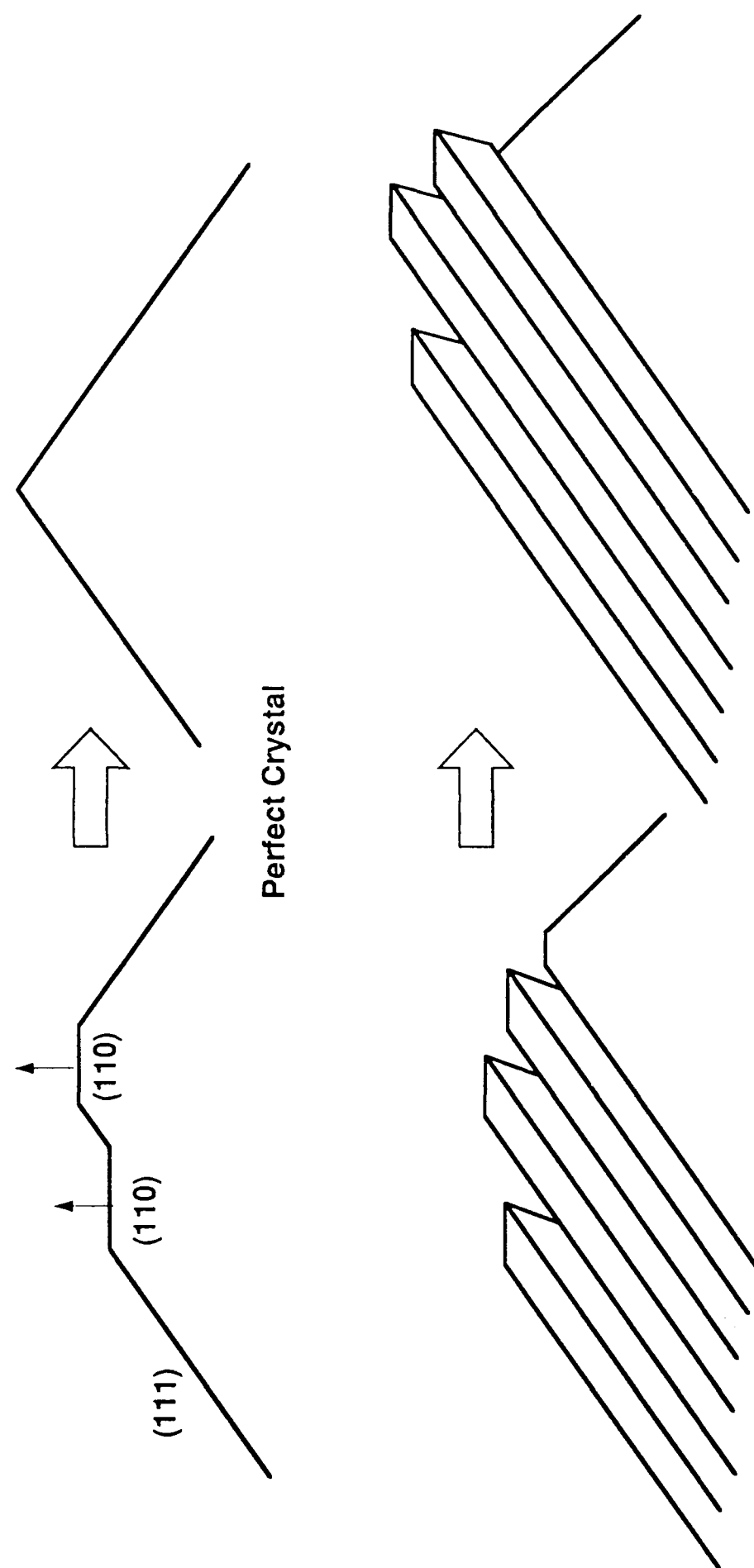


Figure 6

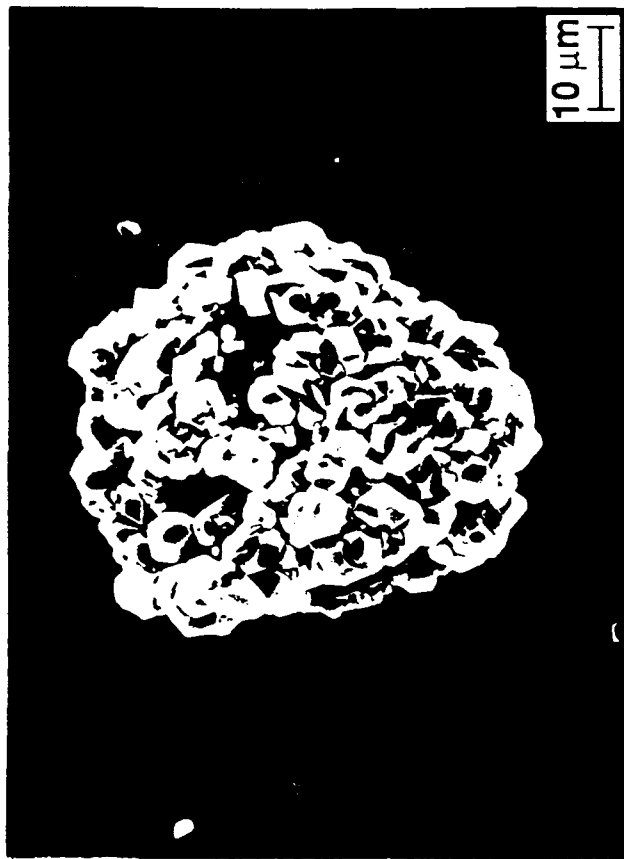
SC-1335-T



**Twinned Crystal**

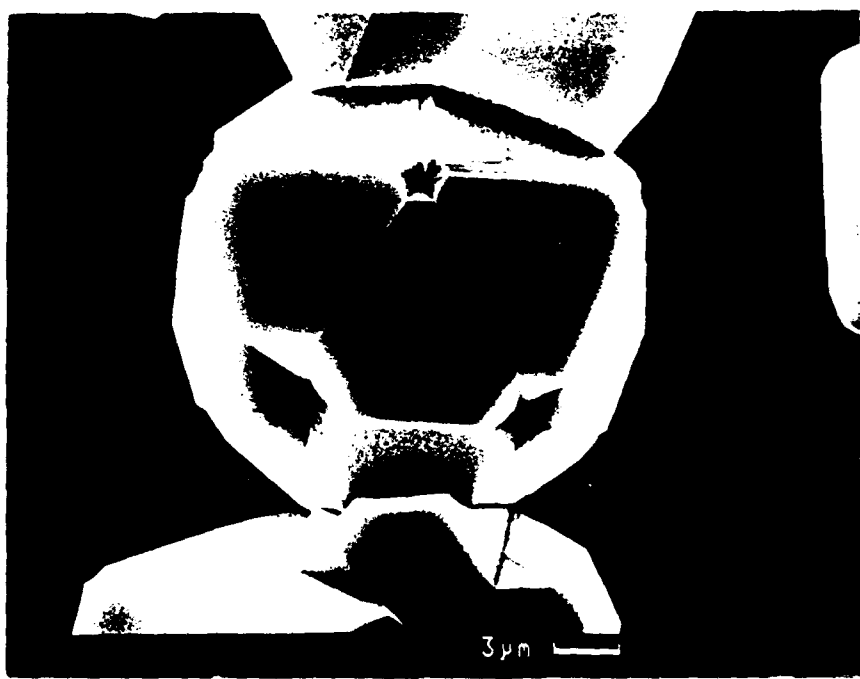
Figure 7

SC52596



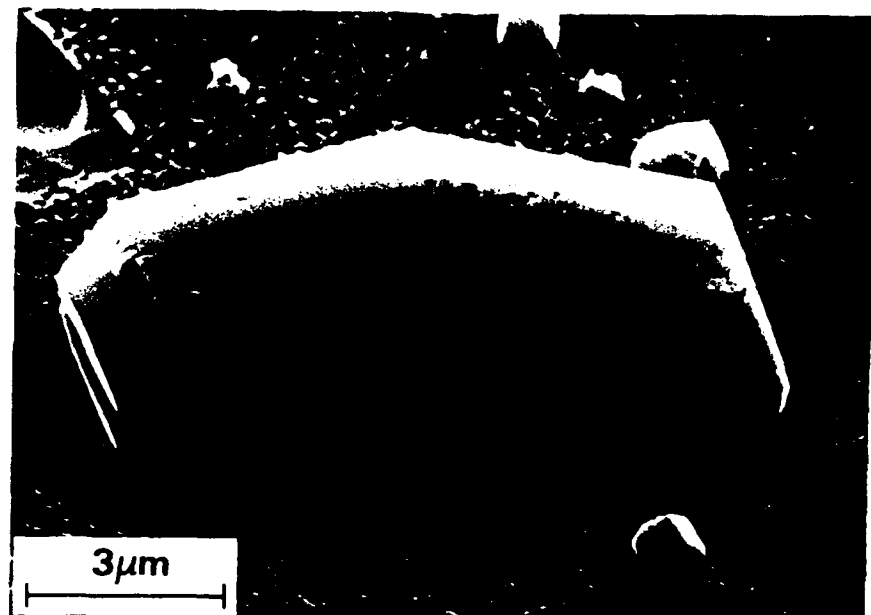
**Surface nucleation of  
polycrystalline diamond on cubic  
boron nitride particulates**

Figure 8



**POLYCRYSTALLINE DIAMOND  
ON (100) SILICON, CUBIC BORON  
NITRIDE POLISH (45 MESH)**

Figure 9



**POLYCRYSTALLINE DIAMOND ON  
FUSED SILICA, SUBMICRON  
DIAMOND PASTE POLISH**

Figure 10

# PROCEEDINGS REPRINT

 SPIE—The International Society for Optical Engineering

*Reprinted from*

## Diamond Optics III

**9-11 July 1990**  
San Diego, California



**Volume 1325**

# The polishing of polycrystalline diamond films

Alan B. Harker, John Flintoff, and J.F. DeNatale

Rockwell International Science Center

P.O. Box 1085

1049 Camino Dos Rios

Thousand Oaks, CA 91360

## ABSTRACT

Optically smooth surfaces can be produced on initially rough polycrystalline diamond films through the combined use of reactive ion etching and high temperature lapping on Fe metal. Protective thin film barriers are first applied to the diamond surface to restrict the reactive oxygen or hydrogen ion etching process to regions of greatest roughness. When the overall surface roughness has been reduced sufficiently by etching, mechanical lapping of the surface on an Fe plate at temperatures of 730°C-900°C in the presence of hydrogen can be used to produce surface roughnesses of less than 10 nm as measured by profilometry. The two techniques are complementary for flat surfaces, while the reactive etching process alone can be used with shaped substrates to produce a surface finish suitable for LWIR optical applications.

## 1. INTRODUCTION

The fundamental processes involved in the growth of polycrystalline diamond film surfaces leads to a high degree of roughness in thicker films. The general roughness is produced by the protrusion of individual faceted particles as shown in the scanning electron micrograph in Fig. 1. This roughness is often overshadowed, however, by the localized preferential growth of large particulates (Fig. 2). This surface roughness greatly limits the use of such thick diamond films for coating friction-wear surfaces and in optical components.

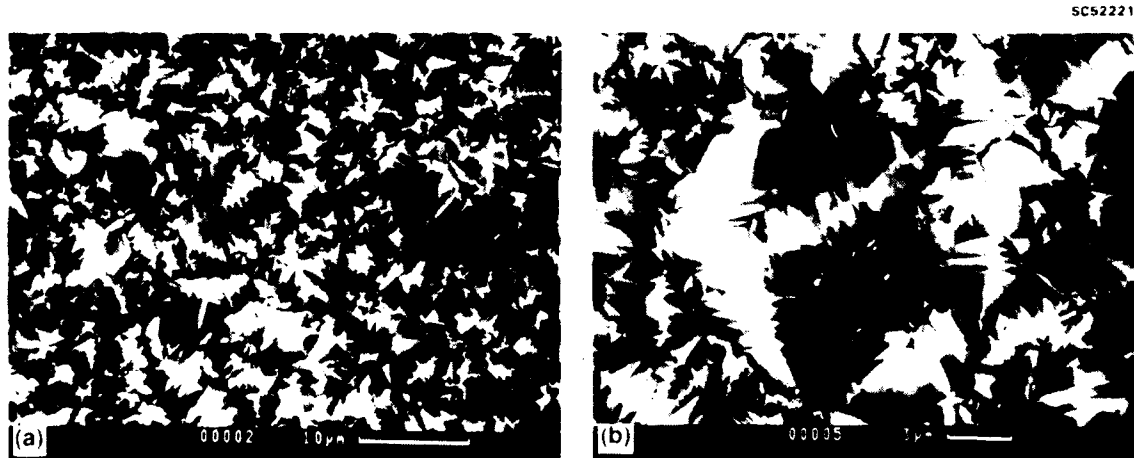


Fig. 1. Electron micrographs of highly faceted polycrystalline diamond surface.

Techniques for limiting such roughness in the deposition process are being explored, but it is reasonable to assume that some degree of postdeposition surface finishing will be required for most thick film applications. Simple room temperature polishing procedures are very difficult

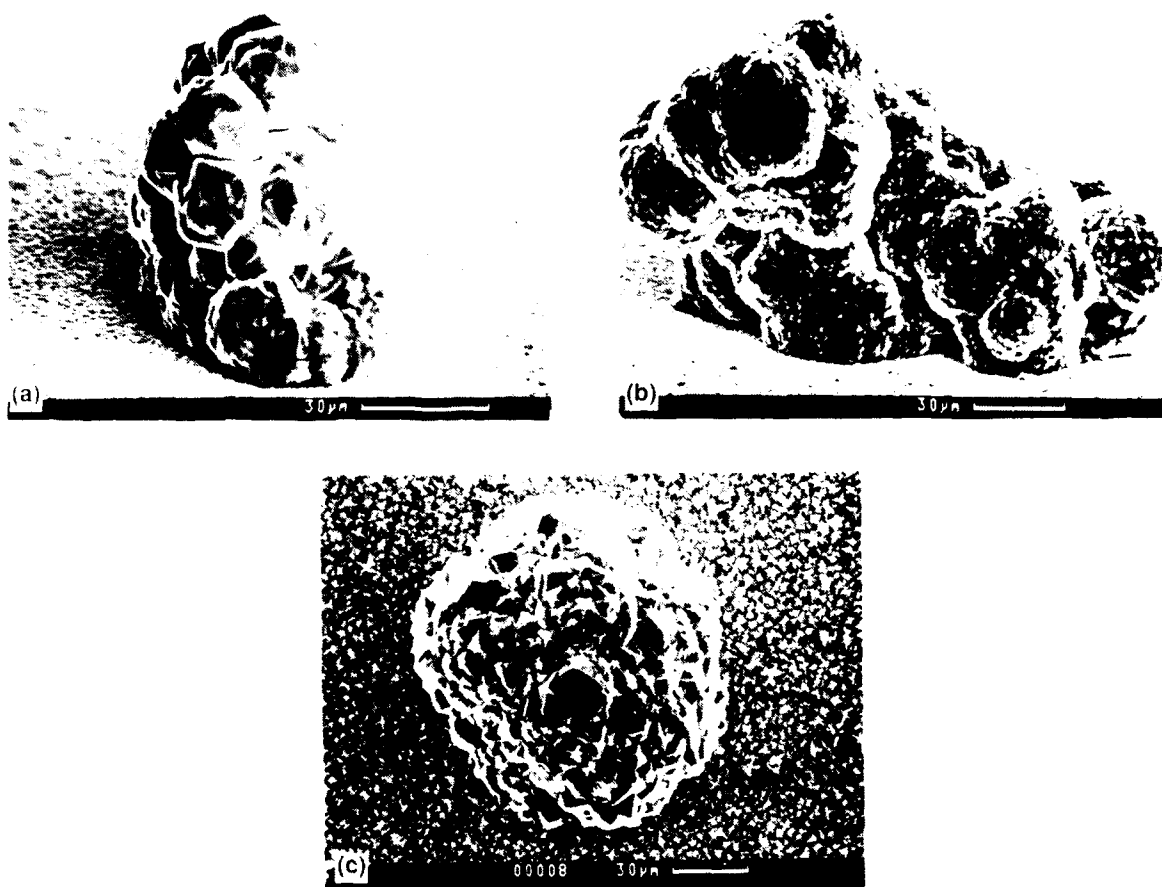


Fig. 2. Electron micrographs of supermicron scale particulates formed during the microwave PACVD growth of polycrystalline diamond.

and time consuming, due both to the mechanical properties of the material and the highly local nature of the roughness. Since the material properties of the diamond greatly limit abrasive polishing, a chemical approach would be preferred.

The polishing of polycrystalline diamond surfaces by contact with iron in a hydrogen atmosphere at elevated temperatures was initially reported in the Japanese literature in 1988.<sup>1</sup> This technique, while quite useful, has severe limitations in terms of scaling to large sample sizes and for use on shaped surfaces. The high temperatures involved ( $> 730^{\circ}\text{C}$ ) also produce mechanical failures and thermal shocking of the film and substrate. The presence of supermicron particulates on the films limits contact of the polishing plate with the general film surface as does any curvature imparted to the substrate by stress from the growth of the diamond films.

To alleviate some of the problems associated with the high temperature polishing process, a means of using ion etching has been pursued to reduce surface roughness to the degree that the diamond films are suitable for use as IR optical components.

## 2. EXPERIMENTAL

The diamond films used in these experiments were prepared on 2.5 cm diameter circular (100) single crystal silicon substrates by microwave plasma assisted CVD (PACVD) in a UHV

chamber equipped with an Astex 1500 W magnetron. Typical conditions were 0.7% methane and 0.3% oxygen in hydrogen at temperatures of 450-750°C. Film thicknesses ranged from 30 to 200  $\mu\text{m}$ . As shown in Fig. 1, the films were polycrystalline with local supermicron particulates and generally exhibited a concave surface curvature of near 5  $\mu\text{m}$  depth from edge to center.

Contact polishing experiments were carried out on a rotating 9 cm diameter iron metal plate in a stainless steel UHV chamber at 600-800°C in a hydrogen atmosphere at pressures of 4 to 80 torr. A tungsten filament was operated in the polisher at 1950°C. Chemical etching experiments were carried out in a stainless steel vacuum chamber in mixtures of oxygen in argon and hydrogen in argon, using an AC discharge.

Scanning electron microscopy (SEM), transmission electron microscopy (TEM), Raman microprobe, x-ray photoelectron spectroscopy (XPS), and profilimetry were used to characterize the diamond film samples and iron plate surfaces.

### 3. RESULTS

#### 3.1 Fe-Plate polishing

The use of the Feplate polishing technique was studied as a function of plate temperature and hydrogen pressure. The progress of the polishing process was observed by SEM and is shown in the series of micrographs in Fig. 3. The major observation is that the primary reactive polishing process occurs only at points of direct contact between the lapping plate and the high points of the faceted film. In areas out of direct contact with the Fe plate, only minor surface roughening was observable by SEM in highly faceted areas, presumably from surface reactions with gaseous species such as residual oxygen, hydrogen atoms and organic radicals produced in the chamber by the hot tungsten filament.

As the lapping process removes the crystalline facets, broader areas of the film contact the plate and eventually a smooth surface is obtained. Profilimetry shows a local surface roughness of  $\pm 100$  nm to 5000 nm before polishing and less than  $\pm 10$  nm after lapping on the Fe plate.

For the current system under study at 750°C in 80 torr of hydrogen, with a tungsten filament operating at 1950°C, local polishing rates of  $> 5 \mu\text{m}$  per hour have been observed. Molybdenum and stainless steel lapping surfaces were also examined. Though limited polishing was observed on the stainless plate, the highest rates of material removal were obtained with elemental iron on which polishing has been observed at temperatures up to 900°C.

The mechanism of the polishing process near 750°C has been studied by Raman scattering spectroscopy and Xray photoelectron spectroscopy (XPS). The carbon 1s electron XPS peak was used to observe the chemical changes occurring at the diamond surface during polishing. The very smooth substrate side of a freestanding diamond film was used in these measurements after being coated by ion beam sputtering with a metallic iron film thin enough (1 - 1.5 nm) such that the XPS carbon peak was still observable. The carbon 1s electron spectrum was determined before and after heating in vacuum and in hydrogen, with and without the Fe metal thin film coating.

The diamond carbon 1s peak shape and chemical shift showed no change after heating in vacuum to 750°C without the Fe film coating. With the Fe overcoating the C 1s peak exhibited broadening and a shift to lower binding energy when heated in excess of 725°C (285.8 $\pm$ 0.2 to 284.4 $\pm$ 0.2 eV). No changes in the C 1s spectrum were observed after heating to 650°C-700°C in

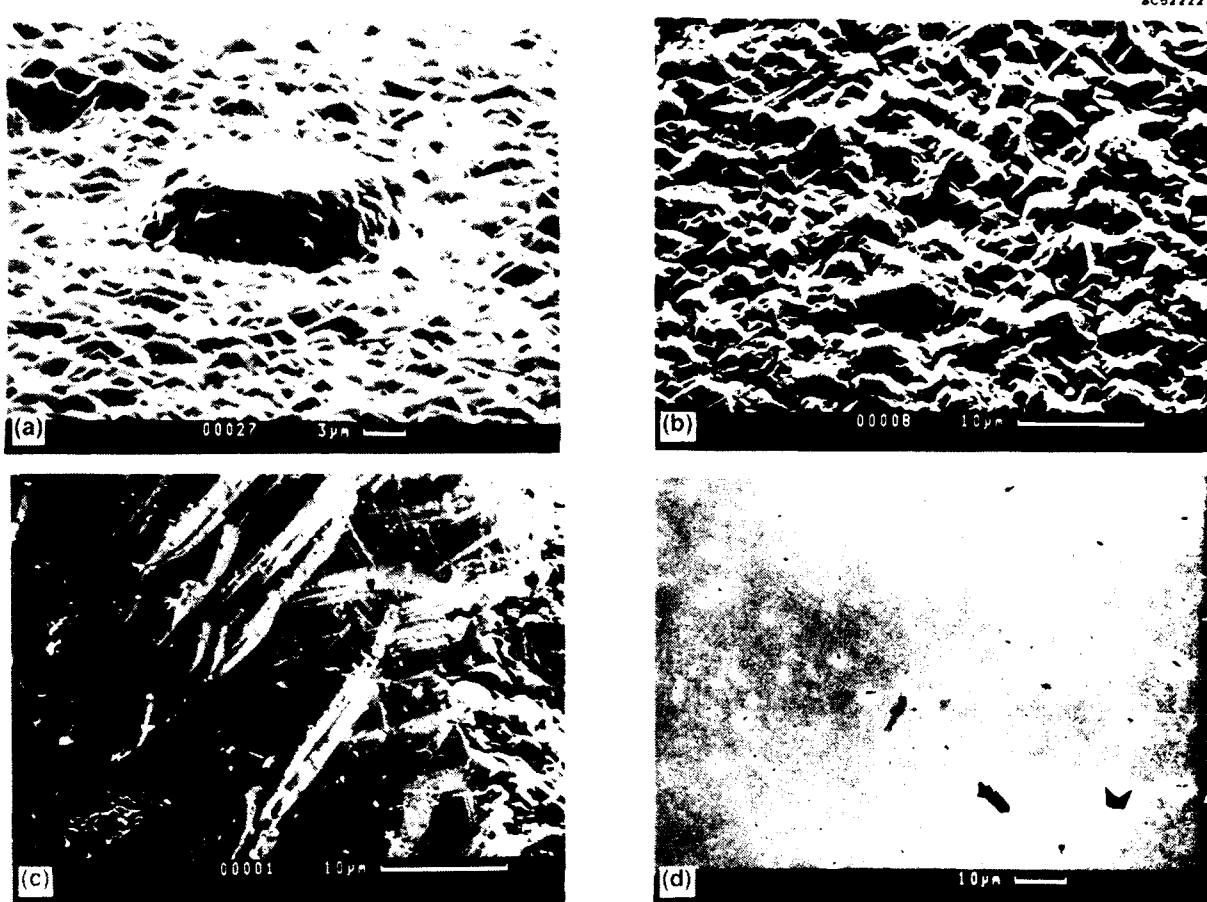


Fig. 3. Electron micrographs showing the progressive polish being developed on a polycrystalline diamond surface during Fe plate lapping at 750°C.

vacuum with the Fe overcoat. This is consistent with the occurrence of the alpha to gamma phase transition occurring in Fe at 723°C. This transition increases the solubility of carbon in the Fe by a factor of 40 to 0.8 wt%.<sup>2</sup>

The broadened C 1s peak observed at 284.4 eV after heating the diamond to 750°C in the presence of Fe is consistent with the diamond surface losing its crystalline properties, but does not indicate the formation of a carbide. However, due to the thinness of the Fe film, any carbide could readily be removed by reaction with residual oxygen in the chamber and is certainly removed by atomic hydrogen. Evidence of this is the observation that the C 1s peak retained its diamond character after heating the Fe coated sample to 750°C in the presence of hydrogen.

Raman spectra taken on the rough polycrystalline diamond surface before and after polishing show that the Fe plate lapping produces an increase in the broad  $1450-1600\text{ cm}^{-1}$  peak associated with  $\text{sp}^2$  bonded carbon. However, after mechanical surface polishing at room temperature and vigorous cleaning, the  $\text{sp}^2$  bonded spectral feature is greatly reduced, indicating that the nondiamond carbon material is localized at the film surface. SEM analysis suggested that at least some of this  $\text{sp}^2$  bonded material might be in the form of polishing debris bound at the surface by electrostatic forces.

The results of the XPS measurements on the smooth diamond surface and the Raman analysis of the rougher growth surface suggest that contact of the Fe plate with the diamond at temperatures above 723°C produces loss of crystalline order, converting the outer surface to a more graphitic  $sp^2$  bonded carbon. This graphitic material is then removed from the diamond by reaction with hydrogen and hydrogen atoms. It is also highly likely that iron carbide forms on the surface of the polishing plate which is also etched away by reaction with hydrogen to form methane.

The observation of graphitic carbon residue on the lapped diamond surface by Raman scattering indicates that not all of the reacted diamond is removed by physical abrasion or hydrogen etching. This residual  $sp^2$  bonded material could possibly exist as polishing debris attached to the surface or as material still chemically bound to the diamond that did not experience sufficient etching by hydrogen to be removed.

### 3.2 Reactive ion etching of diamond

The major limitation to the rapid broad area polishing of thick diamond films is the presence of large particulates of high defect density diamond carbon on the film surface. These particulates are an artifact of the growth process. They are attributed to very rapid growth occurring in local regions of high plasma density around particulate matter initially blown off surfaces in the chamber and deposited on the substrate or particulates formed in the gas phase. Such particulates can achieve dimensions of 20 to 100  $\mu\text{m}$  and cannot readily be removed from the film by mechanical means. During Fe plate lapping these macroscopic particulates are the only diamond surface initially in contact with the lapping plate, greatly reducing the area of polish. Ion etching provides a means to selectively remove these large particulates from the film before further surface polishing.

General area reactive plasma etching with either hydrogen or oxygen has been reported<sup>3,4</sup> and is known to attack nondiamond carbon preferentially. Since the larger particulates have very high defect densities, they are generally more susceptible to ion etching than the strongly faceted grains in the film and at 400-600°C in an oxygen plasma can be etched at a rate near 1  $\mu\text{m}$  per minute.

To insure that the reactive etching is confined to the regions of the large particulates a nonreactive (Au), high-temperature coating can be applied to the whole film and then selectively removed by physical polishing. The exposed areas then can be preferentially etched. Figure 4 shows a micrograph of a 120  $\mu\text{m}$  particle which has been greatly flattened by oxygen plasma etching, while the surrounding finer grained diamond film is unreacted.

Through repetition of the surface coating, mechanical polish, and etching procedure a surface can be obtained with a roughness below  $\pm 50$  nm. Such films are suitable for LWIR applications with no further surface polishing and the approach is suitable for shaped surfaces.

Figure 5 shows an infrared transmission spectrum taken from a 1 cm diameter region of a 35  $\mu\text{m}$  thick diamond film after reactive etching and Fe plate lapping. The film, which was initially totally scattering at wavelengths shorter than 10  $\mu\text{m}$ , shows significant improvement in short wavelength infrared transmission, but does not achieve full optical clarity. The spectrum still shows losses from hydrogen impurities in the film, intrinsic diamond absorption, and retained local scattering centers not fully removed by the polishing process in this sample. The degree of improvement in surface roughness in the diamond films can be seen in the Dektak profiles in Fig. 6. The unpolished film had a roughness exceeding  $\pm 100$  nm and achieved a final local roughness of less than  $\pm 10$  nm after ion etching and Fe plate lapping.

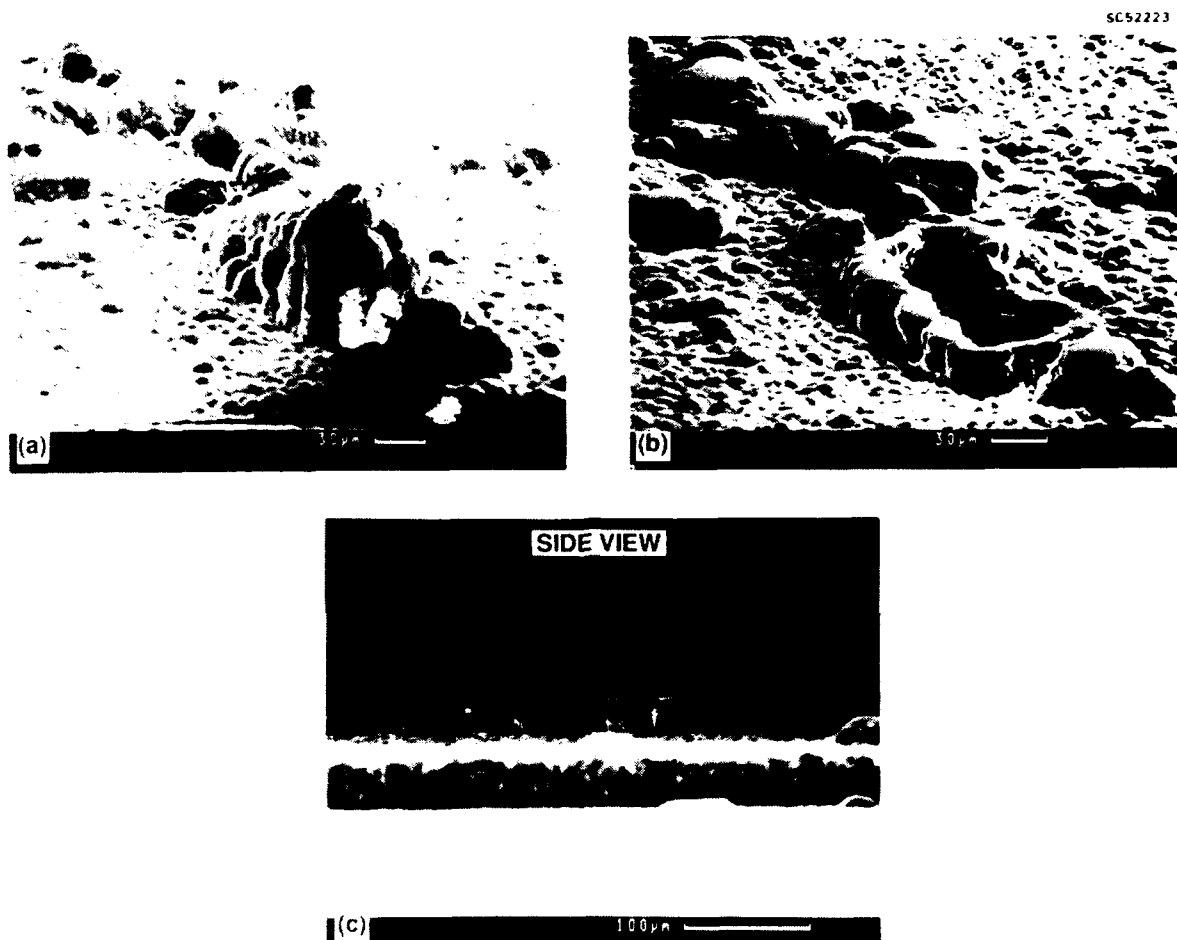


Fig. 4. Electron micrographs showing the progress of local reactive etching of super-micron scale diamond particles.

#### 4. CONCLUSIONS

The combined use of high temperature reactive plasma etching and lapping with an Fe plate in a hydrogen atmosphere can produce a broad area optical polish on the surface of polycrystalline diamond films. The major limitations to the techniques are the stresses and nonuniformities in the initial films themselves. Highly stressed films, poorly adhered to their substrates may not withstand the mechanical and thermal shocks associated with the polishing techniques. However, low stress films deposited on silicon have been shown capable of attaining an optical polish over regions of up to 2 cm in diameter.

#### 5. ACKNOWLEDGEMENT

Portions of this research were sponsored by the Office of Naval Research.

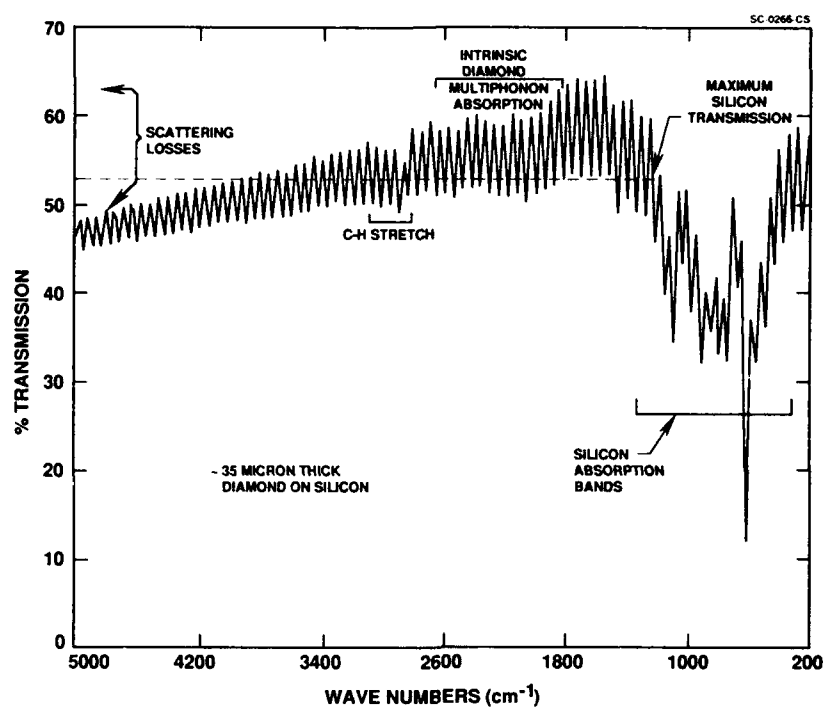


Fig. 5. Infrared transmission spectrum of a partially polished 2.5 cm diameter, 35  $\mu\text{m}$  thick polycrystalline diamond film on silicon.

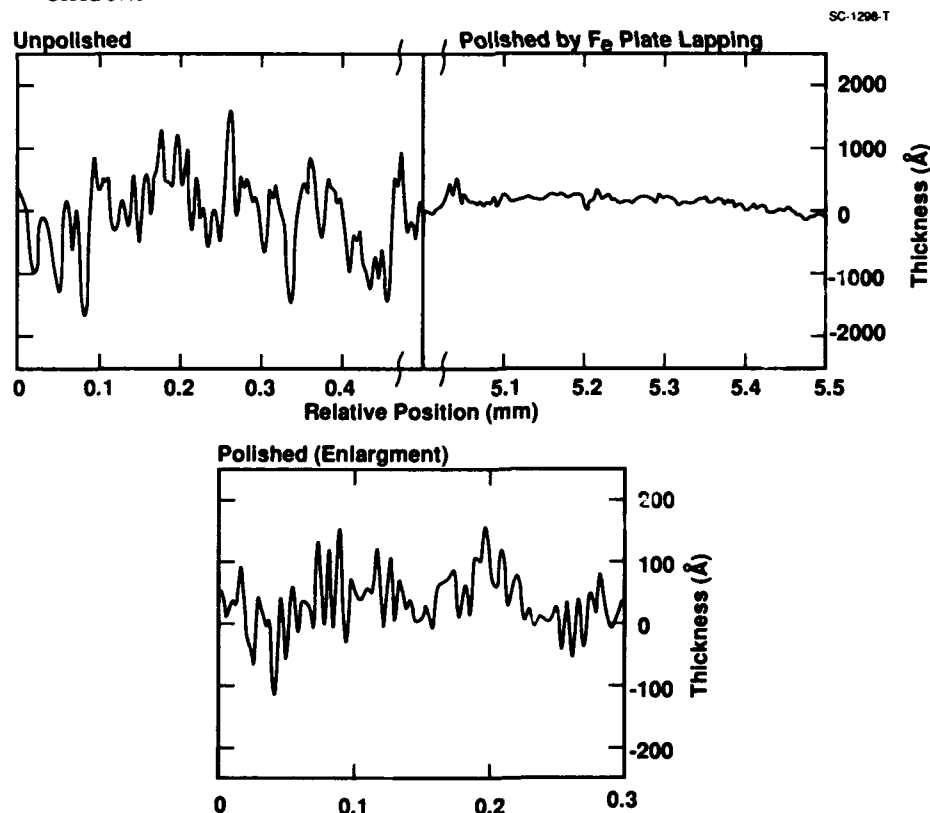


Fig. 6. Dektak stylus profiles of an unpolished and Fe plate final polished polycrystalline diamond film.

## 6. REFERENCES

1. C. Yang, H. Tokura, a M. Yoshikawa, "Polishing of Diamond Film with Metal," internal report, Tokyo Institute of Technology, Ookayama, Meguroku, Tokyo, Japan, 152 (1988).
2. M. Hansen and K. Anderko, Constitution of Binary Alloys, (McGraw Hill Book Co. Inc., N.Y.) p. 353 (1958).
3. N. Uchida, T. Kurita, K. Uematsu, and K. Saito, "Thermochemical Etching Effect on CVD Diamond in an Oxygen Atmosphere," *J. Mat. Sci. Lett.* 9, 249-250 (1990).
4. N. Uchida, T. Kurita, K. Uematsu, and K. Saito, "Hydrogen Post-Etching Effect on CVD Diamond Film," *J. Mat. Sci. Lett.* 9, 251-252 (1990).